



Inês Ribeiro Violante

The neurobiological basis of Neurofibromatosis type I:  
new insights into brain  
structure, function and neurochemistry

2012



UNIVERSIDADE DE COIMBRA



**The neurobiological basis of Neurofibromatosis type 1:  
new insights into brain structure, function and neurochemistry**

Contributions to understand impaired cognitive function

**Inês Ribeiro Violante**

**2012**

The studies presented in this thesis were carried out at the Visual Neurosciences Laboratory at IBILI (Instituto Biomédico de Investigação da luz e Imagem), Faculty of Medicine, University of Coimbra, Portugal, and were supported in part by a fellowship from the Portuguese Foundation for Science and Technology (SFRH/BD/41348/2007) and by grants from the University of Coimbra [Grant number III/14/2008] and the Portuguese Foundation for Science and Technology [Grant numbers PIC/IC/83155/2007, PIC/IC/82986/2007].

Cover design: Inês Violante

ISBN: 978-989-20-3250-4

Copyright © 2012 Inês Violante





Universidade de Coimbra  
Faculdade de Medicina



**The neurobiological basis of Neurofibromatosis type 1:  
new insights into brain structure, function and neurochemistry**

Dissertation presented to obtain a Ph.D. degree in Biomedical Sciences at the  
Faculty of Medicine of the University of Coimbra

Dissertação de Doutoramento apresentada à Faculdade de Medicina da Universidade de Coimbra,  
para prestação de provas de Doutoramento em Ciências Biomédicas

**Inês Ribeiro Violante**

**2012**

Supervised by: Miguel Castelo-Branco, M.D., Ph.D.

Co-Supervisor by: Carlos F.G.C. Geraldes, D.Phil.



*Para a Natália e o António*

“Why, sometimes I’ve believed as many as six impossible things before breakfast.”

The White Queen

in Lewis Carroll, *Alice Through the Looking Glass*



# CONTENTS

<b>Abbreviations</b>	VIII
<b>Summary</b>	XI
<b>Sumário</b>	XIII
<b>Introduction</b>	
Chapter 1 - Introduction	19
Aims and outline of the Thesis	41
<b>Materials and Methods</b>	
Chapter 2 - Fundamentals of magnetic resonance for the study of brain structure, function and neurochemistry	57
Chapter 3 - Research methodology: patient and control groups	75
<b>Results</b>	
Chapter 4 - Abnormal brain activation in Neurofibromatosis type 1: a link between visual processing and the default mode network	85
Chapter 5 - GABA is reduced in the visual cortex of patients with Neurofibromatosis type 1: a new perspective on the disease mechanism	115
Chapter 6 - Gyrfication, cortical and subcortical morphometry in Neurofibromatosis type 1: an uneven profile of developmental abnormalities	139
<b>Concluding Remarks</b>	
Chapter 7 - Discussion and Conclusions	171
<b>List of Publications</b>	187
<b>Agradecimentos</b>	189
<b>Curriculum Vitae</b>	191

## VIII

### ABBREVIATIONS

AC	Adenylate cyclase / Adenylyl cyclase
AC-PC	Anterior commissure - posterior commissure
ADC	Apparent diffusion coefficient
ADHD	Attention deficit hyperactive disorder
AKT	Serine/threonine protein kinase
ANCOVA	Analysis of covariance
ANOVA	Analysis of variance
BA	Brodman area
BOLD	Blood-oxygen-level-dependent
CC	Corpus callosum
cDNA	Complementary DNA
Cho	Choline
cpd	Cycles per degree
Cr	Creatine
CSF	Cerebrospinal fluid
d	Dorsal
DMN	Default-mode-network
DNA	Deoxyribonucleic acid
DSM-IV	Diagnostic and statistical manual of mental disorders - fourth edition
DTI	Diffusion tensor imaging
EPI	Echo planar imaging
ERK	Extracellular signal-regulated kinase
FA	Fractional anisotropy
FA	Flip angle
FID	Free induction decay
FDA	Food and drug administration
FDR	False discovery rate
FLAIR	Fluid attenuated inversion recovery
fMRI	Functional magnetic resonance imaging
FOV	Field of view
FRT	Facial recognition test
FSIQ	Full-scale intelligent quotient
FWHM	Full width at half maximum
GABA	$\gamma$ -Aminobutyric acid

GABA-T	GABA transaminase
GAD	Glutamic acid decarboxylase
GAP	GTPase activating protein
GATs	GABA transporters
GC	Ganglion cell
GEFs	Guanine-nucleotide exchange factors
GLM	General linear model
Gln	Glutamine
Glu	Glutamate
Glx	Glutamate + Glutamine
GM	Grey matter
GPCR	G protein-coupled receptor
Hb	Deoxyhaemoglobin
HbO <sub>2</sub>	Oxyhaemoglobin
Ins	Inositol
IPSP	Inhibitory postsynaptic potentials
IQ	Intelligent quotient
JLO	Judgment of line orientation
LGI	Local gyrification index
LGN	Lateral geniculate nucleus
LTP	Long-term potentiation
M	Magnocellular
MAPK	Mitogen-activated protein kinase
mEPSCs	Miniature excitatory postsynaptic currents
mIPSCs	Miniature inhibitory postsynaptic currents
MLPA	Multiplex ligation-dependent probe amplification
MPNST	Malignant peripheral nerve sheath tumours
MPRAGE	Magnetization prepared rapid gradient echo
MR	Magnetic resonance
MRI	Magnetic resonance imaging
MRS	Magnetic resonance spectroscopy
mTOR	Mammalian target of rapamycin
NAA	N-acetylaspartate
NF1	Neurofibromatosis type 1

NMDAR	N-methyl-D-aspartate receptor
NS	Non significant
P	Parvocellular
PCr	Phosphocreatine
PD	Proton density
PET	Positron emission tomography
PI3K	Phosphatidylinositol 3-kinase
PIQ	Performance intelligent quotient
PK	Protein kinase
RF	Radiofrequency
RFX	Random effects
RNA	Ribonucleic acid
ROI	Region-of-interest
RTK	receptor tyrosine kinase
rut	Rutabaga
SD	Standard deviation
SE	Standard error
SEM	Standard error of the mean
SHP2	Src homology-2 containing tyrosine phosphatase
sIPSCs	Spontaneous inhibitory postsynaptic currents
$T_{1w}$	T1-weighted
$T_{2w}$	T2-weighted
tCr	Total creatine
TD	Typically Developing
TE	Echo time
TI	Inversion Time
TIV	Total intracranial volume
TR	Repetition time
UBOs	Unidentified bright objects
v	Ventral
VGAT	Vesicular neurotransmitter transporter
VIQ	Verbal intelligent quotient
WISC-III	Wechsler intelligence scale for children - third edition
WM	White matter
WT	Wild type



## SUMMARY

Neurofibromatosis type 1 (NF1) is a single-gene disorder associated with complex cognitive dysfunction including learning disabilities, attention deficit hyperactive disorder, executive function, visuospatial and motor coordination deficits. Neuroimaging techniques can contribute to identify the neurobiological basis underlying these impairments. Here, I used spectroscopy, functional and structural brain imaging to identify the neural and neurotransmitter systems involved in the aetiology of the cognitive deficits in NF1. Particularly, I focused on basic physiological features that have the potential to unravel downstream alterations that can cause higher order cognitive deficits. This approach was chosen to scrutinise the contributions of visual sensory processing, neurotransmitter regulation and neuroanatomical characteristics to the NF1 phenotype.

Visual sensory processing was investigated by probing the neural activation of the two main pathways conduction information from the retina to the cortex, the magnocellular and parvocellular streams. This study examined for the first time the function of the early visual cortex in patients with NF1 and identified a pattern of deficient activation to both stimulus types. This analysis was performed in children, adolescents and adults with NF1 to investigate whether deficits in visual sensory processing ameliorated with age. It is shown that this is not the case and that the pattern observed in children persists into adulthood. Furthermore, we investigated the activation pattern of high-level visual and non-visual regions modulated by the different stimuli to examine possible functional consequences of low-level visual impairments. This led to the observation that during M-biased stimulation, patients with NF1 failed to deactivate or even activated anterior and posterior midline regions of the default mode network, while controls deactivated these regions. By definition, the default mode network is composed by a set of brain regions that are active during task-irrelevant thoughts and deactivate during performance of cognitively demanding or engaging tasks. The observation that the early visual magnocellular processing is impaired in NF1 and is specifically associated with a deficient deactivation of the default mode network may provide a neural explanation for high-order cognitive deficits present in NF1, particularly attentional.

NF1 belongs to a cluster of neurodevelopmental disorders for which alterations in the main inhibitory neurotransmitter,  $\gamma$ -aminobutyric acid (GABA), were proposed as the underlying cause of the cognitive deficits. This theory is the result of cellular and molecular studies on a mouse model of the disorder ( $Nf1^{+/-}$ ), which indicated an imbalance in

## XII

excitatory/inhibitory push-pull systems as a consequence of increased GABA-mediated inhibitory neurotransmission. To test whether a similar mechanism translates to the human disorder, magnetic resonance spectroscopy was applied to measure GABA levels in the visual cortex of children and adolescents with NF1 and matched controls. Measurements were performed in the visual cortex to provide further insight into the neural mechanisms causing the deficient visual sensory processing previously observed. We found that patients with NF1 have significantly lower GABA levels than controls and that NF1 mutation type significantly predicted cortical GABA. Our results provide the first evidence of GABAergic dysfunction in patients with NF1. This constitutes a relevant finding to understand the physiological profile of the disorder with implications for the identification of targets for therapeutic strategies.

I finalize the set of studies presented in this thesis by providing novel data on NF1 neuroanatomy. In order to understand how mutations in the *NF1* gene impact brain structure it is essential to characterize in detail the brain structural abnormalities in patients with this condition. Here we investigated the volumes of subcortical structures and for the first time the composite dimensions of the cortex, through the analysis of cortical volume, cortical thickness, cortical surface area and gyrification. It is shown that macrocephaly observed in patients is due to an increase in white matter volume and grey matter subcortical volume. Subcortical analysis revealed disproportionately larger thalami, right caudate and middle corpus callosum in patients with NF1. Moreover, it is shown that patients with NF1 have significant lower gyrification indices than typically developing children, primarily in frontal and temporal lobes, but also affecting the insula, cingulate cortex, parietal and occipital regions. These neuroanatomic abnormalities were localized to specific brain regions indicating that particular areas might constitute selective targets for *NF1* gene mutation. Furthermore, the lower gyrification indices were accompanied by a disproportionate increase in brain size without the corresponding increase in folding in patients with NF1. Taken together these findings suggest that specific neurodevelopmental processes, such as gyrification, are more vulnerable to *NF1* dysfunction than others.

As a single gene disorder, there is a great potential for establishing genetic, neurochemical and brain-behaviour relationships in NF1. The work presented in this thesis contributes to the understanding of these complex connections and identified novel neurobiological markers of NF1.

## SUMÁRIO

A Neurofibromatose de tipo 1 (NF1) é uma doença provocada por alterações no gene da *NF1* e está associada a disfunções cognitivas complexas que incluem dificuldades de aprendizagem, défice de atenção e hiperatividade, alterações da função executiva, visuoespacial e da coordenação motora. O uso de técnicas de neuroimagem pode contribuir para a identificação das bases neurobiológicas que contribuem para estas alterações. Na presente tese foram utilizadas técnicas de espectroscopia, imagem funcional e estrutural por ressonância magnética, para identificar os sistemas neurais e de neurotransmissão envolvidos na etiologia dos défices cognitivos na NF1. O foco destes estudos incidiu sobre a investigação de padrões fisiológicos cujas alterações possuem potencial para causar défices cognitivos. Esta abordagem permitiu escrutinar as contribuições relativas do processamento sensorial visual, da regulação dos níveis de neurotransmissores e as características neuroanatómicas que definem o fenótipo da NF1.

O processamento visual foi investigado recorrendo ao estudo da ativação neuronal das duas principais vias que conduzem informação visual da retina até ao córtex, ou seja, as vias magnocelular e parvocelular. Este estudo examinou pela primeira vez a função do córtex visual em doentes com NF1, permitindo a identificação de um padrão de ativação deficitária em resposta a ambos os estímulos (magnocelular e parvocelular). A análise destes padrões de ativação foi efetuada em crianças, adolescentes e adultos com NF1, com o objetivo de determinar se os défices no processamento visual são atenuados com a idade. Mostramos que tal não ocorre e que o padrão observado nas crianças persiste na idade adulta. Investigámos ainda o padrão de ativação em regiões de processamento visual de alto nível e outras regiões cerebrais moduladas pelos dois tipos de estímulo, com o propósito de identificar as consequências funcionais de alterações visuais de baixo nível. Esta análise permitiu observar que, em resposta ao estímulo visual magnocelular os doentes com NF1 não evidenciavam deativação ou ainda ativaram regiões da linha média anterior e posterior da “rede neuronal de funcionamento por defeito” (em inglês, default mode network (DMN)). Por definição, a DMN é composta por um conjunto de áreas cerebrais que estão ativas durante pensamentos irrelevantes para uma determinada tarefa e que deativam durante a performance de tarefas cognitivas exigentes ou que necessitam atenção. A observação de que a via magnocelular tem um funcionamento deficitário na NF1 e está especificamente associada a um défice do funcionamento da DMN, pode contribuir para a explicação das dificuldades cognitivas presentes na doença, principalmente as de cariz atencional.

## XIV

A NF1 pertence a um grupo de doenças do neurodesenvolvimento para as quais foi proposto que alterações no principal neurotransmissor inibitório, o ácido  $\gamma$ -aminobutírico (GABA), conduzem a défices cognitivos. Esta teoria é o resultado de estudos celulares e moleculares efetuados num modelo animal da doença, o ratinho *Nf1<sup>+/-</sup>*. Estes estudos evidenciaram um aumento da neurotransmissão GABAérgica que acarreta uma alteração no balanço dos sistemas inibitórios e excitatórios. Por forma a testar se um mecanismo similar se traduz para a doença humana, a espectroscopia por ressonância magnética foi aplicada para medir os níveis de GABA no córtex visual de crianças e adolescentes com NF1 e respetivos participantes controlo. Esta medição foi efetuada no córtex visual para aprofundar os mecanismos neuronais que causam os défices do processamento visual verificados no estudo anterior. Identificámos por um lado, uma redução significativa dos níveis de GABA nos doentes com NF1 em relação aos controlos e por outro, que o tipo de mutação no gene da *NF1* permite prever esta diminuição dos níveis de GABA. Estes resultados estabelecem a primeira evidência de alteração GABAérgica nos doentes com NF1, constituindo um achado relevante para compreender o perfil fisiológico da doença, com implicações para a identificação de alvos terapêuticos.

Finalizo o conjunto de estudos apresentado nesta tese expondo novos dados sobre a neuroanatomia da NF1. Para compreender a forma como mutações no gene da *NF1* interferem com a estrutura cerebral é essencial caracterizar em detalhe as alterações da estrutura do cérebro nos doentes com NF1. Desta forma, investigámos os volumes subcorticais e explorámos ainda, pela primeira vez, as diversas dimensões do córtex, através de análises de volume, espessura, superfície e girificação corticais. Mostramos que a macrocefalia observada em doentes é devida a um aumento do volume da matéria branca e da matéria cinzenta subcortical. A análise subcortical detalhada revelou aumentos desproporcionados dos tálamos, do núcleo caudado direito e do corpo caloso médio nos doentes com NF1. Identificámos ainda que os doentes com NF1 possuem índices de girificação reduzidos em comparação com os observados em crianças com desenvolvimento típico, particularmente dos lobos frontais e temporais, mas que afetam também a ínsula, o córtex cingulado, e regiões parietais e occipitais. Estas alterações neuroanatômicas foram localizadas em regiões cerebrais específicas, indicando que determinadas áreas podem constituir alvos seletivos das mutações no gene da NF1. Os índices de girificação reduzidos nos doentes com NF1 apresentaram-se acompanhados de um aumento do tamanho do cérebro, na ausência do correspondente incremento de convoluções corticais. Em suma, estes achados sugerem que processos específicos do desenvolvimento neural, tal como a girificação, são mais vulneráveis

do que outros a disfunções do gene da *NF1*.

Tratando-se de uma doença que afeta um único gene, a *NF1* possui um elevado potencial para o estabelecimento de relações genéticas, neuroquímicas e ainda entre o funcionamento cerebral e o comportamento. O trabalho apresentado nesta tese contribui para a compreensão destas complexas conexões e identifica novos marcadores neurobiológicos da *NF1*.



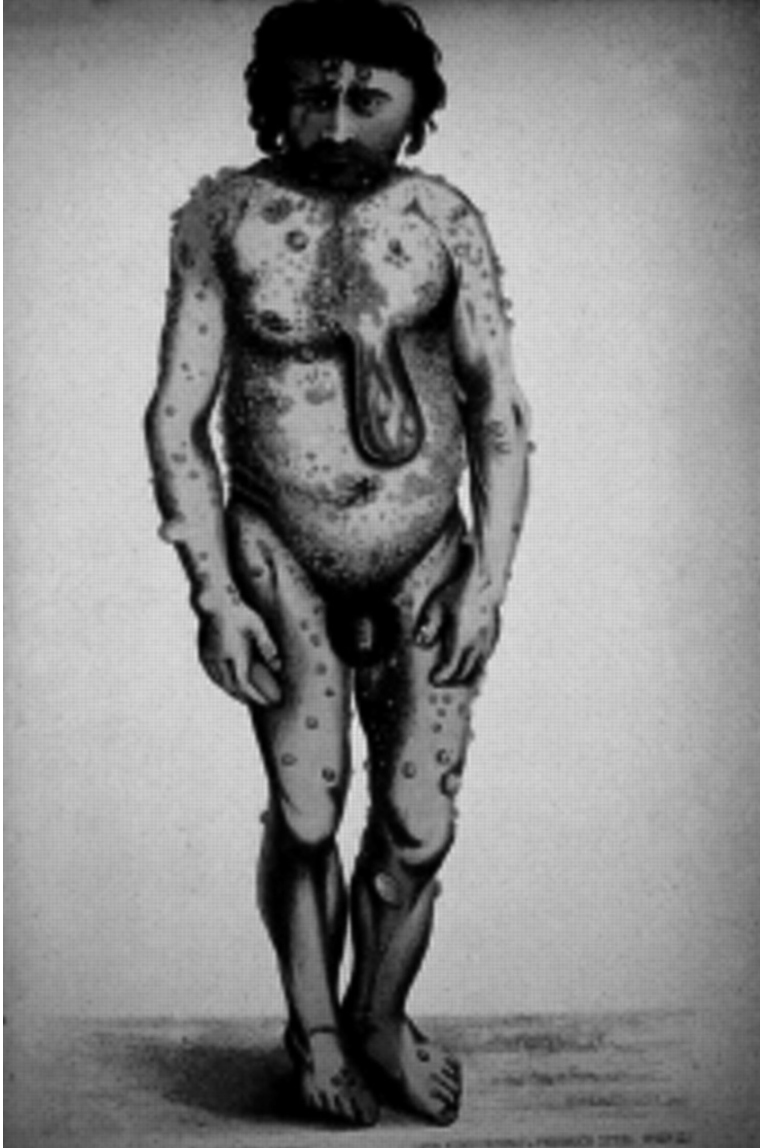
# INTRODUCTION





# CHAPTER I

## Introduction



The “Wart Man”, Johann Gottfried Rheinhard, as reported by Tilesius von Tilenau, 1793.  
Reproduced from Ruggieri and Polizzi, 2003. With permission from the publisher.

Neurofibromatosis constitutes a group of genetic disorders characterized by the development of tumours of the nervous system, particularly of the nerve sheath (Friedman and Riccardi, 1999; McClatchey, 2007). Three major forms of neurofibromatosis are recognized as separate entities on the basis of their genetic origin and pathogenesis: neurofibromatosis type 1, neurofibromatosis type 2 and schwannomatosis (MacCollin et al., 2005; Ferner, 2007).

The focus of this thesis is on the neurobiological basis underlying the cognitive deficits observed in patients with neurofibromatosis type 1 (NF1). Although cognitive deficits constitute the most common neurological complication in NF1 (North et al., 1997; Hyman et al., 2005) and pose a significant impact on patients' quality of life (North, 2000), few studies focused on the neurobiological basis of such impairments. In the present thesis a tripartite methodological approach was followed to acquire functional information on neural activity, and structural and neurochemical profiles of patients with NF1, with the goal of elucidating the pathophysiological mechanisms leading to altered brain function. To gain access into the living human brain, studies were performed using magnetic resonance imaging and spectroscopy. Such techniques revolutionized our ability to study brain anatomy and physiology and have proven to be critical for future understanding of the neurobiological basis underlying cognitive deficits in NF1 and other neurodevelopmental disorders.

This introductory chapter will first present background information on the clinical and genetic features of the disorder and summarize the current understanding on the function of the *NF1* gene. In the second part the focus will be on brain structure and function in NF1 and their relevance to the main research goal of this Thesis. Particularly, I discuss contributions to the neurobiology of cognitive deficits from both animal models of the disorder and studies in human patients. I will finish by providing an outline of the content and specific aims of the following chapters.

## **HISTORICAL PERSPECTIVE ON NF1**

Although descriptions in the literature that could fit the NF1 diagnosis go back to the 13<sup>th</sup> century (Morse, 1999), it was not until 1768 that the first convincing description of NF1 was reported by Mark Akenside (Akenside, 1768):

“ ... a man about three score years of age came to St. Thomas' Hospital. [...] [He]

had been accustomed during the greater part of his life to a constant succession of wens [tumours] that shot out in several places on his head, trunk, arms and legs: which indisposition he inherited from his father.”

However, only at 1882, NF1 was recognized as a disorder and characterized by von Recklinghausen (von Recklinghausen, 1882) on a report entitled “On multiple cutaneous fibromas and their relationship with multiple neuromas” (Wilkins and Brody, 1971; Crump, 1981):

“... it appears that these multiple neuromas and cutaneous fibromas existed simultaneously. It also appears that this was not a fortuitous combination, but rather that the tumours were related structurally [...] the evidence [...] is: 1) the nature of the neoplastic tissue in both types of tumour was almost identical, 2) nerve tumours penetrated the undersurface of the tumours of the skin and sometimes could be peeled out of them, and 3) the cutaneous fibromas presented an arrangement different from the usual multiple fibromatous neoplasms.” (von Recklinghausen, 1882; Wilkins and Brody, 1971).

Recklinghausen gave substantial contributions to the knowledge of the pathological condition by identifying its cutaneous and neurologic manifestations and by demonstrating its nervous origin. He was the first to connect the simultaneous appearance of fibromas and neuromas and he coined the term neurofibroma. On this basis, NF1 is also known as von Recklinghausen’s disease.

## CLINICAL FEATURES

NF1 is one of the most common genetic disorders affecting the human nervous system, occurring with an estimate incidence of 1 per 3500 individuals, independent of ethnicity, race and gender (Huson et al., 1988; Friedman and Riccardi, 1999).

The National Institute of Health Consensus Development Conference formulated the current diagnostic criteria, described in Panel 1, and also proposed the name neurofibromatosis type 1 (National Institutes of Health Consensus Development Conference Statement: neurofibromatosis, 1988).

NF1 is a multisystem disorder, with a wide variety of manifestations affecting the skin, eyes,

**Panel 1 – Diagnostic criteria for NF1 (as defined by the National Institutes of Health Consensus Development Conference Statement: neurofibromatosis., 1988)**

Two or more of the below criteria are required for diagnosis:

- Six or more café-au-lait macules (> 5 mm in diameter in children or > 15 mm in adolescents and adults)
- Two or more cutaneous or subcutaneous neurofibromas or one plexiform neurofibroma
- Axillary or groin freckling
- Two or more Lisch nodules (iris hamatomas)
- Optic pathway glioma
- A distinctive osseous lesion such as sphenoid wing dysplasia or thinning of the long bone cortex with or without pseudoarthrosis
- A first-degree relative with NF1

skeleton, the endocrine system, and blood vessels, as well as the central and peripheral nervous system.

Individuals with NF1 typically present the first manifestations of characteristic pigmentary abnormalities in childhood, including café-au-lait macules, skinfold freckling and Lisch nodules. Café-au-lait spots are local changes in the skin pigmentation that develop in virtually all patients and are usually noticeable at birth and invariably by age 3 years (Huson et al., 1988). Axillary and inguinal freckling is detected most frequently between 3 and 5 years of age (Korf, 2002). Additional sites for freckling include the area above the eyelids, around the neck and under the breasts (Huson et al., 1988). Lisch nodules are melanocytic iris hamatomas that do not affect vision (Huson et al., 1987). Characterization of histopathological and ultrastructural features of a Lisch nodule revealed that it was composed of three main cytotypes: pigmented cells, fibroblast-like cells and mast cells, showing a pattern similar to a neurofibroma (Richetta et al., 2004).

The neurofibroma is the most common tumor seen in individuals with NF1. It arises from the fibrous tissue surrounding peripheral nerve sheaths and is composed of Schwann cells, fibroblasts, perineural cells and mast cells (Gutmann et al., 1997). Neurofibromas manifest as benign, focal cutaneous or subcutaneous lesions, or plexiform tumours. Focal cutaneous or dermal neurofibromas typically appear in late childhood or

early adolescence and do not transform into malignant tumours. Plexiform neurofibromas arise from multiple nerve fascicles and tend to grow along the length of the nerve and often involve multiple nerve fascicles, branches and plexi (Korf, 1999). Individuals with NF1 have a lifetime risk of 8-13% of developing malignant peripheral nerve sheath tumours (MPNST), typically arising from pre-existing plexiform neurofibromas (Evans et al., 2002). MPNSTs are poorly responsive to conventional therapies, prone to metastasize and have a poor overall prognosis.

In children, the most common neoplasms apart from neurofibromas are gliomas, which occur in all parts of the brain but are more likely to appear in the optic pathways, brainstem and cerebellum (Korf, 2000; Sylvester et al., 2006; Ullrich et al., 2007). Within the gliomas, optic pathway gliomas are the most common and are found in ~15% of children with NF1, typically arising in the first decade of life (Listernick et al., 2007).

Several other features are often associated with NF1, including macrocephaly, short stature, at 10<sup>th</sup>–25<sup>th</sup> percentiles, scoliosis, headache, hyperintension, and T<sub>2</sub>-weighted signal intensity lesions on magnetic resonance imaging of the brain (Huson et al., 1989; Gutmann et al., 1997). Furthermore, 30-60% of the individuals with NF1 have learning disabilities (North et al., 1997; Hyman et al., 2005), with a significant impact on quality of life (North, 2000). The cognitive profile of patients with NF1 is discussed in the second part of the Introduction.

## GENETICS OF NF1

Linkage studies were able to identify the disease-causing gene in NF1 to chromosome 17 (Barker et al., 1987; Seizinger et al., 1987). Later, gene mapping identified the *NF1* gene at chromosome 17q11.2 and its protein product, neurofibromin (Cawthon et al., 1990b; Viskochil et al., 1990; Wallace et al., 1990).

The *NF1* gene is large, spanning over 350 kb of genomic DNA (Figure 1) (Marchuk et al., 1991) and can be classified as a tumour suppressor gene, since mutations in both alleles are detected in neurofibromas (Colman et al., 1995) and malignant tumours associated with NF1 (Legius et al., 1993; Shannon et al., 1994; Cichowski and Jacks, 2001). The gene contains 60 exons organized into four clusters, which are separated by four large introns (Li et al., 1995). Intron 27b contains three small unrelated genes, EV12A, EV12B and OMGP, each of which containing two exons (Cawthon et al., 1990a). These

genes are transcribed in the reverse orientation to the *NF1* gene and their role in regulating the *NF1* gene expression is presently unknown.

The *NF1* gene is ubiquitously expressed, in line with the diverse clinical manifestations of the disorder (Gutmann et al., 1991; Daston et al., 1992). However, the highest level of gene expression is seen in neural tissues, including neurons and glial cells (Daston et al., 1992). Additionally, *NF1* expression occurs across multiple brain systems including subcortical and cortical structures. In the cortex, expression spans all cortical layers, whereas in the striatum, is sparse, occurring in a pattern suggestive of interneuronal expression (Gutmann et al., 1995a).

The large size of the *NF1* gene may help explain the high incidence of mutations at

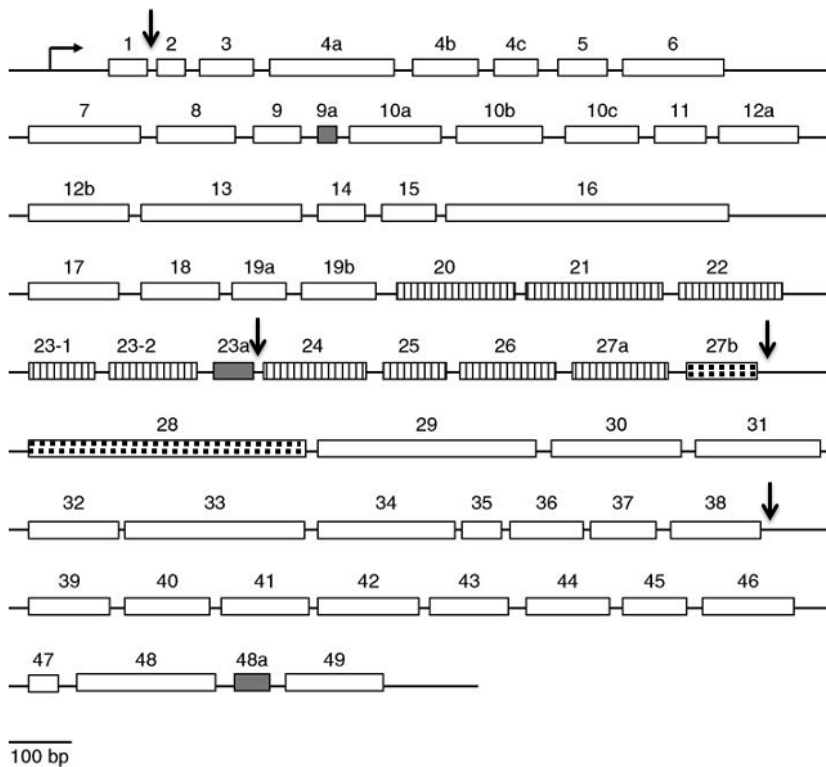


**Figure 1. Diagram of the *NF1* gene.** The arrow at the superior left corner represents the transcription start site. Exons are represented as rectangular boxes and the scale bar in the left corner indicates their size. The exons of the *NF1* Ras-GAP-related domain are striped and those of the Sec14 domain have a squared pattern. Alternatively spliced exons (9a, 23a and 48a) are filled in. Introns are not drawn to scale and the four large introns are marked with facing-down arrows. Adapted from Thomas and De Vries, 2009.

the NF1 locus. Indeed it has one of the highest mutation rates in humans (Fahsold et al., 2000) and approximately 50% of the patients with NF1 present new mutations without a family history of NF1 (Thomson et al., 2002). The disease is supposed to result from loss-of-function mutations because >80% of germline mutations described cause truncation of the gene product (Ars et al., 2000; Messiaen et al., 2000; Ars et al., 2003). Several types of mutations have been observed, including missense and nonsense mutations, small and large deletions, insertions, intronic changes affecting splicing, alterations of the 3' untranslated region of the gene and gross chromosomal rearrangements (Jett and Friedman, 2010). Individuals affected by NF1 are heterozygous for the mutation, as homozygous mutations appear to be lethal (Friedman and Riccardi, 1999).

### THE PROTEIN NEUROFIBROMIN AND ITS FUNCTIONS

The protein product of the *NF1* gene is neurofibromin (RefSeq: NP\_000258.1, UniProtKB P21359-2), a large protein with 2818 amino acids and a calculated molecular mass of 250-280 kDa (DeClue et al., 1991; Gutmann et al., 1991). Neurofibromin is a cytoplasmatic protein expressed in all tissues and cell lines examined. Is detected in human, rat, and mouse neurons, astrocytes, oligodendrocytes, Schwann cells, adrenal medullary cells, white blood cells and gonadal tissue (DeClue et al., 1991; Gutmann et al., 1991; Daston et al., 1992). During early embryonic development is ubiquitously expressed (Daston and Ratner, 1992; Baizer et al., 1993; Huynh et al., 1994; Gutmann et al., 1995a) and in adults the expression is highest in the nervous system and adrenal glands (Daston and Ratner, 1992; Daston et al., 1992; Golubic et al., 1992; Gutmann et al., 1995a).

Despite its large size, the function of neurofibromin is not clearly understood and a variety of mutations across the entire gene are associated with NF1 (Castle et al., 2003). To date, it is known to have two functional domains, Sec14 and RasGAP related domain (Trovo-Marqui and Tajara, 2006). Sec14-interactive domain (see Figure 1) is homologous to the yeast Sec14p, which is known to regulate intracellular proteins and lipid trafficking in yeast (Mousley et al., 2006). However, the biological role of Sec14 domain in NF1 is currently unknown, although structural studies seem to support its role in lipid binding (Welti et al., 2011). The RasGAP domain (see Figure 1), allows neurofibromin to act as a Ras-GAP (GTPase activating protein) protein to negatively regulate Ras signal-



ling (Martin et al., 1990; Weiss et al., 1999), while it can also influence the adenylyl cyclase pathway, as observed in the fruit fly (*Drosophila melanogaster*) and mice (Tong et al., 2002; Dasgupta et al., 2003).

The Ras protein belongs to a large super-family of low-molecular weight G-proteins, known as GTPases, which mediate signalling from membrane receptor to intracellular cascades of kinases. Ras GTPases promote the hydrolysis of active Ras-GTP to inactive Ras-GDP (Bernards and Settleman, 2004).

In NF1, haploinsufficiency resulting in reduced levels of functional neurofibromin leads to enhanced activation of Ras, which in turn hyperactivates the cascades of downstream signalling pathways, including those that involve mitogen-activated protein kinase (MAPK)/ERK (MEK), phosphatidylinositol 3-kinase (PI3K), protein kinase B (PKB) and mammalian target of rapamycin (mTOR) kinase (see Figure 2). MEK activates members of the extracellular signal-regulated kinase (ERK), which then phosphorylates a variety of targets. A number of these signals are then transmitted to the nucleus, regulating the expression of genes controlling cell proliferation, cell death, differentiation and migration (see Trovo-Marqui and Tajara, 2006 for a comprehensive review). mTOR functions involve the regulation of cell growth, proliferation and motility as well as signal integration from different pathways important for controlling cellular processes (Raught et al., 2001; Hay and Sonenberg, 2004; Dasgupta et al., 2005; Johannessen et al., 2005).

Neurofibromin also holds a microtubule association function (Gregory et al., 1993), which is relevant for the integrity of neuronal axonal and dendritic projections and consequently to signal transduction and neuronal connections.

Collectively, these findings argue that alterations in neurofibromin function may affect different intracellular signalling pathways in specific cell types.

To complicate matters further, neurofibromin has five isoforms (II, 3, 4, 9a and 10a-2), arising from the four alternatively splicing exons (9a, 10a-2, 23a and 48a) (Figure 1) (Gutmann et al., 1995b; Gutmann et al., 1999), with varied functional roles and exhibiting differential expression in distinct tissues. Neurofibromin type II is an isoform to which a functional role has been established. It results from the insertion of exon 23a and has a reduced GAP ability (Andersen et al., 1993; Gutman et al., 1993) and loss of association with microtubules (Gutmann et al., 1995b). This isoform was proven to be relevant for cognition, as mice lacking exon 23a presented learning deficits with no elevated tumour predisposition (Costa et al., 2001). This indicates a critical role of the

GAP domain in modulating learning and memory. Although type I and II isoforms appear to be ubiquitously expressed in the brain, type I is the major form expressed by neurons, whereas type II is mainly expressed in glial cells (Gutmann et al., 1995a).

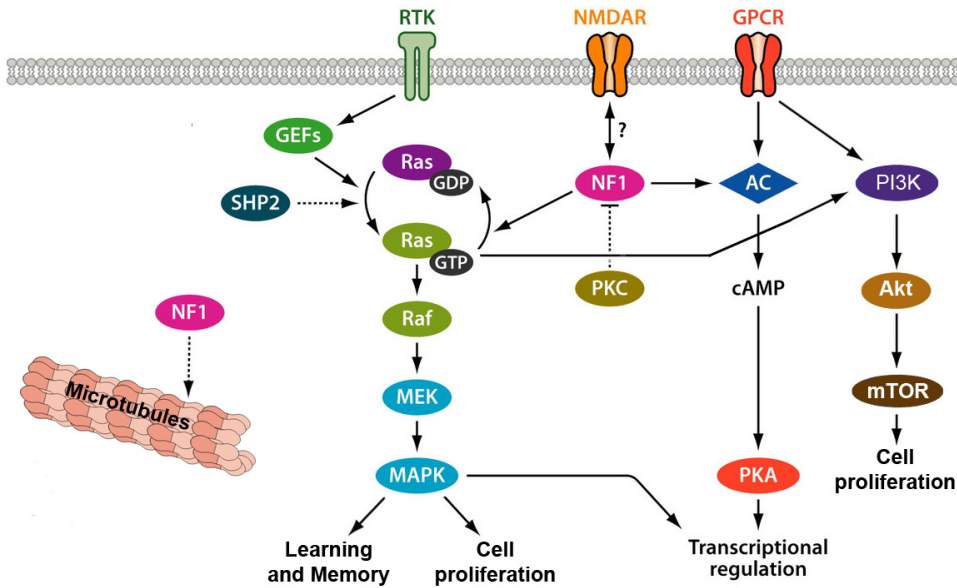


**Figure 2. Interactions of neurofibromin (NF1) with different cell signaling pathways.** NF1 is a GTPase activating protein (GAP) that negatively regulates Ras-MAPK signaling cascade. The GAP function of NF1 can be counteracted by guanine-nucleotide exchange factors (GEFs). NF1 also acts as an activator of adenylate cyclase (AC) and the phosphatidylinositol 3-kinase (PI3K)-AKT-mTOR cascade. Some of these signals are then transmitted to the nucleus, regulating the expression of genes controlling cell proliferation, cell death, differentiation and migration. NF1 also holds a microtubule association function. Arrows and barred lines indicate activation and suppression, respectively. MEK, mitogen-activated protein kinase or extracellular signal-regulated kinase; NMDAR, N-methyl-D-aspartate receptor; GPCR, G protein-coupled receptor; RTK, receptor tyrosine kinase; PKA, protein kinase A; PKC, protein kinase C; SHP2, Src homology 2-containing tyrosine phosphatase; AKT, serine/threonine protein kinase, mTOR, mammalian target of rapamycin. Adapted from Shilyansky et al., 2010a.

## THE VARIATION OF PHENOTYPES IN NF1 OR THE HARD TASK OF FINDING GENOTYPE-PHENOTYPE CORRELATIONS

In NF1, there is complete genetic penetrance but variable expressivity. This means that all the individuals with NF1 carrying a disease-causing allele, express the disease phenotype, however, the degree to which the genotype is phenotypically expressed varies among individuals.

In this regard, the highly variable clinical expressivity observed in NF1 is manifested by marked inter- and intra-familial variation in both the number of major features and the occurrence of complications (Ward and Gutmann, 2005). Accordingly, it has been difficult to establish correlations between specific mutation and clinical presentations (Castle et al., 2003). In general, no solid correlation was observed between the type of mutation and a distinctive phenotypic expression of the disease. Exceptions to this are the patients with a NF1 microdeletion, who have earlier onset of neurofibromas, profound developmental delays and distinctive facial features (Tonsgard et al., 1997; Upadhyaya et al., 1998), and also a substantially higher lifetime risk for the development of MPNSTs (De Raedt et al., 2003).

Contributing to the low number of known genotype-phenotype correlations is the fact that, on one hand, mutational analysis has proven to be difficult due to the large size of the gene, the occurrence of mutations in nearly every exon, the presence of pseudogenes in other chromosomes, and the great variety of possible mutations. On the other hand, variable phenotypes can be caused by several factors including modifier genes (Easton et al., 1993; Sabbagh et al., 2009), environmental factors, and complex genetic and environmental interactions.

Despite the difficulties to identify genotype-phenotype correlations, patients that participated in the studies presented in this thesis were genotyped for the NF1 gene. Genotyping allows a better characterization of the NF1 population studied and the identification of the disease causing mutations. In fact, we were able to show that the NF1 mutation type significantly predicted cortical  $\gamma$ -aminobutyric acid (GABA) levels in the visual cortex of our cohort of patients, and thereby succeeded in identifying a genotype-phenotype correlation.

## COGNITIVE PROFILE OF PATIENTS WITH NF1

The most common neurological complication of NF1 in childhood is cognitive impairment, which does not seem to resolve in adulthood (North et al., 1997; Hyman et al., 2005) and has significant impact in quality of life (North, 2000). In spite of the plethora of studies investigating cognition in NF1, there is not a general consensus regarding the exact cognitive profile (Levine et al., 2006). This might reflect in part methodological differences regarding the variety of comparison groups used (unaffected siblings or unrelated controls), controlling or not for intelligent quotient (IQ) or including children with brain tumours.

Typically, studies report IQs in the low-average range as compared with siblings, controls and norms (as reviewed by Levine et al., 2006). However, mental retardation (IQ < 70) occurs only in 4 - 8% of the NF1 population (North, 2000). The reported frequency of learning disabilities is high and ranges between 30-65% (Ozonoff, 1999).

Learning disabilities constitute an umbrella term applied to define a significant discrepancy between *ability* (intellect) and *achievement* in a specific domain (Kronenberger and Dunn, 2003). The Diagnostic and Statistical Manual of Mental Disorders, Fourth Edition (DSM-IV) divides learning disabilities into five main categories: reading disorders, mathematical performance disorders, disorders of written expression, nonverbal learning disorders, and learning disorders not otherwise specified. In general, neuropsychological evaluation has identified deficits in the NF1 population involving visuospatial, executive function, motor, language and memory domains. Therefore, a single learning disability category is insufficient to describe the NF1 phenotype.

Visuospatial deficits are considered one of the hallmark characteristics of the NF1 cognitive profile, and the most common impairment is observed in the judgment of line (JLO) test (Eldridge et al., 1989; Dilts et al., 1996; Hyman et al., 2005; Levine et al., 2006; Clements-Stephens et al., 2008; Ribeiro et al., 2012). Indeed, visuospatial performance represents a strong predictor of NF1 diagnosis and the pattern of performance on a set of visuospatial measures was able to identify 90% of over 100 children and adolescents with NF1, providing a strong predictor of diagnosis (Schrimsher et al., 2003). Nevertheless, from the four visuospatial/motor tests used by the authors (JLO, BlockDesign subtest of the Wechsler Intelligence Scale for Children-third edition (WISC-III), the Recognition-Discrimination Test, and the Beery Visual-Motor Integration Test), the JLO alone had essentially the same discriminative outcome as the multivariate combination of all the other tests in terms of correctly classifying NF1 cases. In agreement

with this observation, Levine et al (2006) pointed out that other tasks used to assess visuospatial function do not present the same degree of impairment, and tasks requiring recognition of complex objects are matched between NF1 and control groups. In addition, there is evidence suggesting that the visuospatial deficits observed in the JLO test might be linked to executive functions. In particular, NF1 affects planning, working memory, cognitive flexibility and inhibitory control (Descheemaeker et al., 2005; Rowbotham et al., 2009; Huijbregts et al., 2010). Furthermore, there is a high comorbidity (~50%) between NF1 and attention deficit hyperactive disorder (ADHD) (Koth et al., 2000; Rosser and Packer, 2003), which is commonly associated with deficits in executive function. Besides visuospatial and executive function, motor coordination is also frequently impaired in NF1 (Feldmann et al., 2003; Levine et al., 2006; Huijbregts et al., 2010).

Patients with NF1 also show aspects of verbal learning deficits, particularly in expressive and receptive language, vocabulary, visual naming and phonological awareness (Ozonoff, 1999; Levine et al., 2006).

## **BRAIN STRUCTURAL AND FUNCTIONAL NEUROIMAGING CONTRIBUTIONS TO UNDERSTAND THE NF1 COGNITIVE PROFILE**

### **Neuroanatomy**

The most evident brain structural alteration observed in NF1 is macrocephaly, which occurs in approximately 50% of children with this condition (North et al., 1994; Van Es et al., 1996). Macrocephaly is defined as a head circumference greater than the 95<sup>th</sup> percentile. The commonest cause for macrocephaly is megalencephaly, i.e. larger brain volume (Steen et al., 2001). There is no known association between macrocephaly and neuropsychological function in NF1 and there is still a debate on the structures contributing to this enlargement and their impact on cognitive function (Payne et al., 2010).

The neuroimaging studies performed so far can be divided between volumetric measurements of overall grey matter and white matter tissues (Said et al., 1996; Steen et al., 2001) and studies that included brain parcellation to identify regions with abnormal volume (Moore et al., 2000; Cutting et al., 2002b; Greenwood et al., 2005). The majority of these studies points to macrocephaly being caused by increased white matter (Said et al., 1996; Steen et al., 2001) or a combination of white and grey matter

(Cutting et al., 2002a; Greenwood et al., 2005).

The most consistent structural finding across studies is an enlargement of the corpus callosum in patients with NF1 (Kayl et al., 2000; Moore et al., 2000; Dubovsky et al., 2001; Steen et al., 2001; Cutting et al., 2002b; Wignall et al., 2010). The corpus callosum is the major commissural structure in the human brain and it connects the left and right cerebral hemispheres. Its principal function is to facilitate interhemispheric communication and transfer motor, sensory, and cognitive information between the hemispheres. Other brain structure anomalies observed included increased brainstem growth rate, suggestive of abnormal cell proliferation (DiMario et al., 1999) and smaller surface area and grey matter volume of the left *planum temporal* of NF1 boys compared with controls (Billingsley et al., 2002).

It is clear that the study of neuroanatomy in NF1 has a lot to gain from recent methodological advances, which can provide information on the composite dimensions of the cortex (volume, thickness and surface area) and additional morphometric parameters. Moreover, the application of powerful statistical methods to brain imaging data can aid in the identification of structures that contain information to distinguish patients from controls without an *a priori* hypothesis. Recently, our group employed a multivariate statistical pattern analysis to classify whole-brain anatomical images. We were able to reveal the existence of brain structural differences in grey matter and white matter tissue that could accurately discriminate individuals with NF1 from controls (Duarte et al., 2012). The statistical map provided by the classifier showed spatially distributed clusters enclosing a number of regions, thus providing strong indications for localized abnormalities in patients with NF1. Those regions included the hippocampus, basal ganglia, thalamus, and occipital cortex.

Attempts to find relationships between structural alterations and cognitive function did not result, so far, on any firm conclusions. However, there is some evidence that grey matter properties influence cognitive function (Said et al., 1996; Moore et al., 2000; Steen et al., 2001).

Besides morphometric and volumetric studies, there are several reports of altered white matter microstructure as investigated using diffusion tensor imaging (DTI) (Sheikh et al., 2003; Zamboni et al., 2007; van Engelen et al., 2008; Ferraz-Filho et al., 2012). This technique can reveal microscopic details about tissue architecture by probing water molecule diffusion patterns (Schaefer et al., 2000; Hagmann et al., 2006). Two main parameters can be determined from diffusion-weighted MRI data: the apparent diffusion

coefficient (ADC), which indicates the degree of diffusion of water molecules, and fractional anisotropy (FA), that describes the degree of anisotropy of a diffusion process. Low FA values indicate that diffusion is isotropic, i.e. it is unrestricted in all directions, this typically occurs in the cerebrospinal fluid (CSF). High values of FA indicate that diffusion occurs mainly according to one axis and is restricted along other directions, which is seen for white matter fibers.

Despite of the fact that there is no published DTI study on the context of cognitive function, alterations in white matter microstructure of the thalamus were consistently found (Zamboni et al., 2007; van Engelen et al., 2008; Ferraz-Filho et al., 2012). The thalamus is a highly interactive structure, with widespread connections to multiple cortical regions, that provides selection and transformation of different sensory inputs to the cortex. The various nuclei of the thalamus are involved in the integration of sensory and motor information, memory and executive functions (Schmahmann and Pandya, 2008), competences in which NF1 patients show disabilities (Hyman et al., 2005; Levine et al., 2006; Roy et al.). Moreover, patients with NF1 presented significantly reduced FA values and/or elevated ADC of several other anatomical brain locations, including brain stem, cerebellar white matter, basal ganglia, corpus callosum, and frontal and parietal white matter regions (Zamboni et al., 2007; van Engelen et al., 2008). Given the importance of white matter integrity to efficient information transit, alterations in white matter microstructure and structural connectivity could have significant contributions to impaired cognition (Nagy et al., 2004).

### **Unidentified bright objects**

Neuroimaging studies applying magnetic resonance imaging (MRI) identified focal areas of hyperintensity on  $T_2$ -weighted images. Those have a frequency of 55-90% in childhood (Payne et al., 2010) and commonly occur in the basal ganglia, cerebellum, thalamus, brain stem and subcortical white matter (Van Es et al., 1996; Lopes Ferraz Filho et al., 2008). These lesions are isointense on  $T_1$ -weighted images and are not visible on computed tomographic scans, they exert no mass effect, there is no surrounding oedema and they do not enhance with contrast. These hyperintensities are often referred as unidentified bright objects (UBOs) to reflect their mysterious nature. A neuropathologic autopsy study of MRI-confirmed UBOs in NF1 demonstrated an atypical astrocytic infiltrate with areas of microscopic fluid-filled vacuoles (DiPaolo et al., 1995). Although it was initially thought that UBOs resolved with age, a prospective study involving a large

number of patients showed that the natural history of these lesions is more complex than initially envisioned (Gill et al., 2006). Their disappearance seems to depend on their location; with UBOs in the basal ganglia, thalamus, brainstem and cerebellum regressing with age, while those in cerebellar cortex and deep white matter not.

The high frequency of UBOs in NF1 leads to the hypothesis that these lesions might be associated with the cognitive profile. This relationship has been studied with several approaches focusing on the presence, location, number of locations, and/or volume of UBOs (see North, 2000; Levine et al., 2006 for a review). However, the results are not consensual. In terms of IQ, evidence suggests that patients with NF1 and UBOs have lower IQs than patients without UBOs (Hofman et al., 1994; North et al., 1994; Feldmann et al., 2003; Hyman et al., 2003; Chabernaude et al., 2009), however this was not reproducible across all studies (Duffner et al., 1989; Dunn and Roos, 1989; Ferner et al., 1993; Legius et al., 1995). More detailed studies focusing on the impact of UBOs on specific locations have observed that their presence in thalamic (Moore et al., 1996; Hyman et al., 2007) or thalamo-striatal (Goh et al., 2004; Chabernaude et al., 2009) structures negatively influence cognitive performances. Future studies should discern the role of UBOs on cognitive impairment and establish whether they constitute a causal relation. For now, there is no sufficient clear evidence that UBOs can predict cognitive deficits in NF1.

### **Functional neuroimaging studies**

A more complete understanding of the neural correlates underlying the cognitive deficits requires methods that can assess functional activity. However, there are very few functional (f) MRI studies in patients with NF1.

The first fMRI study in NF1 focused on phonological processing (Billingsley et al., 2003b), a core component of reading. Participants performed two phonologic processing tasks, an auditory and an orthographic task, and they were required to determine whether two pronounceable nonsense words rhymed. In the auditory task, patients with NF1 revealed greater activation than controls in the inferior frontal cortex, middle temporal and parietal regions. However, patients also showed reduced activation of dorso-lateral prefrontal cortical areas, relative to posterior (temporal, parietal, and occipital), in comparison with controls. This pattern, was found to be similar to the one observed in dyslexic patients by Shaywitz and colleagues (Shaywitz et al., 1998). However, while the pattern of neural deficits in dyslexia is also characterized by decrease activity of the left



hemisphere, the opposite pattern was seen in NF1, with greater underactivation of the right hemisphere. Concerning the written task, patients with NF1 displayed relatively less frontal compared with posterior activity, a pattern opposite to the one observed with the auditory task. The authors interpreted this variation in the patterns of regional activity between tasks as a reflection of compensatory neural recruitment, due to either inefficient or dysfunctional neural networks, particularly of the frontal lobe.

Two studies have investigated the neural correlates of visuospatial processing in NF1 (Billingsley et al., 2004; Clements-Stephens et al., 2008). Billingsley et al presented alphanumeric stimuli in either their conventional form, inverted or rotated (Billingsley et al., 2004). Participants were asked to respond if the stimulus presented was a letter or a number. Patients relied to a greater degree than controls on posterior cortex (including occipital, parietal, and middle temporal cortices), relative to lateral and inferior frontal regions. This pattern was related to patients' behavioural performance on the task. The authors hypothesized that the increase in posterior activity may reflect a compensatory mechanism for deficient frontal activation, which could be related to morphological abnormalities in the inferior frontal areas observed in a previous study (Billingsley et al., 2003a). Clement-Stephens *et al* conducted a study using an adaptation of the judgment of line orientation task (Clements-Stephens et al., 2008). The authors reported that subjects with NF1 relied more on left than right hemisphere structures for task completion, while controls did the opposite. This left hemisphere dominance for visuospatial processing suggests that visuospatial problems occur due to inefficient right hemisphere network. Moreover, this pattern was accompanied by an unexpected underactivation of the primary visual cortex in NF1, while parietal regions did not present between-group differences.

A more recent study assessed working memory in humans and mice (Shilyansky et al., 2010b). Two visuospatial working memory tasks were applied to human subjects: 1) a spatial working memory maintenance and manipulation task (task 1), and 2) a parametric spatial working memory capacity task (task 2). In both tasks subjects were shown an array of dots. In task 1, subjects had to either hold the array as it was or flip it across the horizontal axis. After a fixed delay, subjects were shown a probe array and were asked to determine if the probe was in the same position as the previously shown array (maintenance condition) or corresponded to the flipped array (manipulation condition). In task 2, the difficulty of the task increased parametrically, as subjects were shown an array of one, three, five or seven dots. After a delay, subjects were shown a single

probe circle and were asked to determine if the probe was in the same position as one of the target circles. Authors performed a region-of-interest analysis, involving frontal (dorsolateral prefrontal cortex, frontal eye fields), parietal and striatal regions (caudate and putamen) (Shilyansky et al., 2010b). Individuals with NF1 performed significantly worse than controls in both tasks. In task 1, significantly reduced activation in patients compared with controls was observed in frontal, parietal and striatal brain regions, while in task 2 differences were observed only for frontal and parietal regions. Furthermore, the neural activation in the right dorsolateral prefrontal cortex was significantly correlated with patients' performance in both tasks. Interestingly, during task 2, patients with NF1 showed impaired deactivation of the medial prefrontal cortex when compared to controls. This region belongs to the brain default mode network, which is composed by a set of regions that are active during task irrelevant thoughts (McKiernan et al., 2003), and deactivate during performance of cognitively demanding tasks (Shulman et al., 1997; Raichle et al., 2001; McKiernan et al., 2003). This study points once more to frontal impairments in patients with NF1.

Unfortunately, none of these studies performed whole-brain between-groups comparisons, being limited to the investigation of activity in a priori defined regions. This approach has the disadvantage of limiting the overall identification of the functional networks involved in task completion. Importantly, fMRI can also be used to monitor response to therapy at the level of brain functional connectivity, as performed as a part of an ongoing clinical trial on NF1 (Chabernaude et al., 2012).

### **Other evidences of regional brain alterations**

Positron emission tomography (PET) constitutes an additional valuable tool to study metabolism and can identify patterns of abnormal brain activity. Studies employing radiotracers of glucose observed altered metabolism of the thalamus in patients with NF1 (Kaplan et al., 1997; Buchert et al., 2008), indicating that this structure could be of potential relevance for the NF1 cognitive phenotype. Moreover, decreased levels of the neuronal marker N-acetylaspartate were observed using magnetic resonance spectroscopy (Wang et al., 2000), indicating either neuronal loss or neuronal dysfunction.

## STUDIES ON ANIMAL MODELS OF NF1

Genetic manipulations in animal models have provided important insights to study and improve our understanding of human genetic diseases. A variety of models capturing different features of the disease can be used to understand the complexity of the human disorder. In that sense, several NF1 models were developed using mice, the fruit fly (*Drosophila melanogaster*) and zebrafish.

Regardless of the species being studied, neurofibromin is involved in cognitive processes and neural development. Even so, it is important to keep in mind that the biological consequences of the alterations seen in animal models might not be conserved across species.

### Mice models

The main mice model applied to study NF1 bears a heterozygous null mutation in the *Nf1* gene (*Nf1*<sup>+/-</sup>) (Jacks et al., 1994), whereas homozygous *Nf1*<sup>-/-</sup> mice die in utero, as a result of a cardiac anomaly (Brannan et al., 1994).

Although *Nf1*<sup>+/-</sup> mice do not develop neurofibromas, the hallmark feature of NF1, they are cancer prone and the behavioural phenotype shows a pattern that is reminiscent of the human cognitive manifestations. Impairments in memory, attention and visuospatial domains have been successfully recapitulated by the mice models (Shilyansky et al., 2010a). Furthermore, studies employing the *Nf1*<sup>+/-</sup> mice, as well as, conditional mutants contributed extensively to identify the cellular and molecular mechanisms that underlie the cognitive and behavioural changes associated with NF1. Conditional mutants were created using the Cre-loxP system, which enables gene deletions to specific time frames, cell types, or areas (Gu et al., 1994).

Overall, *Nf1*<sup>+/-</sup> mice and a number of other *Nf1* mutants, showed impairments in spatial memory and learning in the hidden version of the Morris water maze, which were reversed by increasing the training trials (Silva et al., 1997; Costa et al., 2001; Costa et al., 2002; Li et al., 2005; Cui et al., 2008). The Morris water maze is a test sensitive to hippocampal function (Morris et al., 1982) and long-term potentiation (LTP) mechanisms (Moser et al., 1998). Furthermore, the *Nf1*<sup>+/-</sup> mice also have working memory (Shilyansky et al., 2010b) and attention deficits (Li et al., 2005).

The first key finding contributing to understand learning deficits in mice came from the study of Costa *et al* (2001), where authors related increased Ras signalling with im-

paired learning. Further developments arose from studying LTP to determine whether changes in synaptic plasticity account for the hippocampal related functional deficits observed in mice (Costa et al., 2002). The LTP deficits were revealed by theta-burst stimulation but not high-frequency stimulation indicating that the LTP deficits were more sensitive to alterations in GABA-mediated inhibition. Taking into account this evidence and to further identify cell-type physiological effects, Cui *et al* (2008) developed a series of Cre-LoxP mice to limit neurofibromin heterozygosity to specific brain cell types. They observed that *Nf1* expression in interneurons seems to be critical for behaviour, whereas its role in pyramidal neurons or glia do not alter performance in the Morris water maze and is therefore nonessential for hippocampal learning. Furthermore, it was determined that increased inhibition was related to increase in miniature inhibitory postsynaptic potentials (mIPSPs) frequency as a result of *Nf1* heterozygosity in inhibitory neurons, linking neurofibromin to GABAergic neurotransmission. In turn, increased frequency of mIPSPs was attributable to higher levels of GABA release as a consequence of increased phosphorylation of synapsin 1, a protein with a critical role in the regulation of neurotransmitter storage and release (Hilfiker et al., 1999). Glutamatergic neurotransmission does not seem to be affected, suggesting a shift in the balance between inhibitory and excitatory processes within hippocampal networks. Recently, it was shown that spontaneous IPSPs are also increased in the prefrontal cortex and striatum of the *Nf1*<sup>+/-</sup> mice (Shilyansky et al., 2010b). Overall, these results suggest that neurofibromin may be part of a general feedback mechanism that adjusts the rate of GABA release to match the level of synaptic activity. Inadequate GABA release during high levels of synaptic activity might lead to erroneous synaptic strengthening and learning deficits.

The learning, memory and attention deficits in the *Nf1*<sup>+/-</sup> mice could be rescued by two methods: 1) Reducing of Ras/MAPK activity, as shown by the use of *Nf1*/*Ras* double mutants (*Nf1*<sup>+/-</sup>/*Kras*<sup>+/-</sup>) or farnesyl transferase inhibitors, as lovastatin, that pharmacologically decrease levels of Ras signalling (Costa et al., 2002; Li et al., 2005). 2) Reducing GABAergic neurotransmission. GABA<sub>A</sub> receptor antagonist, picrotoxin, was able to rescue behavioural deficits associated with impaired hippocampal function (Cui et al., 2008) and working memory (Shilyansky et al., 2010b).

Another cognitive domain that has been studied in the animal model is attention. A recent contribution to this subject came from the study of Brown *et al* (2010). Authors used an *Nf1*<sup>+/-</sup> mutant with a complete loss of the *Nf1* gene in GFAP expressing glial cells (*Nf1* OPG mouse) to gain insight into the attention abnormalities seen in children

with NF1. The mice presented non-selective and selective attention deficits (as measured by the frequency of rearing in response to a novel environment) without an accompanying hyperactivity phenotype. This behavioural pattern is the consequence of reduced dopamine levels in the striatum, which is normalized following either methylphenidate or L-dopa administration (Brown et al., 2011).

Given the complex reciprocal modulation of neural transmission, particularly between dopamine, GABA and glutamate, it is probable that an interplay between these neurotransmitters contribute to the cognitive deficits observed in NF1.

Besides the cellular and molecular alterations discussed, studies in the *Nf1* mice also provide relevant information to understand the impact of altered structure in brain function. Particularly, it was shown that mice lacking neurofibromin in the majority of cortical neurons and astrocytes fail to form cortical barrels in the somatosensory cortex, demonstrating a role for neurofibromin in cortical development (Lush et al., 2008).

### ***Drosophila* and zebrafish models**

The fruit fly, *Drosophila melanogaster* has been extensively used as a genetic model to study the neural mechanisms underlying learning and memory deficits. In part because of its rapid generation time, comparatively low cost, and vast battery of genetic and transgenic capabilities available (Gatto and Broadie, 2011). *Drosophila Nf1*-null mutants are viable, fertile, and normally patterned, but display a 15%–20% size reduction (The et al., 1997) and lack a circadian rest–activity rhythm (Williams et al., 2001).

In the *Drosophila*, *Nf1* is involved in both Ras-dependent and cAMP-dependent pathways interacting with the rutabaga (*rut*) gene encoding adenylyl cyclase (AC). Neurofibromin activation of the Rut/AC pathway is an essential component of *Drosophila* learning and memory functions (Guo et al., 2000). Introduction of human *NF1* into the *Drosophila* disease model revealed distinct functional domains of *NF1*. The GAP-related domain was necessary for long-term memory, while the C-terminal for immediate memory (Ho et al., 2007). Recently, it was shown that *Nf1* is required in the operational phase of memory acquisition, but not for stabilization and maintenance (Buchanan and Davis, 2010).

The circadian defect is partially restored by mutations that attenuate Ras signalling (Williams et al., 2001). However, the other analyzed phenotypes are Ras-insensitive. Instead, they are suppressed by decreasing the activity of the cAMP/PKA signalling pathway (Guo et al., 1997; The et al., 1997; Guo et al., 2000).

A zebrafish model of NF1 was recently developed with the purpose to elucidate novel developmental functions of neurofibromin (Padmanabhan et al., 2009). Zebrafish has two genes, *nf1a* and *nf1b* highly similar to NF1 at the amino acid level (90.4% and 90.7%, respectively). Knockdown of the *nf1* genes results in cardiovascular and neural abnormalities in embryos and increased tumorigenesis (Shin et al., 2012). Furthermore *nf1*-null larvae seem to have motor and learning deficits (Shin et al., 2012).

## PHARMACOLOGICAL THERAPIES

Pharmacological therapies to treat the cognitive deficits in patients with NF1 have been inspired by findings in mice models. Researchers have shown that neurofibromin regulates Ras/MAPK signalling presynaptically and deficits in neurofibromin result in augmented GABA release (Costa et al., 2002; Cui et al., 2008) causing learning deficits. If this mechanism translates to the human disorder it would be theoretically possible to reverse learning deficits by either decreasing Ras signalling or GABA activity.

Picrotoxin is a drug that blocks the binding of GABA to its receptors and at sub-convulsant doses reversed LTP and learning deficits on the *Nf1<sup>+/-</sup>* mice (Cui et al., 2008). However, this is an analeptic drug with potential to cause seizures and there is little quantitative information on the effects of picrotoxin in humans. Furthermore, approximately 6% of the individuals with NF1 have epilepsy (Korf et al., 1993), making this group of patients unsuitable to receive this treatment. Moreover, the prominent role of GABA in the central nervous system (Owens and Kriegstein, 2002) might lead to non-specific consequences while there are also uncertainty relatively to the long-term effects of chronic drug use. Concerns raised by the use of GABA antagonists and the sparse information of their effects in humans make pharmacological manipulations of the Ras-MAP-kinase pathway an alternative choice for clinical trials. Particularly, the FDA-approved drug lovastatin, conventionally used for lowering cholesterol levels. Lovastatin decreases the activation of Ras and can reverse LTP and learning impairments of the *Nf1<sup>+/-</sup>* mice (Li et al., 2005).

Pharmacological therapies can additionally be applied to treat attention deficits in children. Studies in a *Nf1* mice showed that attention abnormalities are a consequence of reduced dopamine levels in the striatum, which is normalized by methylphenidate or L-dopa administration (Brown et al., 2011). Moreover, attention deficits in the *Nf1<sup>+/-</sup>*

mice were also rescued by lovastatin (Li et al., 2005). These data suggests that agents that normalize abnormalities in either Ras signalling or dopamine homeostasis, might be potentially used to treat attention deficits in NF1.

The first targeted therapeutic intervention trial in children with NF1 employed an analogue of lovastatin, simvastatin (Krab et al., 2008). The results of this clinical trial indicated that simvastatin did not improve cognitive function in children with NF1 (Krab et al., 2008). In consequence, another clinical trial was set up using lovastatin. Early reports showed improvements exceeding those of test-retest or practice effects limited to some participants in areas of verbal and nonverbal memory at phase I studies (Acosta et al., 2011). Two additional multicenter double-blind placebo control clinical trials, targeting cognitive deficits in NF1, are currently ongoing (NCT00352599, NCT00853580). Results concerning these clinical trials have not yet been disclosed.

## **AIMS AND OUTLINE OF THE THESIS**

As a single gene disorder, NF1 bears an enormous potential for establishing genetic, neurochemical and brain-behaviour relationships, constituting a relevant model to elucidate the neural mechanisms underlying cognitive impairment in neurodevelopmental disorders.

In *Chapter 1*, the genetics and pathophysiology of the disorder were presented. Genetic alterations in the *NF1* gene disrupt the normal trajectory of neural development in complex ways resulting in a heterogeneous pattern of cognitive and behavioural phenotypes. The cognitive pattern of dysfunction has been extensively examined at the behavioural level, now it remains to be determined the biological mechanisms contributing to the observed phenotype in patients.

The aim of this thesis is to provide new insights into brain structure, function and neurochemical alterations in NF1 that might contribute to identify the aetiology of the cognitive deficits observed in the disorder. This identification of physiological alterations is critical to understand the pathogenesis and find adequate treatments.

In order to explore physiological alterations in the human brain appropriate methodologies are required. Magnetic resonance is a suitable technique as it provides *in vivo*

and non-invasively multidimensional neurological information. *Chapter 2* provides an overview of the fundamentals of magnetic resonance for the study of brain structure, functional activation and neurochemistry that were applied in this thesis.

*Chapter 3* describes the participant's recruitment and selection criteria and the protocols followed for participants' characterization, and overviews the research timeline followed in the course of this work.

The following chapters are presented as individual self-standing contributions. Therefore, each chapter has its own methodology and results sections.

*Chapter 4* describes a study using functional magnetic resonance imaging (fMRI) to test whether information processing in early visual cortical areas is impaired. This study provides the first fMRI study on basic visual processing deficits in children, adolescents and adult patients with NF1. Previous fMRI studies have focused on higher order cognitive mechanisms (i.e. phonological processing, visuospatial processing and working memory). However, it is crucial to assess whether sensory deficits are present in patients with NF1, namely early visual processing deficits, as they can contribute to the poor performance of individuals with NF1 in visuospatial tasks. Moreover they can play a role in impaired function of higher order cognitive mechanisms (Doniger et al., 2002; Dias et al., 2011).

Inspired by studies in NF1 mice models indicating that the balance between excitation and inhibition is altered due to increased GABAergic neurotransmission, we sought to translate this hypothesis to the human disorder. Therefore, in *Chapter 5*, magnetic resonance spectroscopy (MRS) was applied to measure GABA levels in children and adolescents with NF1.

In order to understand how mutations in the NF1 gene impact brain structure it is also essential to characterize in detail the brain structural abnormalities in patients with NF1. *Chapter 6* adds to the present knowledge on structural brain alterations in children with NF1 by investigating the volume of subcortical structures and the composite dimensions of the cortex, through the analysis of cortical volume, cortical thickness, cortical surface area and gyrification.

Finally, the overall results are discussed in *Chapter 7* with the objective of providing a comprehensive and integrative view of the different studies developed in this thesis and its conclusions.



## REFERENCES

- Acosta MT, Kardel PG, Walsh KS, Rosenbaum KN, Gioia GA, Packer RJ. Lovastatin as treatment for neurocognitive deficits in neurofibromatosis type 1: phase I study. *Pediatr Neurol.* 45:4 (2011) 241-245.
- Akenside M. Observations on cancers. *Med Trans Coll Phys Lond.* 1:(1768) 64-92.
- Andersen LB, Ballester R, Marchuk DA, Chang E, Gutmann DH, Saulino AM, Camonis J, Wigler M, Collins FS. A conserved alternative splice in the von Recklinghausen neurofibromatosis (NF1) gene produces two neurofibromin isoforms, both of which have GTPase-activating protein activity. *Mol Cell Biol.* 13:1 (1993) 487-495.
- Ars E, Serra E, Garcia J, Kruyer H, Gaona A, Lazaro C, Estivill X. Mutations affecting mRNA splicing are the most common molecular defects in patients with neurofibromatosis type 1. *Hum Mol Genet.* 9:2 (2000) 237-247.
- Ars E, Kruyer H, Morell M, Pros E, Serra E, Ravello A, Estivill X, Lazaro C. Recurrent mutations in the NF1 gene are common among neurofibromatosis type 1 patients. *J Med Genet.* 40:6 (2003) e82.
- Baizer L, Ciment G, Hendrickson SK, Schafer GL. Regulated expression of the neurofibromin type I transcript in the developing chicken brain. *J Neurochem.* 61:6 (1993) 2054-2060.
- Barker D, Wright E, Nguyen K, Cannon L, Fain P, Goldgar D, Bishop DT, Carey J, Baty B, Kivlin J, et al. Gene for von Recklinghausen neurofibromatosis is in the pericentromeric region of chromosome 17. *Science.* 236:4805 (1987) 1100-1102.
- Bernards A, Settleman J. GAP control: regulating the regulators of small GTPases. *Trends Cell Biol.* 14:7 (2004) 377-385.
- Billingsley RL, Schrimsher GW, Jackson EF, Slopis JM, Moore BD, 3rd. Significance of planum temporale and planum parietale morphologic features in neurofibromatosis type 1. *Arch Neurol.* 59:4 (2002) 616-622.
- Billingsley RL, Slopis JM, Swank PR, Jackson EF, Moore BD, 3rd. Cortical morphology associated with language function in neurofibromatosis, type I. *Brain Lang.* 85:1 (2003a) 125-139.
- Billingsley RL, Jackson EF, Slopis JM, Swank PR, Mahankali S, Moore BD, 3rd. Functional magnetic resonance imaging of phonologic processing in neurofibromatosis 1. *J Child Neurol.* 18:11 (2003b) 731-740.
- Billingsley RL, Jackson EF, Slopis JM, Swank PR, Mahankali S, Moore BD. Functional MRI of visual-spatial processing in neurofibromatosis, type I. *Neuropsychologia.* 42:3 (2004) 395-404.
- Brannan CI, Perkins AS, Vogel KS, Ratner N, Nordlund ML, Reid SW, Buchberg AM, Jenkins NA, Parada LF, Copeland NG. Targeted disruption of the neurofibromatosis type-1 gene leads to developmental abnormalities in heart and various neural crest-derived tissues. *Genes Dev.* 8:9 (1994) 1019-1029.
- Brown JA, Gianino SM, Gutmann DH. Defective cAMP generation underlies the sensitivity of CNS neurons to neurofibromatosis-1 heterozygosity. *J Neurosci.* 30:16 (2010) 5579-5589.
- Brown JA, Xu J, Diggs-Andrews KA, Wozniak DF, Mach RH, Gutmann DH. PET imaging for attention deficit preclinical drug testing in neurofibromatosis-1 mice. *Exp Neurol.* 232:2 (2011) 333-338.

- Buchanan ME, Davis RL. A distinct set of *Drosophila* brain neurons required for neurofibromatosis type 1-dependent learning and memory. *J Neurosci.* 30:30 (2010) 10135-10143.
- Buchert R, von Borczyskowski D, Wilke F, Gronowsky M, Friedrich RE, Brenner W, Mester J, Clausen M, Mautner VF. Reduced thalamic 18F-fluorodeoxyglucose retention in adults with neurofibromatosis type 1. *Nucl Med Commun.* 29:1 (2008) 17-26.
- Castle B, Baser ME, Huson SM, Cooper DN, Upadhyaya M. Evaluation of genotype-phenotype correlations in neurofibromatosis type 1. *J Med Genet.* 40:10 (2003) e109.
- Cawthon RM, O'Connell P, Buchberg AM, Viskochil D, Weiss RB, Culver M, Stevens J, Jenkins NA, Copeland NG, White R. Identification and characterization of transcripts from the neurofibromatosis 1 region: the sequence and genomic structure of *EVI2* and mapping of other transcripts. *Genomics.* 7:4 (1990a) 555-565.
- Cawthon RM, Weiss R, Xu GF, Viskochil D, Culver M, Stevens J, Robertson M, Dunn D, Gesteland R, O'Connell P, et al. A major segment of the neurofibromatosis type 1 gene: cDNA sequence, genomic structure, and point mutations. *Cell.* 62:1 (1990b) 193-201.
- Chabernaud C, Sirinelli D, Barbier C, Cottier JP, Sembely C, Giraudeau B, Deseille-Turlotte G, Lorette G, Barthez MA, Castelnau P. Thalamo-striatal T2-weighted hyperintensities (unidentified bright objects) correlate with cognitive impairments in neurofibromatosis type 1 during childhood. *Dev Neuropsychol.* 34:6 (2009) 736-748.
- Chabernaud C, Mennes M, Kardel PG, Gaillard WD, Kalbfleisch ML, Vanmeter JW, Packer RJ, Milham MP, Castellanos FX, Acosta MT. Lovastatin regulates brain spontaneous low-frequency brain activity in Neurofibromatosis type 1. *Neurosci Lett.* 515:1 (2012) 28-33.
- Cichowski K, Jacks T. NF1 tumor suppressor gene function: narrowing the GAP. *Cell.* 104:4 (2001) 593-604.
- Clements-Stephens AM, Rimrodt SL, Gaur P, Cutting LE. Visuospatial processing in children with neurofibromatosis type 1. *Neuropsychologia.* 46:2 (2008) 690-697.
- Colman SD, Williams CA, Wallace MR. Benign neurofibromas in type 1 neurofibromatosis (NF1) show somatic deletions of the NF1 gene. *Nat Genet.* 11:1 (1995) 90-92.
- Costa RM, Yang T, Huynh DP, Pulst SM, Viskochil DH, Silva AJ, Brannan CI. Learning deficits, but normal development and tumor predisposition, in mice lacking exon 23a of *Nf1*. *Nat Genet.* 27:4 (2001) 399-405.
- Costa RM, Federov NB, Kogan JH, Murphy GG, Stern J, Ohno M, Kucherlapati R, Jacks T, Silva AJ. Mechanism for the learning deficits in a mouse model of neurofibromatosis type 1. *Nature.* 415:6871 (2002) 526-530.
- Crump T. Translation of case reports in Ueber die multiplen Fibrome der Haut und ihre Beziehung zu den multiplen Neuromen by F v. Recklinghausen. *Adv Neurol.* 29:(1981) 259-275.
- Cui Y, Costa RM, Murphy GG, Elgersma Y, Zhu Y, Gutmann DH, Parada LF, Mody I, Silva AJ. Neurofibromin regulation of ERK signaling modulates GABA release and learning. *Cell.* 135:3 (2008) 549-560.
- Cutting LE, Huang GH, Zeger S, Koth CW, Thompson RE, Denckl MB. Growth curve analyses of neuropsychological profiles in children with neurofibromatosis type 1: specific cognitive tests remain "spared"

- and “impaired” over time. *J Int Neuropsychol Soc.* 8:6 (2002a) 838-846.
- Cutting LE, Cooper KL, Koth CW, Mostofsky SH, Kates WR, Denckla MB, Kaufmann WE. Megalencephaly in NF1: predominantly white matter contribution and mitigation by ADHD. *Neurology.* 59:9 (2002b) 1388-1394.
- Dasgupta B, Dugan LL, Gutmann DH. The neurofibromatosis 1 gene product neurofibromin regulates pituitary adenylate cyclase-activating polypeptide-mediated signaling in astrocytes. *J Neurosci.* 23:26 (2003) 8949-8954.
- Dasgupta B, Yi Y, Chen DY, Weber JD, Gutmann DH. Proteomic analysis reveals hyperactivation of the mammalian target of rapamycin pathway in neurofibromatosis 1-associated human and mouse brain tumors. *Cancer Res.* 65:7 (2005) 2755-2760.
- Daston MM, Ratner N. Neurofibromin, a predominantly neuronal GTPase activating protein in the adult, is ubiquitously expressed during development. *Dev Dyn.* 195:3 (1992) 216-226.
- Daston MM, Scrable H, Nordlund M, Sturbaum AK, Nissen LM, Ratner N. The protein product of the neurofibromatosis type 1 gene is expressed at highest abundance in neurons, Schwann cells, and oligodendrocytes. *Neuron.* 8:3 (1992) 415-428.
- De Raedt T, Brems H, Wolkenstein P, Vidaud D, Pilotti S, Perrone F, Mautner V, Frahm S, Sciot R, Legius E. Elevated risk for MPNST in NF1 microdeletion patients. *American Journal of Human Genetics.* 72:5 (2003) 1288-1292.
- DeClue JE, Cohen BD, Lowy DR. Identification and characterization of the neurofibromatosis type 1 protein product. *Proc Natl Acad Sci U S A.* 88:22 (1991) 9914-9918.
- Descheemaeker MJ, Ghesquiere P, Symons H, Fryns JP, Legius E. Behavioural, academic and neuropsychological profile of normally gifted Neurofibromatosis type 1 children. *J Intellect Disabil Res.* 49:Pt 1 (2005) 33-46.
- Dias EC, Butler PD, Hoptman MJ, Javitt DC. Early sensory contributions to contextual encoding deficits in schizophrenia. *Arch Gen Psychiatry.* 68:7 (2011) 654-664.
- Dilts CV, Carey JC, Kircher JC, Hoffman RO, Creel D, Ward K, Clark E, Leonard CO. Children and adolescents with neurofibromatosis 1: a behavioral phenotype. *J Dev Behav Pediatr.* 17:4 (1996) 229-239.
- DiMario FJ, Jr., Ramsby GR, Burleson JA. Brain morphometric analysis in neurofibromatosis 1. *Arch Neurol.* 56:11 (1999) 1343-1346.
- DiPaolo DP, Zimmerman RA, Rorke LB, Zackai EH, Bilaniuk LT, Yachnis AT. Neurofibromatosis type 1: pathologic substrate of high-signal-intensity foci in the brain. *Radiology.* 195:3 (1995) 721-724.
- Doniger GM, Foxe JJ, Murray MM, Higgins BA, Javitt DC. Impaired visual object recognition and dorsal/ventral stream interaction in schizophrenia. *Arch Gen Psychiatry.* 59:11 (2002) 1011-1020.
- Duarte JV, Ribeiro MJ, Violante IR, Cunha G, Silva E, Castelo-Branco M. Multivariate pattern analysis reveals subtle brain anomalies relevant to the cognitive phenotype in Neurofibromatosis type 1. *Hum Brain Mapp.* (2012) *in press.*
- Dubovsky EC, Booth TN, Vezina G, Samango-Sprouse CA, Palmer KM, Brasseux CO. MR imaging of the corpus callosum in pediatric patients with neurofibromatosis type 1. *AJNR Am J Neuroradiol.* 22:1 (2001) 190-195.

- Duffner PK, Cohen ME, Seidel FG, Shucard DW. The significance of MRI abnormalities in children with neurofibromatosis. *Neurology*. 39:3 (1989) 373-378.
- Dunn DW, Roos KL. Magnetic resonance imaging evaluation of learning difficulties and incoordination in neurofibromatosis. *Neurofibromatosis*. 2:1 (1989) 1-5.
- Easton DF, Ponder MA, Huson SM, Ponder BA. An analysis of variation in expression of neurofibromatosis (NF) type 1 (NF1): evidence for modifying genes. *Am J Hum Genet*. 53:2 (1993) 305-313.
- Eldridge R, Denckla MB, Bien E, Myers S, Kaiser-Kupfer MI, Pikus A, Schlesinger SL, Parry DM, Dambrosia JM, Zasloff MA, et al. Neurofibromatosis type 1 (Recklinghausen's disease). Neurologic and cognitive assessment with sibling controls. *Am J Dis Child*. 143:7 (1989) 833-837.
- Evans DG, Baser ME, McGaughan J, Sharif S, Howard E, Moran A. Malignant peripheral nerve sheath tumours in neurofibromatosis 1. *J Med Genet*. 39:5 (2002) 311-314.
- Fahsold R, Hoffmeyer S, Mischung C, Gille C, Ehlers C, Kucukceylan N, Abdel-Nour M, Gewies A, Peters H, Kaufmann D, Buske A, Tinschert S, Nurnberg P. Minor lesion mutational spectrum of the entire NF1 gene does not explain its high mutability but points to a functional domain upstream of the GAP-related domain. *Am J Hum Genet*. 66:3 (2000) 790-818.
- Feldmann R, Denecke J, Grenzbach M, Schuierer G, Weglage J. Neurofibromatosis type 1: motor and cognitive function and T2-weighted MRI hyperintensities. *Neurology*. 61:12 (2003) 1725-1728.
- Ferner RE. Neurofibromatosis 1 and neurofibromatosis 2: a twenty first century perspective. *Lancet Neurol*. 6:4 (2007) 340-351.
- Ferner RE, Chaudhuri R, Bingham J, Cox T, Hughes RA. MRI in neurofibromatosis 1. The nature and evolution of increased intensity T2 weighted lesions and their relationship to intellectual impairment. *J Neurol Neurosurg Psychiatry*. 56:5 (1993) 492-495.
- Ferraz-Filho JR, da Rocha AJ, Muniz MP, Souza AS, Goloni-Bertollo EM, Pavarino-Bertelli EC. Diffusion tensor MR imaging in neurofibromatosis type 1: expanding the knowledge of microstructural brain abnormalities. *Pediatr Radiol*. 42:4 (2012) 449-454.
- Friedman JM, Riccardi VM *Neurofibromatosis : phenotype, natural history, and pathogenesis*, 3rd Edition. Baltimore: Johns Hopkins University Press 1999.
- Gatto CL, Broadie K. Drosophila modeling of heritable neurodevelopmental disorders. *Curr Opin Neurobiol*. 21:6 (2011) 834-841.
- Gill DS, Hyman SL, Steinberg A, North KN. Age-related findings on MRI in neurofibromatosis type 1. *Pediatr Radiol*. 36:10 (2006) 1048-1056.
- Goh WH, Khong PL, Leung CS, Wong VC. T2-weighted hyperintensities (unidentified bright objects) in children with neurofibromatosis 1: their impact on cognitive function. *J Child Neurol*. 19:11 (2004) 853-858.
- Golubic M, Roudebush M, Dobrowolski S, Wolfman A, Stacey DW. Catalytic properties, tissue and intracellular distribution of neurofibromin. *Oncogene*. 7:11 (1992) 2151-2159.
- Greenwood RS, Tupler LA, Whitt JK, Buu A, Dombeck CB, Harp AG, Payne ME, Eastwood JD, Krishnan KR, MacFall JR. Brain morphometry, T2-weighted hyperintensities, and IQ in children with neurofibromatosis type 1. *Arch Neurol*. 62:12 (2005) 1904-1908.

- Gregory PE, Gutmann DH, Mitchell A, Park S, Boguski M, Jacks T, Wood DL, Jove R, Collins FS. Neurofibromatosis type 1 gene product (neurofibromin) associates with microtubules. *Somat Cell Mol Genet.* 19:3 (1993) 265-274.
- Gu H, Marth JD, Orban PC, Mossmann H, Rajewsky K. Deletion of a DNA polymerase beta gene segment in T cells using cell type-specific gene targeting. *Science.* 265:5168 (1994) 103-106.
- Guo HF, The I, Hannan F, Bernards A, Zhong Y. Requirement of *Drosophila* NF1 for activation of adenylyl cyclase by PACAP38-like neuropeptides. *Science.* 276:5313 (1997) 795-798.
- Guo HF, Tong J, Hannan F, Luo L, Zhong Y. A neurofibromatosis-1-regulated pathway is required for learning in *Drosophila*. *Nature.* 403:6772 (2000) 895-898.
- Gutman DH, Andersen LB, Cole JL, Swaroop M, Collins FS. An alternatively-spliced mRNA in the carboxy terminus of the neurofibromatosis type 1 (NF1) gene is expressed in muscle. *Hum Mol Genet.* 2:7 (1993) 989-992.
- Gutmann DH, Wood DL, Collins FS. Identification of the neurofibromatosis type 1 gene product. *Proc Natl Acad Sci U S A.* 88:21 (1991) 9658-9662.
- Gutmann DH, Zhang Y, Hirbe A. Developmental regulation of a neuron-specific neurofibromatosis 1 isoform. *Ann Neurol.* 46:5 (1999) 777-782.
- Gutmann DH, Geist RT, Wright DE, Snider WD. Expression of the neurofibromatosis 1 (NF1) isoforms in developing and adult rat tissues. *Cell Growth Differ.* 6:3 (1995a) 315-323.
- Gutmann DH, Geist RT, Rose K, Wright DE. Expression of two new protein isoforms of the neurofibromatosis type 1 gene product, neurofibromin, in muscle tissues. *Dev Dyn.* 202:3 (1995b) 302-311.
- Gutmann DH, Aylsworth A, Carey JC, Korf B, Marks J, Pyeritz RE, Rubenstein A, Viskochil D. The diagnostic evaluation and multidisciplinary management of neurofibromatosis 1 and neurofibromatosis 2. *JAMA.* 278:1 (1997) 51-57.
- Hagmann P, Jonasson L, Maeder P, Thiran JP, Wedeen VJ, Meuli R. Understanding diffusion MR imaging techniques: from scalar diffusion-weighted imaging to diffusion tensor imaging and beyond. *Radiographics.* 26 Suppl 1:(2006) S205-223.
- Hay N, Sonenberg N. Upstream and downstream of mTOR. *Genes Dev.* 18:16 (2004) 1926-1945.
- Hilfiker S, Pieribone VA, Czernik AJ, Kao HT, Augustine GJ, Greengard P. Synapsins as regulators of neurotransmitter release. *Philos Trans R Soc Lond B Biol Sci.* 354:1381 (1999) 269-279.
- Ho IS, Hannan F, Guo HF, Hakker I, Zhong Y. Distinct functional domains of neurofibromatosis type 1 regulate immediate versus long-term memory formation. *J Neurosci.* 27:25 (2007) 6852-6857.
- Hofman KJ, Harris EL, Bryan RN, Denckla MB. Neurofibromatosis type 1: the cognitive phenotype. *J Pediatr.* 124:4 (1994) S1-8.
- Huijbregts S, Swaab H, de Sonnevile L. Cognitive and motor control in neurofibromatosis type I: influence of maturation and hyperactivity-inattention. *Dev Neuropsychol.* 35:6 (2010) 737-751.
- Huson S, Jones D, Beck L. Ophthalmic manifestations of neurofibromatosis. *Br J Ophthalmol.* 71:3 (1987) 235-238.
- Huson SM, Harper PS, Compston DA. Von Recklinghausen neurofibromatosis. A clinical and population study in south-east Wales. *Brain.* 111 ( Pt 6):(1988) 1355-1381.

- Huson SM, Compston DA, Harper PS. A genetic study of von Recklinghausen neurofibromatosis in south east Wales. II. Guidelines for genetic counselling. *J Med Genet.* 26:11 (1989) 712-721.
- Huynh DP, Nechiporuk T, Pulst SM. Differential expression and tissue distribution of type I and type II neurofibromins during mouse fetal development. *Dev Biol.* 161:2 (1994) 538-551.
- Hyman SL, Shores A, North KN. The nature and frequency of cognitive deficits in children with neurofibromatosis type 1. *Neurology.* 65:7 (2005) 1037-1044.
- Hyman SL, Gill DS, Shores EA, Steinberg A, North KN. T2 hyperintensities in children with neurofibromatosis type 1 and their relationship to cognitive functioning. *J Neurol Neurosurg Psychiatry.* 78:10 (2007) 1088-1091.
- Hyman SL, Gill DS, Shores EA, Steinberg A, Joy P, Gibikote SV, North KN. Natural history of cognitive deficits and their relationship to MRI T2-hyperintensities in NF1. *Neurology.* 60:7 (2003) 1139-1145.
- Jacks T, Shih TS, Schmitt EM, Bronson RT, Bernard A, Weinberg RA. Tumour predisposition in mice heterozygous for a targeted mutation in Nf1. *Nat Genet.* 7:3 (1994) 353-361.
- Jett K, Friedman JM. Clinical and genetic aspects of neurofibromatosis 1. *Genet Med.* 12:1 (2010) 1-11.
- Johannessen CM, Reczek EE, James MF, Brems H, Legius E, Cichowski K. The NF1 tumor suppressor critically regulates TSC2 and mTOR. *Proc Natl Acad Sci U S A.* 102:24 (2005) 8573-8578.
- Kaplan AM, Chen K, Lawson MA, Wodrich DL, Bonstelle CT, Reiman EM. Positron emission tomography in children with neurofibromatosis-1. *J Child Neurol.* 12:8 (1997) 499-506.
- Kayl AE, Moore BD, 3rd, Slopis JM, Jackson EF, Leeds NE. Quantitative morphology of the corpus callosum in children with neurofibromatosis and attention-deficit hyperactivity disorder. *J Child Neurol.* 15:2 (2000) 90-96.
- Korf BR. Plexiform neurofibromas. *Am J Med Genet.* 89:1 (1999) 31-37.
- Korf BR. Malignancy in neurofibromatosis type 1. *Oncologist.* 5:6 (2000) 477-485.
- Korf BR. Clinical features and pathobiology of neurofibromatosis 1. *J Child Neurol.* 17:8 (2002) 573-577
- Korf BR, Carrazana E, Holmes GL. Patterns of seizures observed in association with neurofibromatosis 1. *Epilepsia.* 34:4 (1993) 616-620.
- Koth CW, Cutting LE, Denckla MB. The association of neurofibromatosis type 1 and attention deficit hyperactivity disorder. *Child Neuropsychol.* 6:3 (2000) 185-194.
- Krab LC, de Goede-Bolder A, Aarsen FK, Pluijm SM, Bouman MJ, van der Geest JN, Lequin M, Catsman CE, Arts WF, Kushner SA, Silva AJ, de Zeeuw CI, Moll HA, Elgersma Y. Effect of simvastatin on cognitive functioning in children with neurofibromatosis type 1: a randomized controlled trial. *JAMA.* 300:3 (2008) 287-294.
- Kronenberger WG, Dunn DW. Learning disorders. *Neurol Clin.* 21:4 (2003) 941-952.
- Legius E, Marchuk DA, Collins FS, Glover TW. Somatic deletion of the neurofibromatosis type 1 gene in a neurofibrosarcoma supports a tumour suppressor gene hypothesis. *Nat Genet.* 3:2 (1993) 122-126.
- Legius E, Descheemaeker MJ, Steyaert J, Spaepen A, Vlietinck R, Casaer P, Demaerel P, Fryns JP. Neurofibromatosis type 1 in childhood: correlation of MRI findings with intelligence. *J Neurol Neurosurg Psychiatry.* 59:6 (1995) 638-640.

- Levine TM, Materek A, Abel J, O'Donnell M, Cutting LE. Cognitive profile of neurofibromatosis type 1. *Semin Pediatr Neurol.* 13:1 (2006) 8-20.
- Li W, Cui Y, Kushner SA, Brown RA, Jentsch JD, Frankland PW, Cannon TD, Silva AJ. The HMG-CoA reductase inhibitor lovastatin reverses the learning and attention deficits in a mouse model of neurofibromatosis type 1. *Curr Biol.* 15:21 (2005) 1961-1967.
- Li Y, O'Connell P, Breidenbach HH, Cawthon R, Stevens J, Xu G, Neil S, Robertson M, White R, Viskochil D. Genomic organization of the neurofibromatosis 1 gene (NF1). *Genomics.* 25:1 (1995) 9-18.
- Listernick R, Ferner RE, Liu GT, Gutmann DH. Optic pathway gliomas in neurofibromatosis-1: controversies and recommendations. *Ann Neurol.* 61:3 (2007) 189-198.
- Lopes Ferraz Filho JR, Munis MP, Soares Souza A, Sanches RA, Goloni-Bertollo EM, Pavarino-Bertelli EC. Unidentified bright objects on brain MRI in children as a diagnostic criterion for neurofibromatosis type 1. *Pediatr Radiol.* 38:3 (2008) 305-310.
- Lush ME, Li Y, Kwon CH, Chen J, Parada LF. Neurofibromin is required for barrel formation in the mouse somatosensory cortex. *J Neurosci.* 28:7 (2008) 1580-1587.
- MacCollin M, Chiocca EA, Evans DG, Friedman JM, Horvitz R, Jaramillo D, Lev M, Mautner VF, Niimura M, Plotkin SR, Sang CN, Stemmer-Rachamimov A, Roach ES. Diagnostic criteria for schwannomatosis. *Neurology.* 64:11 (2005) 1838-1845.
- Marchuk DA, Saulino AM, Tavakkol R, Swaroop M, Wallace MR, Andersen LB, Mitchell AL, Gutmann DH, Boguski M, Collins FS. cDNA cloning of the type 1 neurofibromatosis gene: complete sequence of the NF1 gene product. *Genomics.* 11:4 (1991) 931-940.
- Martin GA, Viskochil D, Bollag G, McCabe PC, Crosier WJ, Haubruck H, Conroy L, Clark R, O'Connell P, Cawthon RM, et al. The GAP-related domain of the neurofibromatosis type 1 gene product interacts with ras p21. *Cell.* 63:4 (1990) 843-849.
- McClatchey AI. Neurofibromatosis. *Annu Rev Pathol.* 2:(2007) 191-216.
- McKiernan KA, Kaufman JN, Kucera-Thompson J, Binder JR. A parametric manipulation of factors affecting task-induced deactivation in functional neuroimaging. *J Cogn Neurosci.* 15:3 (2003) 394-408.
- Messiaen LM, Callens T, Mortier G, Beysen D, Vandenbroucke I, Van Roy N, Speleman F, Paepe AD. Exhaustive mutation analysis of the NF1 gene allows identification of 95% of mutations and reveals a high frequency of unusual splicing defects. *Hum Mutat.* 15:6 (2000) 541-555.
- Moore BD, Slopis JM, Schomer D, Jackson EF, Levy BM. Neuropsychological significance of areas of high signal intensity on brain MRIs of children with neurofibromatosis. *Neurology.* 46:6 (1996) 1660-1668.
- Moore BD, 3rd, Slopis JM, Jackson EF, De Winter AE, Leeds NE. Brain volume in children with neurofibromatosis type 1: relation to neuropsychological status. *Neurology.* 54:4 (2000) 914-920.
- Morris RG, Garrud P, Rawlins JN, O'Keefe J. Place navigation impaired in rats with hippocampal lesions. *Nature.* 297:5868 (1982) 681-683.
- Morse RP. Neurofibromatosis type 1. *Arch Neurol.* 56:3 (1999) 364-365.
- Moser EI, Krobot KA, Moser MB, Morris RG. Impaired spatial learning after saturation of long-term potentiation. *Science.* 281:5385 (1998) 2038-2042.

- Mousley CJ, Davison JM, Bankaitis VA. Sec14 Like PTPs Couple Lipid Metabolism with Phosphoinositide Synthesis to Regulate Golgi Functionality. *Subcell Biochem.* 59:(2006) 271-287.
- Nagy Z, Westerberg H, Klingberg T. Maturation of white matter is associated with the development of cognitive functions during childhood. *J Cogn Neurosci.* 16:7 (2004) 1227-1233.
- National Institutes of Health Consensus Development Conference Statement: neurofibromatosis. Bethesda, Md., USA, July 13-15 1987. *Neurofibromatosis.* 1:3 (1988) 172-178.
- North K. Neurofibromatosis type 1. *Am J Med Genet.* 97:2 (2000) 119-127.
- North K, Joy P, Yuille D, Cocks N, Mobbs E, Hutchins P, McHugh K, de Silva M. Specific learning disability in children with neurofibromatosis type 1: significance of MRI abnormalities. *Neurology.* 44:5 (1994) 878-883.
- North KN, Riccardi V, Samango-Sprouse C, Ferner R, Moore B, Legius E, Ratner N, Denckla MB. Cognitive function and academic performance in neurofibromatosis. 1: consensus statement from the NF1 Cognitive Disorders Task Force. *Neurology.* 48:4 (1997) 1121-1127.
- Owens DF, Kriegstein AR. Is there more to GABA than synaptic inhibition? *Nat Rev Neurosci.* 3:9 (2002) 715-727.
- Ozonoff S. Cognitive impairment in neurofibromatosis type 1. *Am J Med Genet.* 89:1 (1999) 45-52.
- Padmanabhan A, Lee JS, Ismat FA, Lu MM, Lawson ND, Kanki JP, Look AT, Epstein JA. Cardiac and vascular functions of the zebrafish orthologues of the type I neurofibromatosis gene *NF1*. *Proc Natl Acad Sci U S A.* 106:52 (2009) 22305-22310.
- Payne JM, Moharir MD, Webster R, North KN. Brain structure and function in neurofibromatosis type 1: current concepts and future directions. *J Neurol Neurosurg Psychiatry.* 81:3 (2010) 304-309.
- Raichle ME, MacLeod AM, Snyder AZ, Powers WJ, Gusnard DA, Shulman GL. A default mode of brain function. *Proc Natl Acad Sci U S A.* 98:2 (2001) 676-682.
- Raught B, Gingras AC, Sonenberg N. The target of rapamycin (TOR) proteins. *Proc Natl Acad Sci U S A.* 98:13 (2001) 7037-7044.
- Ribeiro MJ, Violante IR, Bernardino I, Ramos F, Saraiva J, Reviriego P, Upadhyaya M, Silva ED, Castelo-Branco M. Abnormal achromatic and chromatic contrast sensitivity in neurofibromatosis type 1. *Invest Ophthalmol Vis Sci.* 53:1 (2012) 287-293.
- Richetta A, Giustini S, Recupero SM, Pezza M, Carlomagno V, Amoroso G, Calvieri S. Lisch nodules of the iris in neurofibromatosis type 1. *J Eur Acad Dermatol Venereol.* 18:3 (2004) 342-344.
- Rosser TL, Packer RJ. Neurocognitive dysfunction in children with neurofibromatosis type 1. *Curr Neurol Neurosci Rep.* 3:2 (2003) 129-136.
- Rowbotham I, Pit-ten Cate IM, Sonuga-Barke EJ, Huijbregts SC. Cognitive control in adolescents with neurofibromatosis type 1. *Neuropsychology.* 23:1 (2009) 50-60.
- Roy A, Roulin JL, Charbonnier V, Allain P, Fasotti L, Barbarot S, Stalder JF, Terrien A, Le Gall D. Executive dysfunction in children with neurofibromatosis type 1: a study of action planning. *J Int Neuropsychol Soc.* 16:6 (2010) 1056-1063.
- Ruggieri M, Polizzi A. From Aldrovandi's "Homuncio" (1592) to Buffon's girl (1749) and the "Wart Man" of Tilesius (1793): antique illustrations of mosaicism in neurofibromatosis? *Journal of Medical Genetics.*



- 40:3 (2003) 227-232.
- Sabbagh A, Pasmant E, Laurendeau I, Parfait B, Barbarot S, Guillot B, Combemale P, Ferkal S, Vidaud M, Aubourg P, Vidaud D, Wolkenstein P. Unravelling the genetic basis of variable clinical expression in neurofibromatosis 1. *Hum Mol Genet.* 18:15 (2009) 2768-2778.
- Said SM, Yeh TL, Greenwood RS, Whitt JK, Tupler LA, Krishnan KR. MRI morphometric analysis and neuropsychological function in patients with neurofibromatosis. *Neuroreport.* 7:12 (1996) 1941-1944.
- Schaefer PW, Grant PE, Gonzalez RG. Diffusion-weighted MR imaging of the brain. *Radiology.* 217:2 (2000) 331-345.
- Schmahmann JD, Pandya DN. Disconnection syndromes of basal ganglia, thalamus, and cerebrotocerebellar systems. *Cortex.* 44:8 (2008) 1037-1066.
- Schrimsher GW, Billingsley RL, Slopis JM, Moore BD, 3rd. Visual-spatial performance deficits in children with neurofibromatosis type-1. *Am J Med Genet A.* 120A:3 (2003) 326-330.
- Seizinger BR, Rouleau GA, Ozelius LJ, Lane AH, Faryniarz AG, Chao MV, Huson S, Korf BR, Parry DM, Pericak-Vance MA, et al. Genetic linkage of von Recklinghausen neurofibromatosis to the nerve growth factor receptor gene. *Cell.* 49:5 (1987) 589-594.
- Shannon KM, O'Connell P, Martin GA, Paderanga D, Olson K, Dinndorf P, McCormick F. Loss of the normal NF1 allele from the bone marrow of children with type 1 neurofibromatosis and malignant myeloid disorders. *N Engl J Med.* 330:9 (1994) 597-601.
- Shaywitz SE, Shaywitz BA, Pugh KR, Fulbright RK, Constable RT, Mencl WE, Shankweiler DP, Liberman AM, Skudlarski P, Fletcher JM, Katz L, Marchione KE, Lacadie C, Gatenby C, Gore JC. Functional disruption in the organization of the brain for reading in dyslexia. *Proc Natl Acad Sci U S A.* 95:5 (1998) 2636-2641.
- Sheikh SF, Kubal WS, Anderson AW, Mutalik P. Longitudinal evaluation of apparent diffusion coefficient in children with neurofibromatosis type 1. *J Comput Assist Tomogr.* 27:5 (2003) 681-686.
- Shilyansky C, Lee YS, Silva AJ. Molecular and cellular mechanisms of learning disabilities: a focus on NF1. *Annu Rev Neurosci.* 33:(2010a) 221-243.
- Shilyansky C, Karlsgodt KH, Cummings DM, Sidiropoulou K, Hardt M, James AS, Ehninger D, Bearden CE, Poirazi P, Jentsch JD, Cannon TD, Levine MS, Silva AJ. Neurofibromin regulates corticostriatal inhibitory networks during working memory performance. *Proc Natl Acad Sci U S A.* 107:29 (2010b) 13141-13146.
- Shin J, Padmanabhan A, de Groh ED, Lee JS, Haidar S, Dahlberg S, Guo F, He S, Wolman MA, Granato M, Lawson ND, Wolfe SA, Kim SH, Solnica-Krezel L, Kanki JP, Ligon KL, Epstein JA, Look AT. Zebrafish neurofibromatosis type 1 genes have redundant functions in tumorigenesis and embryonic development. *Dis Model Mech.* (2012).
- Shulman GL, Corbetta M, Buckner RL, Raichle ME, Fiez JA, Miezin FM, Petersen SE. Top-down modulation of early sensory cortex. *Cereb Cortex.* 7:3 (1997) 193-206.
- Silva AJ, Frankland PW, Marowitz Z, Friedman E, Laszlo GS, Cioffi D, Jacks T, Bourchouladze R. A mouse model for the learning and memory deficits associated with neurofibromatosis type I. *Nat Genet.* 15:3 (1997) 281-284.

- Steen RG, Taylor JS, Langston JW, Glass JO, Brewer VR, Reddick WE, Mages R, Pivnick EK. Prospective evaluation of the brain in asymptomatic children with neurofibromatosis type 1: relationship of macrocephaly to T1 relaxation changes and structural brain abnormalities. *AJNR Am J Neuroradiol.* 22:5 (2001) 810-817.
- Sylvester CL, Drohan LA, Sergott RC. Optic-nerve gliomas, chiasmal gliomas and neurofibromatosis type 1. *Curr Opin Ophthalmol.* 17:1 (2006) 7-11.
- The I, Hannigan GE, Cowley GS, Reginald S, Zhong Y, Gusella JF, Hariharan IK, Bernards A. Rescue of a *Drosophila* NF1 mutant phenotype by protein kinase A. *Science.* 276:5313 (1997) 791-794.
- Thomas SL, De Vries GH. Neurofibromatosis Type I: From Genetic Mutation to Tumor Formation. In: *Handbook of Neurochemistry and Molecular Neurobiology* (Lajtha A, ed), pp 107-129: Springer US 2009.
- Thomson SA, Fishbein L, Wallace MR. NF1 mutations and molecular testing. *J Child Neurol.* 17:8 (2002) 555-561.
- Tong J, Hannan F, Zhu Y, Bernards A, Zhong Y. Neurofibromin regulates G protein-stimulated adenylyl cyclase activity. *Nat Neurosci.* 5:2 (2002) 95-96.
- Tonsgard JH, Yelavarthi KK, Cushner S, Short MP, Lindgren V. Do NF1 gene deletions result in a characteristic phenotype? *American Journal of Medical Genetics.* 73:1 (1997) 80-86.
- Trovo-Marqui AB, Tajara EH. Neurofibromin: a general outlook. *Clin Genet.* 70:1 (2006) 1-13.
- Ullrich NJ, Raja AI, Irons MB, Kieran MW, Goumnerova L. Brainstem lesions in neurofibromatosis type 1. *Neurosurgery.* 61:4 (2007) 762-766.
- Upadhyaya M, Ruggieri M, Maynard J, Osborn M, Hartog C, Mudd S, Penttinen M, Cordeiro I, Ponder M, Ponder BAJ, Krawczak M, Cooper DN. Gross deletions of the neurofibromatosis type 1 (NF1) gene are predominantly of maternal origin and commonly associated with a learning disability, dysmorphic features and developmental delay. *Human Genetics.* 102:5 (1998) 591-597.
- van Engelen SJ, Krab LC, Moll HA, de Goede-Bolder A, Pluijm SM, Catsman-Berrevoets CE, Elgersma Y, Lequin MH. Quantitative differentiation between healthy and disordered brain matter in patients with neurofibromatosis type I using diffusion tensor imaging. *AJNR Am J Neuroradiol.* 29:4 (2008) 816-822.
- Van Es S, North KN, McHugh K, De Silva M. MRI findings in children with neurofibromatosis type 1: a prospective study. *Pediatr Radiol.* 26:7 (1996) 478-487.
- Viskochil D, Buchberg AM, Xu G, Cawthon RM, Stevens J, Wolff RK, Culver M, Carey JC, Copeland NG, Jenkins NA, et al. Deletions and a translocation interrupt a cloned gene at the neurofibromatosis type 1 locus. *Cell.* 62:1 (1990) 187-192.
- von Recklinghausen F. Ueber die multiplen Fibrome der Haut und ihre Beziehung zu den multiplen Neuromen Berlin: Hirschwald 1882.
- Wallace MR, Marchuk DA, Andersen LB, Letcher R, Odeh HM, Saulino AM, Fountain JW, Brereton A, Nicholson J, Mitchell AL, et al. Type 1 neurofibromatosis gene: identification of a large transcript disrupted in three NF1 patients. *Science.* 249:4965 (1990) 181-186.
- Wang PY, Kaufmann WE, Koth CW, Denckla MB, Barker PB. Thalamic involvement in neurofibromatosis

- type 1: evaluation with proton magnetic resonance spectroscopic imaging. *Ann Neurol.* 47:4 (2000) 477-484.
- Ward BA, Gutmann DH. Neurofibromatosis 1: from lab bench to clinic. *Pediatr Neurol.* 32:4 (2005) 221-228.
- Weiss B, Bollag G, Shannon K. Hyperactive Ras as a therapeutic target in neurofibromatosis type 1. *Am J Med Genet.* 89:1 (1999) 14-22.
- Welti S, Kuhn S, D'Angelo I, Brugger B, Kaufmann D, Scheffzek K. Structural and biochemical consequences of NF1 associated nontruncating mutations in the Sec14-PH module of neurofibromin. *Hum Mutat.* 32:2 (2011) 191-197.
- Wignall EL, Griffiths PD, Papadakis NG, Wilkinson ID, Wallis LI, Bandmann O, Cowell PE, Hoggard N. Corpus callosum morphology and microstructure assessed using structural MR imaging and diffusion tensor imaging: initial findings in adults with neurofibromatosis type 1. *AJNR Am J Neuroradiol.* 31:5 (2010) 856-861.
- Wilkins RH, Brody IA. Von Recklinghausen's neurofibromatosis. *Arch Neurol.* 24:4 (1971) 374-377.
- Williams JA, Su HS, Bernards A, Field J, Sehgal A. A circadian output in *Drosophila* mediated by neurofibromatosis-1 and Ras/MAPK. *Science.* 293:5538 (2001) 2251-2256.
- Zamboni SL, Loenneker T, Boltshauser E, Martin E, Il'yasov KA. Contribution of diffusion tensor MR imaging in detecting cerebral microstructural changes in adults with neurofibromatosis type 1. *AJNR Am J Neuroradiol.* 28:4 (2007) 773-776.



MATERIALS  
AND  
METHODS



# CHAPTER 2

Fundamentals of  
magnetic resonance  
for the study of brain  
structure, function  
and neurochemistry

Neuroimaging modalities constituted a revolution in the ability to investigate brain anatomy and physiology. Magnetic resonance imaging (MRI) is broadly applied to map the human brain because of its noninvasive nature and its versatility, thereby conferring potential to improve diagnosis, monitor therapeutic approaches and provide insights into the mechanisms of brain disease.

This chapter provides an overview of the magnetic resonance (MR) methods employed throughout this thesis to assess brain morphology, metabolism, physiology and function of the NF1 brain.

## MR PHYSICAL PRINCIPLES – SEMI-CLASSICAL APPROACH

MRI is based on the magnetic excitation of a tissue and the recording of returned electromagnetic signals. More precisely, it is based upon the interaction between an applied magnetic field and a nucleus that possesses spin.

Nuclear spin or spin angular momentum is one of the intrinsic properties of a nucleus and its value depends on atomic composition. The spin,  $I$ , is quantized meaning that it can only admit certain discrete values. These values depend on the atomic number and atomic weight of the nucleus. Three groups of values are possible for  $I$ : zero, half-integral-values, and integral values. Nuclei with an overall spin different from zero (e.g.  $^1\text{H}$ ,  $^{13}\text{C}$ ,  $^{31}\text{P}$ ,  $^{15}\text{N}$ ,  $^{19}\text{F}$ ) are susceptible to the MR technique, whereas those with an overall spin of zero (e.g.  $^{12}\text{C}$ ,  $^{16}\text{O}$ ,  $^{32}\text{S}$ ) are not because they do not interact with the external magnetic field. In MRI, the nucleus that is mostly accessible to experimental research is  $^1\text{H}$  ( $I = 1/2$ ), as it is widely abundant in human tissue and possesses favourable magnetic properties. The two biggest sources of protons in human tissue are water followed by fat.

The nucleus can be considered to be rotating about an axis at a constant velocity. Normally, the orientation of the nuclear spins is random. However, when placed in a strong static magnetic field ( $B_0$ ) precession occurs (rotation around the direction of  $B_0$ ). The precession of the nucleus occurs at the Larmor or resonance frequency  $\omega_0$ , given by the Larmor equation:

$$\omega = \gamma B_0 \quad [\text{Equation 1}]$$

The Larmor frequency, schematically represented in Figure 1, is dependent on the gyromagnetic ratio ( $\gamma$ ), a constant unique of each nucleus, and the external magnetic



field ( $B_0$ ). This precession process generates an electric field with frequency  $\omega_0$ . For hydrogen protons,  $\gamma = 42.56$  MHz per Tesla. Therefore, at the magnetic field strength of a 3 Tesla scanner, the precession frequency of hydrogen protons is 128 MHz.

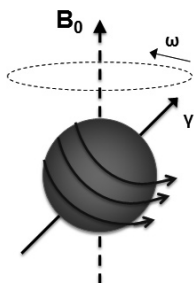


**Figure 1. A nuclear spin precessing in an external magnetic field  $B_0$  at the Larmor frequency ( $\omega$ ).** The Larmor frequency is dependent on the gyromagnetic ratio ( $\gamma$ ) and the external magnetic field ( $B_0$ ).

The orientations that a nucleus' magnetic moment can take against an external magnetic field are not of equal energy. Spin states which are oriented parallel to the external field are lower in energy than in the absence of an external field. In contrast, spin states whose orientations oppose the external field are higher in energy than in the absence of an external field (Figure 2). The nuclei will be distributed throughout the various spin states available. The number of nuclei in each spin state is described by the Boltzmann distribution so that at thermal equilibrium the lower energy level will have a relatively small excess of population of spins. Where energy separation occurs there is a possibility to induce a transition between the various spin states. By irradiating the nucleus with electromagnetic radiation of the correct energy (as determined by its resonance

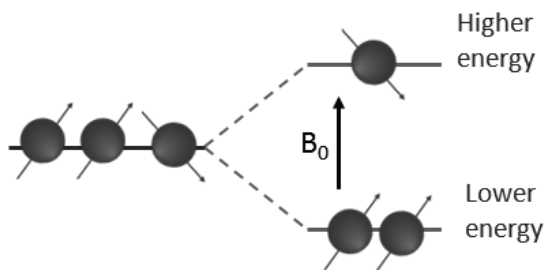


**Figure 2. The orientations that a nucleus' magnetic moment can take against an external magnetic field are not of equal energy.** In the absence of a magnetic field (left side of figure), spins will have equal energy so that there is no preferential alignment between the spin up and spin down orientations. In the presence of a magnetic field (right side), the spin up orientation (parallel to  $B_0$ ) is of lower energy and its configuration contains more protons than the higher energy, spin down configuration. The difference in energy between the two levels is proportional to  $B_0$ .

frequency), a nucleus with a low energy orientation can be induced to “transition” to an orientation with a higher energy. The absorption of energy during this transition forms the basis of the MR method.

The difference in spin population results in a net microscopic magnetization  $M_0$ , aligned parallel to the magnetic field  $B_0$ . This net (or longitudinal) magnetization can be manipulated, which is done in MR experiments.

In a typical MR experiment, the net macroscopic magnetization  $M_0$  is tilted from its original orientation along  $B_0$  (or z-axis) to the transversal orientation by a radio frequency (RF) pulse at the Larmor frequency, as indicated by an effective field  $B_1$  (Figure 3).

During the application of the RF pulse,  $M_0$  will rotate towards the xy-plane ( $M_{xy}$ ). The power and length of the RF pulse can be adjusted, and by this way modulate the extension of rotation. Directly after the application of the RF excitation pulse, the spins are still precessing along  $B_0$ , but their precession is no longer random; they precess in phase, and a maximum signal is detected. When the pulse ends, the nuclei relax and return to their original equilibrium positions, and the MR signal decays. This decaying signal contains the sum of the frequencies from all the target nuclei in the sample. It is picked up by the coil as an oscillating voltage generated by the magnetic moments

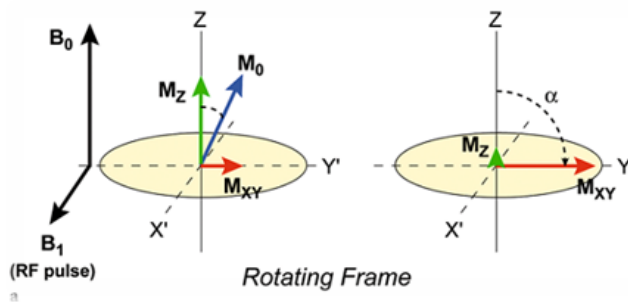


**Figure 3. Schematic representation of a typical MR experiment in the rotation frame of reference.** In a rotating frame, the coordinate system rotates about one axis while the other two axes vary with time. In this rotation frame of reference,  $B_1$  and  $M_0$  are stationary, while the x and y axes rotate at the Larmor frequency. When viewed in this fashion, the precessing spin appears stationary in space with a fixed set of x, y, and z coordinates. A short RF pulse is applied along the x' axis. The magnetic field of this radiation is given by the symbol  $B_1$ . The radiofrequency (RF) pulse causes the bulk magnetization vector,  $M_0$ , to rotate clockwise about the x' axis. The longitudinal component  $M_z$  decreases over time while the transverse component  $M_{xy}$  increases. Reproduced from Goebel, 2007.

precessing/relaxing back to equilibrium. The signal received by the coil is called free induction decay (FID).

The relaxation process is crucial for the MR experiment. Because of local interactions between individual spins, such as translation and rotation, phase coherence will be lost, and  $M_{xy}$  will decrease. Two types of relaxation occur simultaneously: longitudinal (spin-lattice) relaxation and transverse (spin-spin) relaxation. In longitudinal relaxation, the z component of M returns to its original position by transferring vibrational or translational energy to the molecular framework, the lattice. The time required for the system to recover 63% of its equilibrium value after a  $90^\circ$  pulse is  $T_1$  or the spin-lattice relaxation time (Figure 4a). In transverse relaxation, energy is transferred to a neighbouring nucleus in the same molecular environment and precessing in the transverse plane

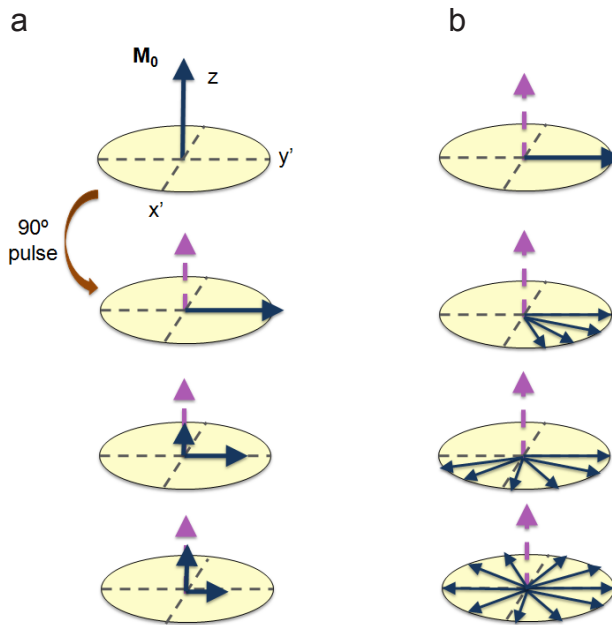


**Figure 4. Representation of  $T_1$  and  $T_2$  relaxation processes.** **a.** Longitudinal relaxation. The magnetization  $M_0$  is tipped by a  $90^\circ$  pulse. After the pulse the system relaxes and magnetization will start its return to the equilibrium state. This effect causes recovery of the longitudinal (z) component of magnetization towards  $M_0$ , at an exponential rate with time-constant  $T_1$ . **b.** Transverse relaxation. Transverse relaxation induce an increase in dephasing of individual spins, so a progressive decrease of the macroscopic magnetization is observed. This process causes shortening of the transverse component of magnetization, at an exponential rate with time-constant  $T_2$ .

at the same  $\omega_0$  frequency.  $T_2$  is the time it takes for the magnetization to reach 37% of its initial value.  $T_2$  occurs due to energy transferred from one excited nucleus to another nucleus nearby. This energy transfer can occur as long as nucleuses are in close proximity and retain the same  $\omega_0$ . Intermolecular and intramolecular interactions such as vibrations or rotations cause  $\omega_0$  to fluctuate, which leads to a gradual loss of phase coherence and reduce the magnitude of transverse magnetization and consequently the signal (Figure 4b).

In addition, a sample always experiences a certain degree of magnetic field inhomogeneity leading to a heterogeneous distribution of resonance frequencies. This inhomogeneity comes from three sources: 1) *Main field inhomogeneity* as a consequence of nonuniformity to  $B_0$  due to imperfections in magnet manufacturing; 2) *Sample-induced inhomogeneity* due to differences in the magnetic susceptibility of adjacent tissues (e.g., air, bone) that distort the local magnetic field at the interface between different tissues; 3) *Imaging gradients* used for spatial localization that induce a transient inhomogeneity during the measurement. Consequently, the MR signal actually decreases more rapidly than it will be expected only by the contribution of  $T_2$ , with a decay constant  $T_2^*$ .

For the production of an image, a sequence of RF pulses is usually combined with specific magnetic gradient pulses superimposed upon the large external field  $B_0$ . The formation of an image involves the following procedures:

*Localization of the region of interest* - Linear magnetic field gradients applied along the x, y, and z axes allow for spatial encoding (Figure 5). As referred previously the Larmor frequency is proportional to the magnetic field strength. By varying the magnetic field linearly one can vary the frequency of the signal.

*Excitation of spins in the region of interest* - Excitation of the spins is performed through the application of RF pulses. However, the application of gradients to signal localization will amplify the dephasing of spins. To avoid losing the signal a gradient-echo or a spin-echo pulse are used (Figure 6).

*Spatial encoding of the spins signal* - Spatial encoding is performed by frequency encoding and phase encoding, both of which contain spatial information needed for image reconstruction.

*Signal detection and reconstruction.*

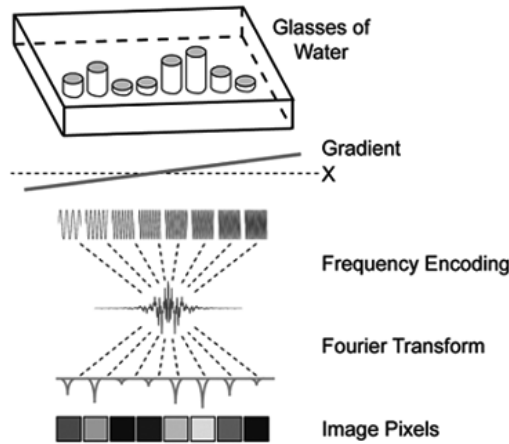


**Figure 5. Image formation.** Assume that eight glasses with different amounts of water are placed in the MRI scanner. If a gradient is applied in the x direction, the spins will precess at frequencies that depend upon their position along the gradient. Spatial information is now frequency-encoded. The strength of the signal at each frequency is directly proportional to the number of protons from the respective glass of water. The time domain signal is the sum of these frequencies and a Fourier Transform can be used to determine the strength of the signal at each frequency. Since frequencies encode different spatial positions, an “image” of eight pixels can be formed. The grey values of these pixels reflect the relative amount of water in the different glasses. Reproduced from Goebel, 2007.

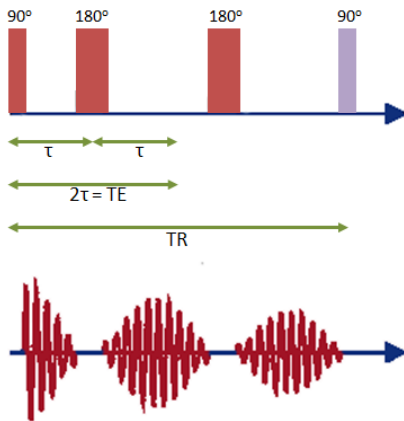
When acquiring MR data, two of the most important parameters to manipulate are the timing values corresponding to the repetition time (TR), and the echo time (TE). TR is the time between successive RF excitation pulses applied and determines the amount of  $T_1$ -weighting contribution to the image contrast. Longer TR allows more time for the RF excitation energy to be dissipated through spin-lattice relaxation, producing images with less  $T_1$  weighting. TE is the time between the excitation pulse and the peak of the echo signal (Figure 6). During this time interval, the transverse magnetization decays due to  $T_2$  and  $T_2^*$  relaxation effects.

Figure 6 contains a simplified scheme of one of the most common pulse sequences used in MRI, the spin-echo sequence. This sequence contains at least two RF pulses, an excitation pulse ( $90^\circ$ ) and one or more  $180^\circ$  refocusing pulses that generate the spin echo(es).

In a spin-echo sequence, the spins are initially excited by a  $90^\circ$  pulse, after which they dephase in the  $x$ - $y$  plane. This dephasing is not homogeneous, i.e., some loose phase faster than others. If, after a time delay  $\tau$ , the system is exposed to a  $180^\circ$  pulse,

a refocusing is initialized. Now the faster spins lie behind the slower ones, but at a time delay  $2\tau$  they catch up, which leads to an echo at time  $TE = 2\tau$ . A common analogy to the formation of an echo is a race (Figure 7) where faster runners separate from slower runners after the starting signal ( $90^\circ$  pulse). However, at a certain time during the race, the runners are transposed ( $180^\circ$  pulse). Now the faster runners are behind the slower ones, but they are able to catch up. All runners will reach the finishing line together (i.e., create an echo at the echo time  $2\tau = TE$ ).

Because of the relatively long  $T_1$  relaxation time of tissues, a delay of a couple of seconds may be necessary before repeating the excitation to let the magnetization recover. During this time a number of parallel slices can be excited. The number of slices obtainable can be calculated by dividing the TR by the time required for each slice. For example, if  $TR = 2000$  ms and  $TE = 80$  ms, the theoretically number of slices is 25 (in practice this number is reduced, since each slice requires slightly more than TE).



**Figure 6. Spin-echo pulse sequence.** The spin system is excited by a  $90^\circ$  pulse. After a time delay ( $\tau$ ) one or several  $180^\circ$  pulse follow. This leads to the formation of an echo. The time between the  $90^\circ$  pulse and the peak of the echo is called echo time (TE). The repetition time (TR) is the time between two complete pulse sequences.

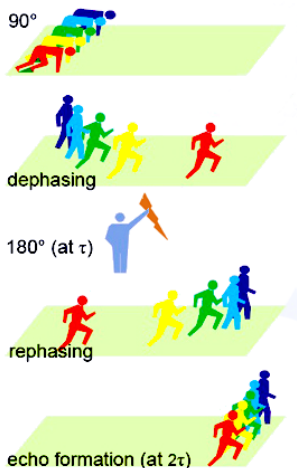


**Figure 7. The race analogy for the echo formation in a spin-echo pulse sequence.** At the time of the  $90^\circ$  pulse, all runners are lined up at the starting line. After the  $90^\circ$  pulse, the faster runners separate from the slower runners (dephasing). At a certain time during the race, the runners are transposed (at the time  $\tau$  when the  $180^\circ$  pulse is transmitted). Now the faster runners are behind the slower ones, but they catch up. All reach the finishing line together (i.e., create an echo at the echo time  $2\tau = TE$ ). Reproduced from Rinck, 2003.

**STRUCTURAL IMAGING**

Structural imaging relies on the fact that different types of tissue have different physical properties providing signals that can be translated in detailed maps of the brain. In a MR image different contrasts can be achieved by using different pulse sequences and manipulating the imaging parameters (e.g. TR, TE, pulse angle). What makes MRI useful for producing images of the brain is that different tissues exhibit different values for both  $T_1$  and  $T_2$  relative to each other. For any given point in time during the relaxation phase, the  $T_1$  of white matter signal is stronger than that of grey matter, and the grey matter signal is stronger than that of the cerebrospinal fluid (CSF) (Figure 8a). These differences in signal intensity are exactly opposite for a  $T_2$  measurement (Figure 8b).

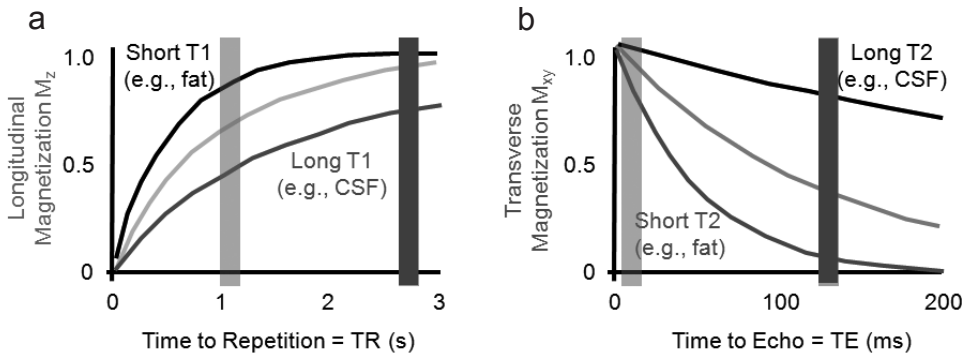


**Figure 8.  $T_1$  and  $T_2$  time constants for brain tissue.** **a.** For any given longitudinal magnetization relaxation time ( $T_1$ ) the white matter signal is stronger than that of grey matter, and the grey matter signal is stronger than that of the CSF. Images acquired at a short TR will be  $T_1$ -weighted (light-grey bar), while images acquired at long TRs will be more  $T_2$ -weighted (dark-grey bar). **b.** For any given transverse magnetization relaxation time ( $T_2$ ), the CSF signal is stronger than grey matter signal and the grey matter signal is stronger than that of white matter. Images acquired at a short TE will be  $T_1$ -weighted (light-grey bar), while images acquired at long TEs will be more  $T_2$ -weighted (dark-grey bar).

In general images have contrast, which depends on either proton density (PD),  $T_1$  or  $T_2$ , Figure 9. Proton density is related to the number of hydrogen atoms in a particular volume. Signal intensities on  $T_1$ ,  $T_2$ , and proton density-weighted images relate to specific tissue characteristics and allow discrimination between different types of tissue.

For quantitative structural brain analysis normally only  $T_1$ -weighted and  $T_2$ -weighted images are used.  $T_1$ -weighted imaging (Figure 9a) offers the greatest segmentation clarity

between grey matter, white matter and CSF, and is therefore most frequently used for quantitative MRI studies of brain morphology. On the other hand,  $T_2$ -weighted imaging (Figure 9b) may be preferably used for quantification of intracranial volume, given that these images have increased signal intensity of CSF that allows easier quantification of CSF and brain parenchyma together.

Furthermore,  $T_2$ -weighted and fluid attenuated inversion recovery (FLAIR) images are routinely used to detect areas of high signal intensity in NF1, Figure 9d. FLAIR images are  $T_2$ -weighted images with the CSF signal suppressed used to provide a better contrast between the lesion and brain parenchyma. The bright lesions observed in several patients with NF1 are nonspecific and tissue composition cannot be deduced based on their visual observation because prolongation of  $T_2$  relaxation occurs with pathologic lesions from different nature.

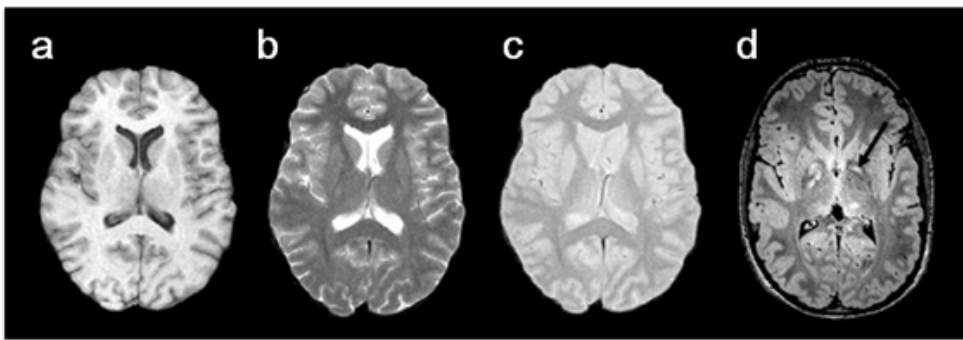


**Figure 9. Brain images with different contrasts.** a.  $T_1$ -weighted image. b.  $T_2$ -weighted image. c. Proton density weighted image. d. FLAIR image of a patient with NF1. Areas of hyperintensity in the image correspond to  $T_2$ w-hyperintensities. A black arrow points to one of these hyperintensities commonly designated unidentified bright objects (UBOs).

## FUNCTIONAL MAGNETIC RESONANCE IMAGING

The purpose of functional magnetic resonance (fMRI) is to measure brain activity. The brain is a highly active organ and neuronal activity consumes energy. To maintain neural cells functioning there is a constant supply of glucose and oxygen to the brain, delivered through an extensive network of blood vessels. The fact that blood flow and energy metabolism are tightly linked to neuronal activity is crucial to many functional imaging methods.



The neurovascular coupling ensures that when neuronal activity increases in a given region there is increased oxygen delivery by increasing blood flow to that region in a process denominated hemodynamic response. Oxygen is transported by haemoglobin and the state of haemoglobin impacts differently the MR signal. Oxyhaemoglobin (oxygenated haemoglobin) has diamagnetic properties (weak, negative susceptibility to magnetic fields, all the electrons are paired so there is no permanent net magnetic moment) and therefore does not distort the surrounding magnetic field, in turn, deoxyhaemoglobin (deoxygenated haemoglobin) is paramagnetic (positive susceptibility to magnetic fields associated with the presence of unpaired electrons) and leads to magnetic field distortions and signal loss. The local field inhomogeneities caused by deoxyhaemoglobin increase the speed of dephasing and the  $T_2^*$  in tissue around the vessels. This effect is the basis of the blood-oxygen-level-dependent (BOLD) contrast used in fMRI (Ogawa et al., 1990). BOLD is the most common functional imaging method applied in neuroscience.

The fMRI BOLD response is dependent on the hemodynamic response (Figure 10c), which can be divided into three phases:

- 1) *Initial dip* immediately after the onset of stimulation caused by a fast transient increase in oxygen consumption, that it is not immediately accompanied by a change in blood flow. It is caused by a small rise in the amount of deoxyhaemoglobin (Figure 10a);
- 2) *Positive BOLD response* as a consequence of increased cerebral blood flow, as well as increased cerebral blood volume. The increase in blood flow overcompensates for the amount of oxygen being extracted, so that an oversupply of oxygenated blood is delivered, Figure 10b. This means that the blood oxygenation actually increases following neural activation and levels of the oxygenated to deoxygenated haemoglobin ratio increase resulting in a more homogeneous local magnetic field. The BOLD effect, thus, measures increased neuronal activity indirectly via a change in local magnetic field homogeneity, which is caused by an oversupply of oxygenated blood. An overshoot might be present especially for long stimulation events as a consequence of a local oversupply of oxygenated haemoglobin;
- 3) *Post-stimulus undershoot* occurs upon cessation of the stimulus before the return of BOLD signal to baseline. This undershoot might be explained by an accumulation of deoxyhaemoglobin in vessels while cerebral blood flow and oxygen extraction rate have already returned to baseline. This could be caused by a vasodilatation of the venules and veins, because of their balloon-like elasticity, which results in an increase in deoxygenated venous blood volume.

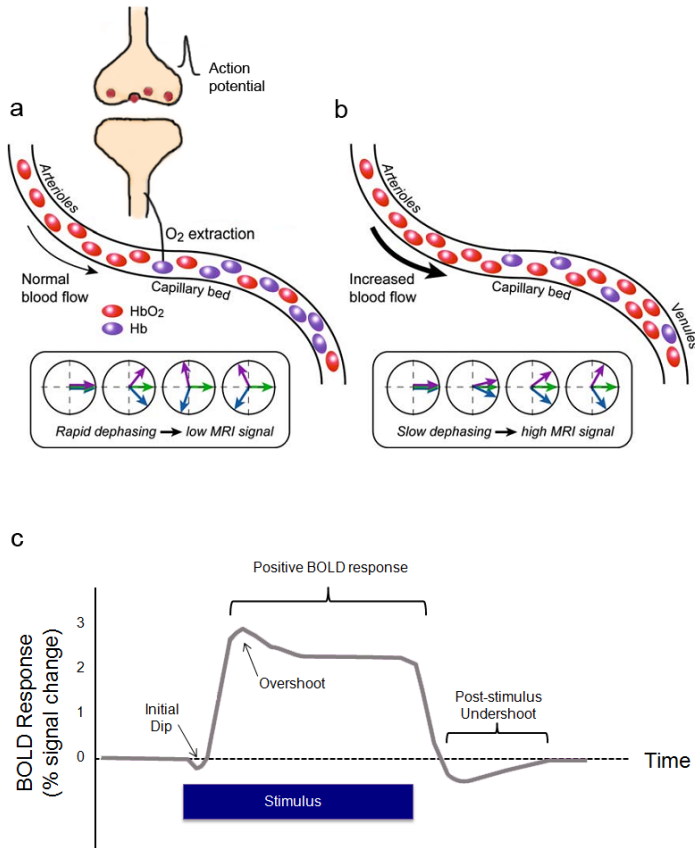


**Figure 10. The hemodynamic BOLD response.** **a.** Immediately after the onset of stimulation there is a fast transient increase in oxygen consumption that it is not immediately accompanied by a change in blood flow. This results in an increase of deoxygenated haemoglobin (Hb) to oxygenated haemoglobin (HbO<sub>2</sub>) ratio in the capillary bed and venules. Since Hb is paramagnetic, it distorts the magnetic field, which leads to rapid dephasing of excited spins resulting in a decrease in the MRI signal. This effect accounts for the initial dip observed in the hemodynamic BOLD response at **c.** **b.** If the cortical region is in activated state there is an increased oxygen extraction rate. However, the blood flow increases delivering oxygen beyond local need, which decreases the amount of Hb and increases HbO<sub>2</sub>. Since HbO<sub>2</sub> does not substantially distort the homogeneity of the local magnetic field, excited spins dephase slower resulting in an enhanced MRI signal (BOLD effect). This effect accounts for the positive BOLD response observed in **c.** When the stimulus is turned off there is an undershoot before returning to baseline, as a result of accumulation of deoxyhemoglobin in the venous blood. Adapted from Goebel, 2007.

In summary, enhanced neuronal activity resulting from activation of neurons leads to a local increase in energy and oxygen consumption in functional areas. However, the BOLD contrast depends not only on blood oxygenation but also on cerebral blood volume and cerebral blood flow, constituting a complex response controlled by several parameters. A relevant question is what neuronal mechanisms underlie BOLD signal. Combined BOLD fMRI and electrophysiological recordings demonstrated that fMRI responses mostly reflect the synaptic input and local intracortical processing, including the activity of excitatory and inhibitory interneurons (Logothetis et al., 2001; Goense and Logothetis, 2008). On the other hand, the interactions between neural activity and the vascular source of the fMRI signal, mainly related with the increase in blood flow remain less understood.

Although a clear understanding of how neuronal activity influences the fMRI response is important to interpret functional imaging data, BOLD fMRI has several advantages, it is noninvasive, has relatively high spatiotemporal resolution, and holds the capacity to demonstrate the network of brain areas engaged when subjects undertake particular tasks. One disadvantage is that it measures a surrogate signal whose spatial specificity and temporal response are subject to both physical and biological constraints.

A major goal in fMRI is to determine the neural bases of sensory, motor and cognitive processes. Additionally, fMRI enables the characterization of the response profile in various regions-of-interest (ROIs) by retrieving plots of averaged signal time courses (Figure 11). To study the activity of a certain brain area a task paradigm has to be developed, i.e. a strategy for presenting stimuli to subjects during an experiment. These paradigms are usually divided in two major categories: blocked designs or event-related designs.

In a blocked design a series of trials in one condition is presented during a discrete epoch of time. The signal acquired during one blocked condition is then compared to other blocks involving different task conditions. In a typical study, task blocks will range in duration from 16 s to a minute and multiple task blocks will be presented to allow the contrast of fMRI signals between task blocks. Event-related paradigms differ from blocked paradigms in that individual trial events (or even sub-components of trial events) are measured. Blocked designs are useful for obtaining high signal-to-noise information in neural processes that last a relatively long time. An example of a block design is shown in Figure 11.

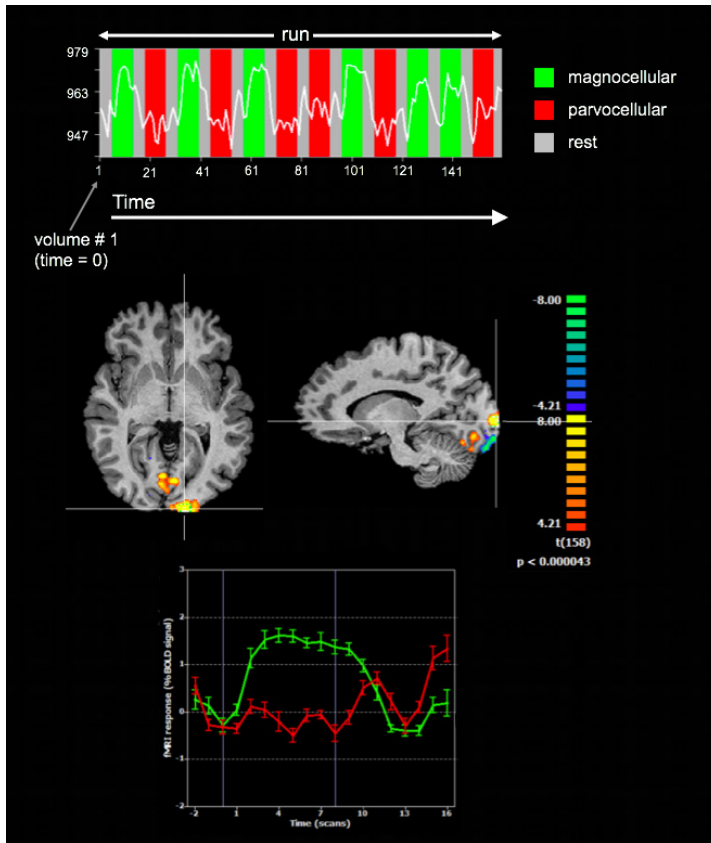


**Figure 11. fMRI activation as a result of a visual experiment comparing activation to magnocellular vs parvocellular stimuli.** An fMRI task paradigm is shown in the upper part of the figure. The horizontal axis represents time (volumes). The vertical axis represents the amplitude of the fMRI response. Each coloured segment corresponds to one condition. The green segments correspond to intervals where subjects were seeing a magnocellular stimulus; the red segments correspond to intervals where subjects were seeing a parvocellular stimulus; grey segments correspond to a control condition. White curves show BOLD responses for a selected group of voxels in the brain that is more activated by magnocellular than parvocellular stimulation. A statistical map of the comparison of activation to magnocellular vs parvocellular stimuli is shown in the middle part of the figure. Voxels responding more to magnocellular than parvocellular stimulus are coloured from red to yellow, while voxels responding more to parvocellular than magnocellular stimulus are coloured from green to blue. A region of 10 voxels was selected from the activation map (white cross indicates the centre of the region). The averaged signal time course plot corresponding to the selected region is shown in the lower part of the figure. The horizontal axis represents time (scans). The vertical axis represents BOLD percentage signal change in relation to the baseline (rest condition). Green depicts the time course of the BOLD response for the magnocellular condition and red for the parvocellular condition.

The presentation and recording of data during the complete task paradigm is called a run (4D volume composed of information on space and time). A run is composed of the repeated measurement of a functional volume (3D volume of the subject's brain every TR). The volume TR specifies the temporal resolution of the functional measurements since all slices comprising one functional volume are obtained once during that time. Each functional volume contains a complete set of slices, 2D representations of the brain that are one voxel thick.

Prior to statistical analysis data is pre-processed to reduce artifact and noise-related signal components. Statistical analysis aims at identifying those brain regions exhibiting increased or decreased responses in specific experimental conditions as compared to other (e.g. control) conditions. In the end, statistical maps are created for visualization and interpretation of the results, Figure 11.

## MAGNETIC RESONANCE SPECTROSCOPY

Magnetic resonance spectroscopy (MRS) makes it possible to directly, *in vivo*, assess biochemistry in localized brain regions, therefore adding a new dimension to non-invasive neuroimaging. MRS allows quantification of neurochemical compounds within localized regions of the brain, allowing assessment of neuronal and glial function, metabolic activity and neuronal degeneration. This technique has been widely applied in clinical research, especially as a biomarker of altered brain metabolism. More recently, its applications to neuroscience gained a new breath through the measurement of neurotransmitters and its correlation with behaviour (Edden et al., 2009; Jung et al., 2009; Stagg et al., 2011).

The product of MRS is a spectrum of different peaks at different radio frequencies and intensities (Figure 12). Specific nuclei contained in a metabolite give rise to either a single peak or multiple peaks that are uniquely positioned along the frequency axis. The peak positions are dependent on the chemical shift. The chemical shift is a consequence of the electronic cloud that surrounds the nucleus, which partially shields each nucleus in a given molecule from  $B_0$ . The electrons around the nucleus generate their own magnetic field, with opposite direction to the lines of force generated by the external magnetic field. This electronic magnetic field effect will cause nuclei with different electronic densities and chemical environments to yield different resonance frequencies from those

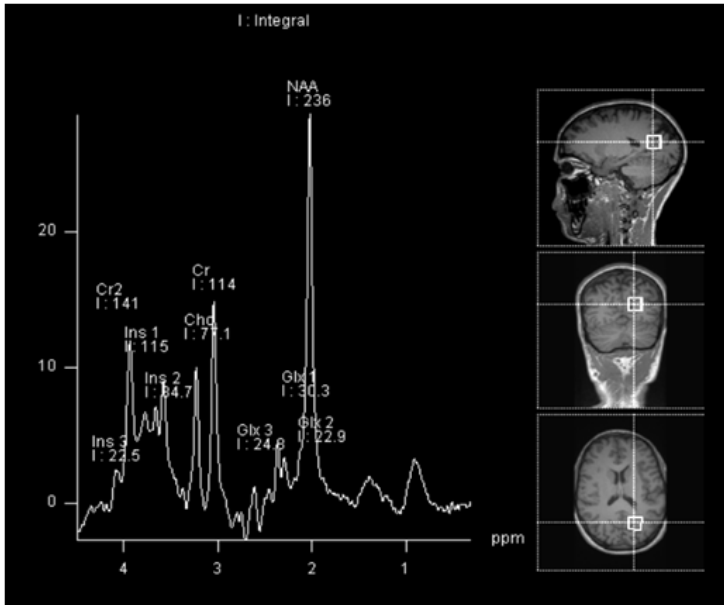


**Figure 12.** 3T spectrum of a voxel in the occipital cortex. The right part of the figure shows the location of the voxel and the left the spectrum. The spectrum is a plot of frequency (horizontal axis) expressed in ppm as a function of signal intensity (vertical axis). The signal intensities are proportional to the concentration of the metabolites in the spectrum. The frequencies are distinct for protons in different chemical environments of different molecules (NAA, N-acetylaspartate; Cr, creatine; Cho, choline; Ins, inositol; Glx, glutamate + glutamine).

defined by the applied external field  $B_0$ .

In general, each nucleus in a molecule experiences a unique shielding factor depending on the chemical environment of the nucleus. This shielding factor results in a slightly different total effective field experienced by each nucleus in a molecule and therefore different frequencies and peak positions in the spectrum.

The signal amplitude of a peak is directly related to the concentration of that metabolite, allowing quantitative determination.

Since molecules resonate at different frequencies when exposed to different magnetic fields, as stated in the Larmor Equation (Equation 1), a normalization of the MRS units was necessary. In that sense, the x-axis is expressed in parts per million (ppm), relative to a reference frequency. In this way, the position of the molecule in the x-axis will be the same regardless of the field strength at which the spectrum was acquired.

Although MRS can be conducted with any nucleus with an overall spin, we will focus on  $^1\text{H}$  MRS. It has several advantages: the proton is the most sensitive stable nucleus, al-

most every compound in living tissue contains hydrogen protons and there is no need for additional hardware to acquire spectra. However, there are technical issues that needed to be overcome. Probably, the biggest problem is the large signal from water molecules that obscures the metabolites signals. Indeed, while the concentration of water is around 36 M (resulting in a proton concentration of 70 M, because each water molecule has two protons), the metabolites we want to measure have a maximum concentration of 10 mM or less. Because of that several methods of water suppression have been developed (De Graaf, 2007). Another disadvantage of  $^1\text{H}$  MRS is the narrow chemical shift range of  $^1\text{H}$  signals (about 15 ppm). To overcome this problem several pulse sequences are designed to exploit  $T_1$  or  $T_2$  relaxation time differences (Frahm et al., 1989), resonance frequency, spin coupling and quantum coherence (Sotak, 1991). In chapter 4 we used a spectral editing technique to detect the neurotransmitter  $\gamma$ -aminobutyric acid (GABA) in the human brain.

Several metabolites are visible in a typical MR spectrum of the brain, but three major peaks characterize the spectrum, N-acetylaspartate (NAA), creatine/phosphocreatine (Cr/PCr) and choline (Cho) compounds. The description of the different metabolites and their biochemical relevance for the human brain can be found in several reports elsewhere (Ross and Bluml, 2001; Hajek and Dezortova, 2008). Briefly, NAA is located in neuronal mitochondria but its exact role as a metabolite is still under discussion (Moffett et al., 2007). NAA is considered to be a neuronal marker because it is almost exclusively located in neurons and its concentration is larger in grey matter than white matter. It constitutes the most prominent signal in  $^1\text{H}$  MRS spectra of the human brain. Cr/PCr are metabolites needed to the cell energetic supply and therefore considered markers of energetic metabolism. Finally, Cho signal is considered a marker of membranes, because it incorporates precursors or degradation products of the membrane phospholipids.

Recently, the application of spectroscopy to quantify the neurotransmitters GABA and glutamate allowed a window into the study of synaptic activity and plasticity important for the understanding of normal and pathological processes in the human brain.

## REFERENCES

- De Graaf RA *In vivo* NMR spectroscopy : principles and techniques, 2nd Edition. Chichester, West Sussex, England ; Hoboken, NJ: John Wiley & Sons 2007.

- Edden RA, Muthukumaraswamy SD, Freeman TC, Singh KD. Orientation discrimination performance is predicted by GABA concentration and gamma oscillation frequency in human primary visual cortex. *J Neurosci.* 29:50 (2009) 15721-15726.
- Frahm J, Bruhn H, Gyngell ML, Merboldt KD, Hanicke W, Sauter R. Localized proton NMR spectroscopy in different regions of the human brain in vivo. Relaxation times and concentrations of cerebral metabolites. *Magn Reson Med.* 11:1 (1989) 47-63.
- Goebel R. Localization of brain activity using functional magnetic resonance imaging. In: *Clinical Functional MRI Presurgical Functional Neuroimaging 2007.*
- Goense JB, Logothetis NK. Neurophysiology of the BOLD fMRI signal in awake monkeys. *Curr Biol.* 18:9 (2008) 631-640.
- Hajek M, Dezortova M. Introduction to clinical in vivo MR spectroscopy. *Eur J Radiol.* 67:2 (2008) 185-193.
- Jung RE, Gasparovic C, Chavez RS, Flores RA, Smith SM, Caprihan A, Yeo RA. Biochemical support for the “threshold” theory of creativity: a magnetic resonance spectroscopy study. *J Neurosci.* 29:16 (2009) 5319-5325.
- Logothetis NK, Pauls J, Augath M, Trinath T, Oeltermann A. Neurophysiological investigation of the basis of the fMRI signal. *Nature.* 412:6843 (2001) 150-157.
- Moffett JR, Ross B, Arun P, Madhavarao CN, Namboodiri AM. N-Acetylaspartate in the CNS: from neurodiagnostics to neurobiology. *Prog Neurobiol.* 81:2 (2007) 89-131.
- Ogawa S, Lee TM, Kay AR, Tank DW. Brain magnetic resonance imaging with contrast dependent on blood oxygenation. *Proc Natl Acad Sci U S A.* 87:24 (1990) 9868-9872.
- Rinck PA *Magnetic resonance in medicine: the basic textbook of the European Magnetic Resonance Forum, 5th Edition.* Oxford ; Boston: Blackwell Scientific Publications. 2003.
- Ross B, Bluml S. Magnetic resonance spectroscopy of the human brain. *Anat Rec.* 265:2 (2001) 54-84.
- Sotak CH. Multiple quantum NMR spectroscopy methods for measuring the apparent self-diffusion coefficient of in vivo lactic acid. *NMR Biomed.* 4:2 (1991) 70-72.
- Stagg CJ, Bachtir V, Johansen-Berg H. The role of GABA in human motor learning. *Curr Biol.* 21:6 (2011) 480-484.



# CHAPTER 3

## Research Methodology: patient and control groups

## **ETHICS STATEMENT**

The studies presented in this thesis were conducted in accordance with the Declaration of Helsinki and all procedures were reviewed and approved by the Ethics Commissions of the Faculty of Medicine of the University of Coimbra (Comissão de Ética da Faculdade de Medicina de Coimbra) and of the Paediatric Hospital of Coimbra (Comissão de Ética do Centro Hospitalar de Coimbra). Written informed consent was obtained from participants older than 18 years of age and from the parents/guardians in the case of participants younger than 18 years of age. Additionally, children and adolescents younger than 18 years of age gave written or oral informed consent.

## **PARTICIPANTS' RECRUITMENT AND SELECTION**

The patients involved in this study were diagnosed in the Genetics Department of the Paediatric Hospital of Coimbra in Portugal and were recruited to meet the following criteria:

### **Inclusion criteria**

- Age > 7 years
- NF1 diagnosis according to the criteria of the National Institutes of Health Consensus (National Institutes of Health Consensus Development Conference Statement: neurofibromatosis, 1988), as described in Panel 1, Chapter 1

### **Exclusion criteria**

- Presence of optic gliomas and/or other brain tumours
- Received cranial radiation therapy or chemotherapy
- Undergone brain surgery
- Epilepsy
- Traumatic brain injury
- History of psychiatric illness
- Being medicated for treating depression
- Severely impaired vision
- Full-scale intelligence quotient (IQ) < 70

The control groups for children and adolescents were recruited from a school with wide socioeconomic coverage and by informal advertising, whereas additional healthy adults were recruited from an adult further education center. Unaffected siblings and parents and spouses of patients with NF1 were also recruited (cases where these participants belong to the control group are explicitly referred in the methods section of the correspondent chapter). We included participants older than 7 years and excluded participants with any neurological disorder or presenting any of the criterion used to exclude patients with NF1. Moreover, the school records of all children and adolescents belonging to control groups were in accordance with their chronological age, indicating adequate intellectual functioning.

In the case of children on stimulant medication (methylphenidate), parents were requested not to give the medication on the days of testing, ensuring that these children were not under the influence of methylphenidate.

## RESEARCH TIMELINE

Patients visited our laboratory at least four times in a period comprised between September 2008 and December 2011, Figure 1.

In the first visit patients and control participants performed contrast sensitivity tasks, to assess achromatic and chromatic contrast sensitivity, and two neuropsychological tests, the Facial Recognition Test (FRT) (Benton, 1983a) (short version) and the Judgment of Line Orientation (JLO) (Benton et al., 1978) (Form H) (see description at section 7). The results of the contrast sensitivity study are published elsewhere (Ribeiro et al., 2012) and are beyond the scope of this thesis. The FRT and JLO neuropsychological tests were designed to probe visuoperceptual and visuospatial functions, respectively. Additionally, participants with 17 years old or older performed the first set of the Raven Standard Progressive Matrices (Raven et al., 1993) as an indication of non-verbal intelligence.

Cognitive evaluation for participants younger than 17 years old was performed using the Portuguese adapted version of the Wechsler Intelligence Scale for Children (WISC-III) (Wechsler, 2003). The administration and scoring of the cognitive tests was performed by a neuropsychologist. Administration of WISC-III was conducted in a separate visit (Visit 2) because of the time required for the evaluation (2 to 3 hours per participant).

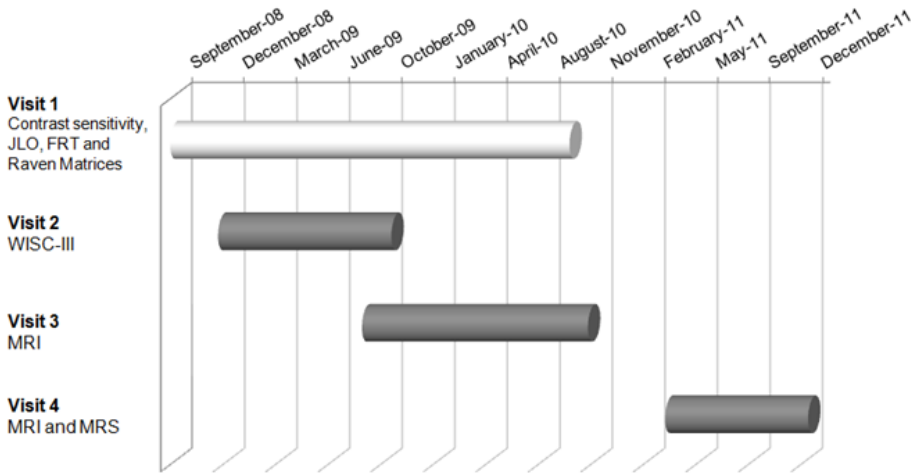


**Figure 1. Research timeline.** Data presented in this thesis are a result of a set of experiments conducted between September 2008 and December 2011. The duration of each period of experiments is showed with bars. The white bar corresponds to a set of studies that are beyond the scope of this thesis and belong to our larger research project on Neurofibromatosis type 1. However, a substantial cohort of patients was included in all our experiments. Additionally, a substantial group of controls participated in the experiments conducted during Visit 3. The scores obtained with the Raven Matrices in Visit 1 were used as part of participants' characterization. Grey bars indicate visits from which experiments were analysed in this thesis. (JLO, Judgment of Line Orientation; FRT, Facial Recognition Test; WISC-III, Wechsler Intelligence Scale for Children; MRI, Magnetic Resonance Imaging; MRS, Magnetic Resonance Spectroscopy).

Although the results of the studies performed during Visit 1 are beyond the scope of this thesis, the same group of patients as well as a substantial group of controls participated in the magnetic resonance imaging (MRI) experiments conducted between September 2009 and November 2010 (Visit 3). Furthermore, the Raven Standard Progressive Matrices scores were used as part of the adult participants' characterization reported in Chapter 4.

During the time period referred as Visit 3, 104 participants were scanned and those that did not presented any exclusion criterion were included in the study presented in Chapter 3. Additionally, a cohort of children and adolescents from this study were selected for the study presented in Chapter 6.

The last visit to our laboratory occurred between April 2011 and December 2011 (Visit 4). For this set of experiments only children and adolescents were recruited. The

group of patients was composed by the same participants and a new cohort of control subjects was recruited. A total of 53 participants were scanned and the results of the study are presented in Chapter 5.

### **GENETIC CHARACTERIZATION OF PARTICIPANTS WITH NF1**

To further characterize the NF1 population, patients' DNA was extracted from peripheral blood using standard procedures. The DNA was sent to the Institute of Medical Genetics at the University of Cardiff, where whole gene sequencing and multiplex ligation-dependent probe amplification analysis were carried out with the aim of identifying the disease causing NF1 mutations (Upadhyaya et al., 2009).

Briefly, the comprehensive NF1 gene mutation screen involved direct DNA sequencing of amplified exons and cDNA fragments and multiplex ligation-dependent probe amplification (MLPA) analysis. The 57 constituent exons of the NF1 gene were individually amplified with an M13-tagged specific primer set. RNA was reverse transcribed and the NF1 gene coding region amplified in 24 overlapping fragments. Mutations identified at the cDNA level were confirmed by direct cycle sequencing of genomic DNA.

### **RADIOLOGICAL ASSESSMENT**

All control and patient subjects were screened for intracranial abnormalities. Radiological examinations were performed by a neuroradiologist using anatomical data from T<sub>1</sub>-weighted Magnetization-Prepared Rapid Gradient-Echo (MPRAGE) and T<sub>2</sub>-weighted Fluid-Attenuated Inversion Recovery (FLAIR) sequences acquired at the Portuguese Brain Imaging Network using a 3T Siemens TimTrio scanner. Unidentified Bright Objects (UBOs), T<sub>2</sub>-hyperintensities commonly found in patients with NF1, were not considered exclusion criteria when present in patients (unless otherwise specified).

### **OPHTHALMOLOGIC ASSESSMENT**

Patients with NF1 were submitted to a complete ophthalmic examination, including best-corrected visual acuity, stereopsis evaluation (Randot Stereotest; Stereo Optical Co., Chicago, IL), slit-lamp examination of anterior chamber structures, and fundus exami-

nation performed by an experience ophthalmologist. This assessment ensured that patients were free of anomalies that could affect vision.

### VISUOSPATIAL AND VISUOPERCEPTUAL FUNCTION IN PATIENTS WITH NF1

The judgement of line orientation (JLO) test (Benton, 1983a) and the facial recognition test (FRT) (Benton, 1983b) are skewed for the function of the ventral (for FRT) and dorsal (for JLO) pathways, and were therefore used for the assessment of visuospatial and visuoperceptual skills in patients.

The JLO is a neuropsychological test widely used to assess visuospatial processing (Lezak, 1995), Figure 2a. It requires subjects to identify the orientation of pairs of lines on a multiple-choice display, which consists of 11 lines, each separated by an angle of  $18^\circ$ . The task consists of five practice examples, which contain test lines of the same length as those in the array. All subsequent lines are shorter than the array lines and comprise either the lower, middle or upper third of the array lines, making it more difficult to correctly assign the line to its match. No time limits are placed on individual items or the test as a whole.

The FRT test is used to assess face recognition abilities (Benton, 1983b). Subjects

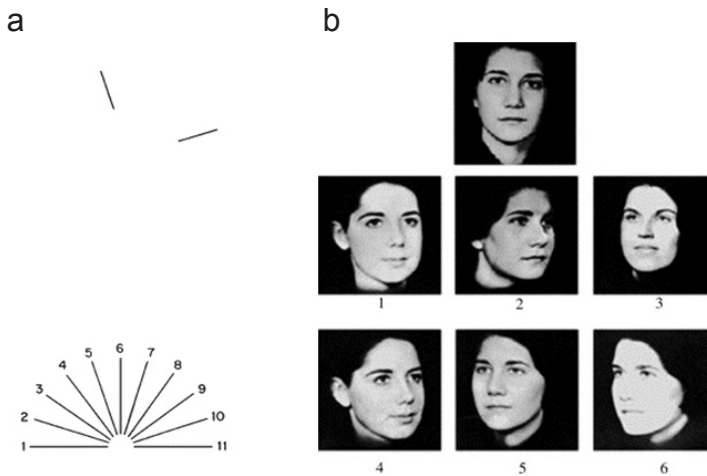


Figure 2. Examples of an item from the Benton judgement of line orientation test (a) and facial recognition test (b).

are presented with a series of items each of which composed of a target face above six test faces, and they are asked to indicate which of the six images match the target face, Figure 2b. Male and female faces are used, and the faces are closely cropped so that no clothing and little hair are visible. The faces are centered within a black background, and the entire image is  $\sim 6.5$  cm x 6.5 cm. For the first six items, only one of the six test faces displays the target individual, and the target image and the test image are identical. In the next seven items, three of the test faces match the target face, and the poses for the test images are different from the target image. No time limits are placed on individual items or the test as a whole.

The group of patients studied during this thesis performed significantly worse than a matched control group in the Facial Recognition Test (FRT) and the Judgment of Line Orientation (JLO) test (Ribeiro et al., 2012).

## REFERENCES

- Benton AL. Contributions to neuropsychological assessment : a clinical manual. New York: Oxford University Press. 1983a.
- Benton AL. Contribution to neuropsychological assessment : a clinical manual. New York ; Oxford: Oxford University Press. 1983b.
- Benton AL, Varney NR, Hamsher KD. Visuospatial judgment. A clinical test. *Arch Neurol.* 35:6 (1978) 364-367.
- Lezak MD. Neuropsychological assessment, 3rd Edition. New York: Oxford University Press 1995.
- National Institutes of Health Consensus Development Conference Statement: neurofibromatosis. Bethesda, Md., USA, July 13-15 1987. *Neurofibromatosis.* 1:3 (1988) 172-178.
- Raven J, Raven JC, Court JH. Manual for Raven's progressive matrices and vocabulary scales, 1993 ed. Edition. Oxford: Oxford Psychologists 1993.
- Ribeiro MJ, Violante IR, Bernardino I, Ramos F, Saraiva J, Reviriego P, Upadhyaya M, Silva ED, Castelo-Branco M. Abnormal achromatic and chromatic contrast sensitivity in Neurofibromatosis type 1. *Invest Ophthalmol Vis Sci.* 53:1 (2012) 287-293.
- Upadhyaya M, Spurlock G, Kluwe L, Chuzhanova N, Bennett E, Thomas N, Guha A, Mautner V. The spectrum of somatic and germline NF1 mutations in NF1 patients with spinal neurofibromas. *Neurogenetics.* 10:3 (2009) 251-263.
- Wechsler D. Escala de Inteligência para Crianças - Terceira Edição (WISC-III): Manual. Lisboa: Cegoc-Tea 2003.





# RESULTS



## CHAPTER 4

Abnormal brain activation in  
Neurofibromatosis type 1:  
a link between visual processing  
and the default mode network

**ABSTRACT**

Neurofibromatosis type 1 (NF1) is one of the most common single gene disorders affecting the human nervous system with a high incidence of cognitive deficits, particularly visuospatial. Nevertheless, neurophysiological alterations at low-levels of visual processing that could be relevant to explain the cognitive phenotype, are poorly understood. Here we used functional magnetic resonance imaging (fMRI) to study early cortical visual pathways in children and adults with NF1. We employed two distinct stimulus types differing in contrast and spatial and temporal frequencies to evoke relatively different activation of the magnocellular (M) and parvocellular (P) pathways. Hemodynamic responses were investigated in retinotopically-defined regions V1, V2 and V3 and then over the acquired cortical volume. Relative to matched control subjects, patients with NF1 showed deficient activation of the low-level visual cortex to both stimulus types. Importantly, this finding was observed for children and adults with NF1, indicating that low-level visual processing deficits do not ameliorate with age. Moreover, only during M-biased stimulation patients with NF1 failed to deactivate or even activated anterior and posterior midline regions of the default mode network. The observation that the magnocellular visual pathway is impaired in NF1 in early visual processing and is specifically associated with a deficient deactivation of the default mode network may provide a neural explanation for high-order cognitive deficits present in NF1, particularly visuospatial and attentional. A link between magnocellular and default mode network processing may generalize to neuropsychiatric disorders where such deficits have been separately identified.

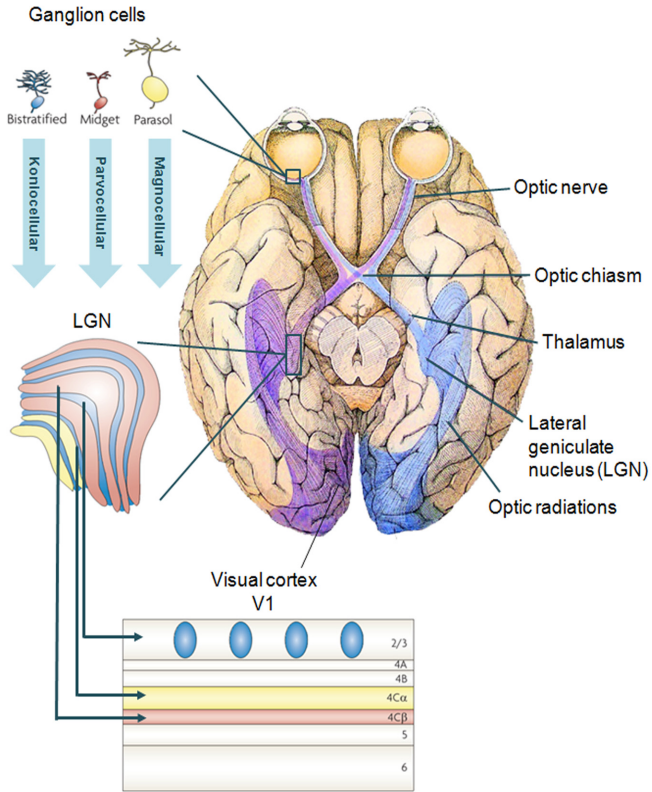
## INTRODUCTION

Neurofibromatosis type 1 (NF1) is commonly associated with cognitive impairment and learning disabilities. The neuropsychological deficits reported include visual perception, motor, visuomotor, language, memory and attention domains (Riccardi, 1992; Friedman et al., 1993; North, 2000; Levine et al., 2006). In particular, visuospatial deficits are considered to be one of the hallmark characteristics of the NF1 cognitive profile (Hyman et al., 2005; Rowbotham et al., 2009).

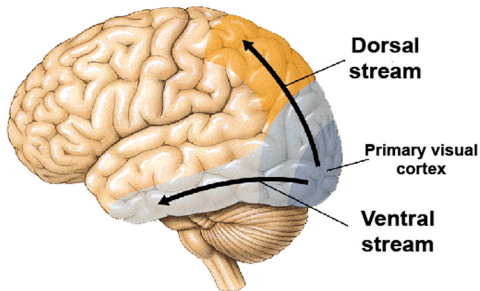
In previous studies visuospatial deficits were mainly assessed using behavioural neuropsychological tests (Eliason, 1986; Eldridge et al., 1989; Hofman et al., 1994; Bawden et al., 1996; Dilts et al., 1996; Schrimsher et al., 2003). The test most often documented to show visuospatial deficits is the Judgment of line Orientation (JLO) test (Levine et al., 2006). In order to unravel the neural mechanisms underlying the JLO deficits in NF1, Clements-Stephens and colleagues (Clements-Stephens et al., 2008) performed a functional magnetic resonance imaging (fMRI) study using an adaptation of this task. They reported that participants with NF1 had more neuronal activity in the left than the right hemisphere across anterior and posterior regions, while controls showed the opposite pattern. Furthermore, they found lower neural activation in Brodmann area 17 of patients with NF1, an area that roughly corresponds to the primary visual cortex (V1). This constituted an early observation of a deficit in the visual cortex. The fact that performance on visuospatial tasks is impaired in individuals with NF1 suggests that information processing in early visual areas might be deficient.

In the early visual system information is transmitted from the retina to the cortex via three parallel channels: the magnocellular (M), parvocellular (P) and koniocellular pathways, Figure 1a. Although these pathways may be difficult to differentiate *in vivo*, one can take advantage of the physiological properties of their constituent neurons and respective circuits (Leventhal, 1991) to generate stimuli with a preferential bias activation of each pathway. Magnocellular population responses are relatively tuned to achromatic stimuli with low spatial and high temporal frequencies and they provide the dominant input to the dorsal stream (Figure 1b), which plays an important role in spatial localization and motion processing. The parvocellular pathway is more sensitive to stimuli with low temporal and high spatial frequencies and projects primarily to the ventral stream (Figure 1b), important in object processing. Additionally, at low contrast levels visual information is primarily conveyed via the magnocellular system (Livingstone and Hubel, 1988). The function of the koniocellular pathway is less defined, but it is known to play a role in colour vision (Hendry and Reid, 2000).

a



b



◀ **Figure 1. Visual Pathways. a.** Visual information is initially encoded in the retina where photoreceptors transduce the pattern of light into an electrochemical signal. Specialized circuits extract basic sensory cues, such as spatial contrast and temporal frequency and encode these properties into the ganglion cells (GC), which fibers form the optic nerve. Each ganglion cell conveys different aspects of the visual input simultaneously to the brain. Three GC types are particularly well characterized: midget, parasol and small and large bistratified. Midget GCs are considered to be the origin of the parvocellular pathway, they project to the parvocellular layers of the lateral geniculate nucleus (LGN), which in turn project to layer 4C $\beta$  of V1 (red). Parasol GCs are considered to be the origin of the magnocellular pathway, they convey information to the magnocellular layers of the LGN, which projects to layer 4C $\alpha$  of V1 (yellow). Small and large bistratified GCs make part of the koniocellular pathway and convey signals to koniocellular layers 3 and 4 of the LGN, which in turn projects to layer 1 and to the cytochrome oxidase blobs of layer 2/3 (blue) in V1. Adapted from Zeki, 1993 and Nassi and Callaway, 2009. **b.** Dorsal and ventral streams originate in the primary visual cortex. The dorsal stream spreads from V1 dorsally to the parietal lobe, while the ventral stream spreads to the temporal lobe.

Recently, we showed abnormalities in low-level sensory processing using psychophysical measures of contrast sensitivity. Our results indicated relative deficits in the M and P channels, with preserved koniocellular function in individuals with NF1 (Ribeiro et al., 2012). However, the neural substrates of visual impairments in this condition are still poorly understood.

In the present study, we focused on the activation of the early cortical visual system, V1, V2 and V3, and we used stimuli with different contrast and different temporal and spatial frequency properties to provide a relative bias concerning the activation of the M or P pathways. Our aim was to establish the functional status of the early visual cortex in patients with NF1. The human visual cortex is divided in several functional areas with distinct local neural properties (Zeki and Shipp, 1988). Area V1 plays a critical role in visual processing because most of the visual information reaching the rest of the visual cortex is first processed in this region. It differs from other cortical areas by having a higher density of neurons, particularly in layer 4 (Rockel et al., 1980). This layer is packed with spiny stellate cells (Douglas and Martin, 1998) and has a thick band of myelinated axons travelling from sublayers 4C $\alpha$  to 4B, known as the stria of Gennari. Because of this band, V1 is historically named striate cortex, and the term extrastriate denotes the rest of visual cortex. V1 neurons are tuned for a number of attributes, including orientation (Hubel and Wiesel, 1959), direction of motion (Carandini et al., 1998), spatial and temporal frequency (De Valois and De Valois, 1988), binocular depth (Cumming and DeAngelis, 2001) and colour selectivity (Horwitz and Hass, 2012).

V1 is bordered by two cortical regions that form area V2. Functionally, V2 has many properties in common with V1, such as selectivity for orientation, colour, stereoscopic disparity and motion (Boynton and Hegde, 2004). While a lesion in V2 spares visual acuity and contrast sensitivity it affects the ability to perform more complex spatial tasks (Merigan et al., 1993). Neurons in V2 are sensible to complex properties such as texture perception (El-Shamayleh and Movshon, 2011) and encoding of illusory contours (Dillenburger and Roe, 2010). There is a relative lack of information concerning the functional role of V3, and its receptive fields are generally larger than in V1 and V2. Studies in the macaque monkey revealed that the dorsal part of V3 has more neurons selective for direction than for colour, while the pattern reverses in ventral V3 (Lyon and Connolly, 2012). M and P information is merged at V1 and V2 and then distributed to both dorsal and ventral streams (Levitt et al., 1996). Dorsal stream connections are more specifically dominated by M inputs whereas ventral connections have a mixed contribution of M and P inputs.

The organization of the visual cortex is such that the visual field is represented several times in the occipital cortex with a topographic organization (Hubel and Wiesel, 1977; Zeki, 1978; Hubel and Livingstone, 1987). This topographic/retinotopic organization means that nearby regions in the retina project to nearby cortical regions. The retinotopic organization is particularly clear in the early visual areas V1, V2, and V3, Figure 2. Retinotopic representations can be mapped using fMRI, provided that the subjects fixate, because the visual field shifts with eye position, and visual stimuli are presented at several locations (Engel et al., 1994; Sereno et al., 1995). Mapping between the retina and the cortex can be described as a log-polar transformation, in which standard axes in the retina are transformed into polar axes in the cortex, according to a logarithmic transformation (Grill-Spector and Malach, 2004). The phase (angle from the horizontal axis) component of the retinotopic map reveals meridian representations (Figure 2a), while eccentricity describes the distance from the fovea. The representation of the fovea is greatly expanded compared to the representations of the periphery, Figure 2b.

In the present study we used retinopic mapping to define cortical visual areas V1, V2 and V3 for each subject, as they provide topological criteria that are the most certain for defining a cortical visual area (Felleman and Van Essen, 1991). Given inter-subject variability (Dougherty et al., 2003), the boundaries of each visual area have to be mapped for each subject. The importance of studying well-defined visual areas is that they constitute an important part of primate brain organization. Moreover, better understanding



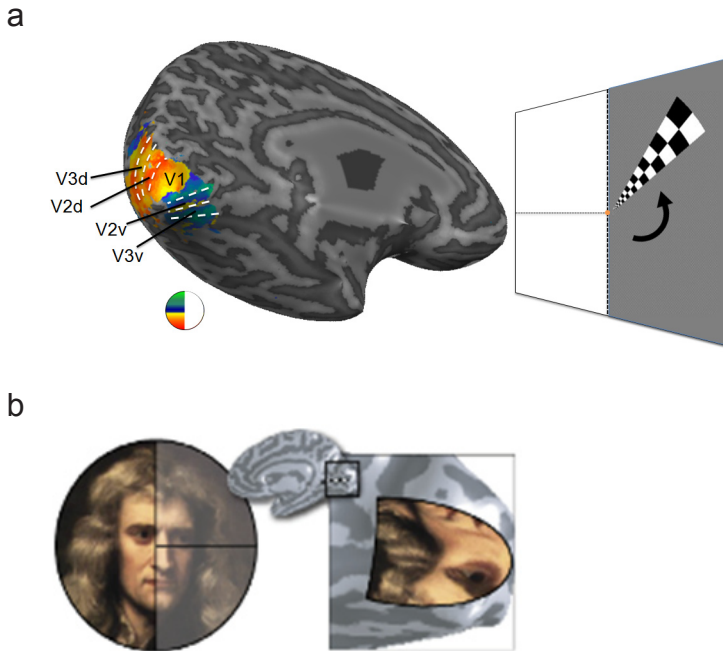


**Figure 2. Representation of the visual field in visual cortex. a.** Visual field maps are measured in the left hemisphere of a single subject using a rotating wedge stimulus. The visual areas V1, V2 and V3 of the left visual field are represented in a smoothed representation of the white matter surface. The colour overlay at the bottom left of the image indicates the angle (with respect to the centre of gaze) that produces the most powerful response at each cortical location. Area V1 represents a hemifield of the contralateral visual space, so that the left hemisphere V1 represents the right half of the visual field and vice versa. Dorsal (d) V2/V3 represents the lower quarter of the visual field and ventral (v) V2/V3 the upper quarter. **b.** Illustration of the visual field map in V1. The left visual field stimulates V1 in the right hemisphere; the image representation is inverted, and the centre of the visual field, near the eye, is greatly expanded (cortical magnification). Adapted from Wandell et al., 2007.

of visual deficits in a neurodevelopmental disorder can be achieved by investigating how visual processing is performed in segregated areas.

Based upon our prior study (Ribeiro et al., 2012), we hypothesized that patients with NF1 would show impairments in activation of low-level visual areas, and therefore we conducted confirmatory analysis in retinotopically-defined areas, V1, V2 and V3. Additionally, we investigated the activation pattern of high-level visual and non visual regions modulated by the different stimuli to examine possible functional consequences of low-level visual impairments.

## MATERIALS AND METHODS

### Participants

Ninety one individuals participated in this study: 25 children and adolescents with NF1, 29 control children and adolescents, 17 adults with NF1 and 20 control adults. Due to the exclusion criteria defined concerning intracranial abnormalities, neuropsychological assessment, performance on the behavioural task and movement within MRI acquisitions (see below), 24 participants were excluded from our analysis. Thus, for analysis, we included: 15 children and adolescents with NF1, 24 chronological age-matched control children and adolescents, 13 female adults with NF1 and 15 chronological age-matched control female adults. Demographic details are shown in Table 1.

Participants with NF1 were recruited and diagnosed in collaboration with the Clinical Genetics Department of the Paediatric Hospital of Coimbra according to the NIH defined diagnostic criteria (National Institutes of Health Consensus Development Conference Statement: neurofibromatosis., 1988). For the children/adolescent control group, participants were recruited among unaffected siblings and from a local school. The adult control group was recruited among the unaffected parents or from an adult educational school. These adult schools provide learning programs for adults with low educational levels and many adult participants with NF1 are also attendants.

In order to ensure that participants included in the study had no central nervous system pathology, a FLAIR MRI sequence was performed in addition to the standard structural scan. Neuroradiological assessment was carried out by an experienced neuroradiologist. Participants were excluded from this study if they had a clinically significant intracranial abnormality on MRI ( $n= 6$  individuals with NF1, 2 controls) such as intracranial tumor, optic glioma or other imaging abnormalities. UBOs (Unidentified Bright Objects - T2 hyperintensities, commonly found in patients with NF1) were not considered exclusion criteria.

None of the participants had a psychiatric illness, epilepsy or were taking medication for treating depression. Participants were also excluded if they had full-scale IQ below 70, for the children/adolescent groups, or Raven score below 3 ( $n= 1$  NF1), in the adult groups. Parents of children on stimulant medication for attention deficit hyperactivity disorder (ADHD) were requested not to give their children the medication on the days of testing ( $n= 2$  NF1, 1 control). All the participants had normal or corrected-to-normal visual acuity.

Ophthalmological assessment was performed by an experienced ophthalmologist to rule out eye disorders in the NF1 group. This included best-corrected visual acuity, stereopsis evaluation using Randot, slit lamp examination of anterior chamber structures and fundus examination. No anomalies that could affect vision were found.

### Neuropsychological assessment

Participants younger than 17 years old received the Portuguese adapted version of the Wechsler Intelligence Scale for Children (WISC-III) (Wechsler, 2003), while 17 years old or older participants performed the first set of the Raven Standard Progressive Matrices (Raven et al., 1993) as an indication of non-verbal intelligence. Three control children/adolescents and one adolescent with NF1 were unavailable to perform IQ tests. However, their school records were in accordance with their chronological age, indicating adequate intellectual functioning. Neuropsychological details are shown in Table 1. Children with NF1 presented significantly lower full-scale IQ (FSIQ) score than control children ( $p=0.013$ ). In the adult groups, the average Raven scores between NF1 and the control group were not statistically different.

**Table 1. Demographic and neuropsychological characteristics of patients and control groups**

	Children and adolescents		Adults	
	NF1, n=15	Controls, n=24	NF1, n=13	Controls, n=15
Age (years)				
Mean $\pm$ SD	11.7 $\pm$ 2.9	12.0 $\pm$ 2.3	33.1 $\pm$ 4.9	32.7 $\pm$ 5.6
Range	7 – 17	7 – 16	25 – 42	26 – 44
Gender ratio				
Female/Male	9/6	13/11	13/0	15/0
Full-scale IQ (WISC-III)				
Mean $\pm$ SD	96.9 $\pm$ 16*	113.0 $\pm$ 19.7	-	-
Raven score				
Mean $\pm$ SD	-	-	6.7 $\pm$ 2.4	7.8 $\pm$ 2.9

Significant differences between NF1 patients and controls are indicated by \* $p<0.05$ .

### Stimuli and task design

*Retinotopic mapping.* The boundaries of low-level retinotopic visual areas were defined

employing a fast approach using the polar angle of the standard retinotopic mapping procedure (Engel et al., 1994; Sereno et al., 1995), Figure 2a. Polar angle maps were obtained using a black and white checkerboard wedge flickering at 8 Hz in counterphase (48 s full cycle, 4 cycles per scan and two scans per subject) centred around an orange-coloured fixation point. Polar angle maps provide the information of angle reversion needed to properly delineate both dorsal and ventral visual areas of V1, V2 and V3.

*M- and P-biased stimulation.* Stimuli were pattern-reversed checkerboards filling the entire screen (30.3° x 23.1°) designed using the Psychophysics Toolbox for Matlab (Brainard, 1997). To bias the activation of the M-pathway we used stimuli with low spatial frequency, 0.25 cycles per degree (cpd) fundamental frequency, and high temporal frequency (18 Hz), with low contrast (18%) that preferentially activates (though not exclusively) the M pathway. This stimulus is similar to the one used by Liu et al (Liu et al., 2006a). P-biased stimulation was achieved using a higher spatial frequency (2 cpd), lower temporal frequency (2 Hz) and 100% contrast. Stimuli were presented in a block-design composed of 6 blocks for each stimulus (16 seconds per block) randomly presented and interleaved with a rest condition (fixation only, 10 seconds), Figure 3. To maintain subjects engaged and to control for attention and fixation participants were asked to fixate a central dot and report a subtle colour change, from red to pink and the other way around, with a button press. Time intervals between colour changes were chosen randomly from 2, 4, 6, 8 or 10 seconds. The task ran throughout the experiment.

Only participants with a high level of detection (>85%) and a low rate of false alarms (<0.3, calculated as the ratio between the number of false alarms and the number of colour changes) were included in these study. 4 patients with NF1 and 4 control participants were excluded by not meeting these criteria.

Stimuli were projected using an LCD projector (AVOTEC Silent Vision 6011, Florida, USA) onto a screen that participants viewed via a fixed mirror placed on the MRI head coil. Participants' eyes were monitored with a camera placed on the mirror system (Avotec Real Eye 5721, Florida, USA).

### **Imaging procedures**

Scanning was performed on a 3T Siemens TimTrio scanner at the Portuguese Brain Imaging Network, using a 12-channel birdcage head coil. For each participant we acquired: i) two T<sub>1</sub>-weighted (T<sub>1w</sub>) MPRAGE sequences, 1x1x1 mm voxel size, repetition time (TR) 2.3 s, echo time (TE) 2.98 ms, flip angle (FA) 9°, field of view (FOV) 256x256, 160 slices;

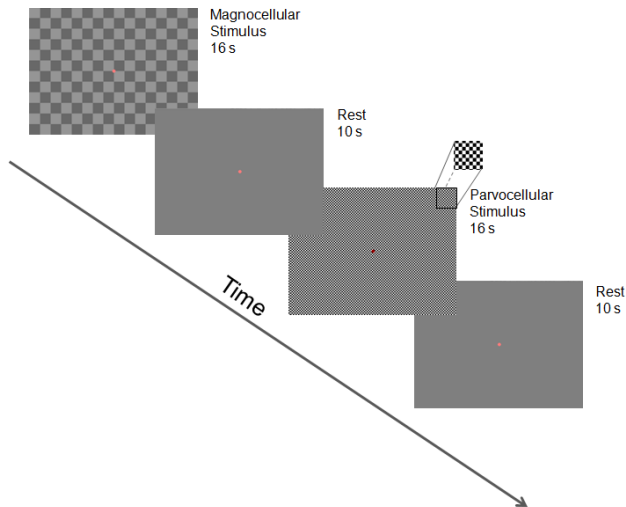


**Figure 3. A schematic diagram of the design for the M/P-biased stimulation.** Stimuli were presented in a random order. Each stimulus was presented 6 times (16 seconds per stimulus) and interleaved with a rest condition (fixation only, 10 seconds). To maintain subjects engaged and to control for attention and fixation participants were asked to fixate a central dot and report a subtle colour change, from red to pink and the other way around, with a button press. A patch of the parvocellular stimulus is shown enlarged.

ii) a  $T_2$ -weighted ( $T_2w$ ) FLAIR sequence, 1x1x1 mm voxel size, TR 5 s, TE 2.98 ms, Inversion Time (TI) 1.8 s, FOV 250x250, 160 slices; iii) one run of fMRI scanning for the M/P-biased stimuli and two runs of the polar angle stimuli using single shot echo planar imaging (EPI) acquired in the axial plane orthogonal to the anterior commissure covering the occipital, temporal and frontal cortices, with 2x2x2 mm voxel size, TR 2 s, TE 39 ms with a 128x128 matrix, FA 90°, FOV 256x256, 26 slices.

FLAIR images were used to identify  $T_2$  hyperintensities, a common neuroradiological finding in patients with NF1. A neuroradiologist, who was blind to the participants' clinical history observed the MR structural scans and reported on the distribution and number of UBOS. Twelve of the fifteen (80 %) children and seven of the thirteen (53.8 %) adults with NF1 had one or more UBOS. The frequency of UBOS is in accordance with published data (Payne et al., 2010). None of the control participants had UBOS.

## Image Analysis

Image processing and analysis were carried out using BrainVoyager QX 2.1 (Brain Innovation, Maastricht, The Netherlands). Analyses to determine total intracranial volume were performed using Statistical Parametric Mapping 8 (SPM8, <http://www.fil.ion.ucl.ac.uk/spm>).

*Image processing and analysis in retinotopically-defined areas:*

*Anatomical Image processing.* High-resolution T<sub>1w</sub> anatomical images were averaged, intensity normalized and re-oriented into a space where the anterior and the posterior commissure lie in the same plane (AC-PC). Afterwards, cortex was segmented using automatic segmentation routines (Kriegeskorte and Goebel, 2001), mesh representations of each hemisphere were created and inflated for polar angle maps projection.

*Functional Image Processing.* We applied slice scan time correction, linear trend removal, temporal high-pass filtering (2 cycles per run), modest spatial smoothing (FWHM 2mm, yielding a small but clear smoothing effect) and a correction for small interscan head movements. Participants were excluded from further analysis if any within-run movement exceeding 2 mm was detected (n= 2 NF1, 4 controls).

*Retinotopic mapping.* Polar angle maps were obtained from the average of two runs, created based on linear regression analysis and projected onto the AC-PC anatomical surfaces of each subject. The cross-correlation was calculated for each run, as a function of the time lag (in TR units, 2 seconds per lag). Lag values at each voxel were encoded in pseudocolors, voxels were included into the statistical map if  $r > 0.25$ ,  $p < 0.05$ . Retinotopic areas V1, V2 dorsal (d), V2 ventral (v), V3d and V3v were manually defined for each subject in each hemisphere in the inflated meshes, Figure 2a. Obtained regions-of-interest (ROIs) were used as “masks” to the analysis of the blood-oxygen-level-dependent (BOLD) signal elicited by M- and P-biased stimulation.

*M- and P-biased stimulation.* Statistical analyses were performed on individual and group data using the general linear model (GLM). Predictors for the response to M- and P- biased stimulation were obtained by convolution of a condition box-car time course with a two-gamma function (Friston et al., 1998). Retinotopically-defined areas were used as ROIs to perform ROI analysis on each subject in the AC-PC space. Within each ROI, a GLM for the M/P-biased stimuli experiment, corrected for temporal serial correlations, was computed and the individual beta values evoked by each stimulus were retrieved and analysed using PAWS Statistics 18.

*Volume-based processing and analysis of cortical activation:*

We were interested in effects that could be generalized to children, adults and overall population irrespective of age and thus we compared the NF1 studied group (children, adolescents and adults) with a matched control group.

Since benign macrocephaly is common in NF1, previous fMRI studies were restricted to ROI analysis (Billingsley et al., 2003; Clements-Stephens et al., 2008; Shilyansky et al., 2010). To overcome this methodological difficulty and be able to perform whole-brain analysis we ensured that the total intracranial volume was not statistically different between matched clinical groups.

*Total intracranial volume measurements.* Total intracranial brain volume for each subject was calculated with the VBM8 toolbox in SPM8. Group comparisons for brain volume were evaluated with independent samples t-tests.

In the children groups, we observed no significant differences in total intracranial volume, which makes it valid to perform normalization procedures and group analysis since it is unlikely that systematic variances in the warping procedure result in false group differences. Adults, however, presented a significant difference in total intracranial volume. Therefore, for this analysis we excluded the 4 control participants with the smallest brain volumes. We analysed 13 patients with NF1 and 11 controls with no intracranial volume significant group difference. Moreover, the overall control and NF1 groups composed by children and adults (without the 4 previously excluded adult participants) did not present a difference in total intracranial volume.

*Cortex-based alignment.* Whole-volume statistical comparisons regarding the activation to the M/P-biased stimuli were conducted in the cortical surface space after performing cortex-based alignment. In order to do that, brains previously transformed to AC-PC space were normalized into Talairach standard space (Talairach and Tournoux, 1988). Following normalization we performed the segmentation routine applied in BrainVoyager. The reconstructed folded cortical representations of each subject and hemisphere were morphed into a spherical representation and aligned to all the other subjects' spheres iteratively (Formisano et al., 2004; Goebel et al., 2006). This procedure was conducted to improve the spatial correspondence mapping between subjects' brains (Fischl et al., 1999). It has been demonstrated that cortical alignment substantially improves group results by reducing anatomical variability (Fischl et al., 1999; Jo et al., 2007). Cortex-based alignment was performed for the children, adult and overall groups separately.

*Group comparisons of the neural activity elicited by the M- and P-biased stimuli in aligned cortices.* Statistical analysis was performed using Random effects (RFX) analyses in order to generalize findings to the population level (Penny, 2003). In the first stage, a whole-volume RFX GLM was performed to estimate condition effects (beta values) separately for each subject and stimuli. At the second level, an independent samples t-test was used to compare patients and controls for each stimulus category. Statistical maps were corrected for multiple comparisons using cluster-size thresholding (Forman et al., 1995; Goebel et al., 2006). Each map was thresholded at  $p < 0.01$  uncorrected and, for correction, submitted to cortex-based cluster threshold estimation based on a Monte Carlo simulation with 1000 iterations. This procedure yielded a statistical map with a cluster size of 45 mm<sup>2</sup> for the adults group and 41 mm<sup>2</sup> for the children and overall groups, corresponding to a corrected  $\alpha$  value of  $p < 0.05$ .

We examined the BOLD timecourses in voxel clusters with statistical significant differences between the clinical groups, NF1 and control. The functional response profiles for each group were reported after the subtraction of the fixation condition from the timecourse.

### **Demographic, Neuropsychological, Behavioural and BOLD activation in retinotopically defined areas analyses**

Statistical analyses were performed with PAWS Statistics 18 (SPSS Inc., Chicago, USA). First, we verified the normality assumption for the different parameters using the Shapiro Wilk's test. For normally distributed data, we used independent samples t-tests, ANOVA and Pearson's correlation analyses. When the data did not meet assumptions of sphericity, we used the epsilon value to choose the type of correction applied: the Huynh-Feldt (for  $\epsilon > 0.75$ ) or the Greenhouse–Geiser (for  $\epsilon < 0.75$ ). For the non-normal data, we used the Mann-Whitney test for comparison between two independent samples.

## **RESULTS**

### **Behaviour**

There was no between group differences on the performance in the behavioural task, neither for children nor for adult clinical groups. Both NF1 patients and controls responded to the fixation task, which imposed a moderate attentional load, with a high



degree of accuracy (above 95% correct trials) and low number of false alarms.

### Activity in retinotopically defined areas

The magnitude of activation elicited by the M- and P-biased stimuli was retrieved from low-level visual areas V1, V2d, V2v, V3d and V3v of each subject's hemispheres. Analysis was performed on 15 children with NF1, 24 control children, 13 adults with NF1 and 15 control adults. First, we performed a repeated measures ANOVA using stimuli (M-biased vs P-biased), visual area (V1, V2d, V2v, V3d, V3v) and hemisphere (left vs right) as within subjects variables and clinical group (NF1 vs controls) and age group (children vs adults) as between subjects factors.

We found a highly significant effect of clinical group [ $F_{(1,63)}=12.892, p<0.001$ ] and a significant effect of age group [ $F_{(1,63)}=5.988, p=0.017$ ] with no interaction between clinical group and age group [ $F_{(1,63)}=0.133, \text{NS}$ ], indicating a similar deficit in visual activation in both children and adults with NF1. Besides, we found a significant effect of stimulus type [ $F_{(1,63)}=76.818, p<0.001$ ], visual area [ $F_{(1,63)}=38.039, p<0.001$ ] and an interaction between stimulus type and visual area [ $F_{(4, 236)}=84.595, p<0.001$ ]. Differences between patients and controls were indicated by the overall clinical group effect and also by significant interactions in visual area x clinical group [ $F_{(4, 228.3)}=2.445, p=0.05$ ] and stimulus type x visual area x clinical group [ $F_{(4,236)}=3.483, p=0.01$ ]. Differences between children and adults were revealed by the overall age group effect and also by significant visual area x age group [ $F_{(4, 228.3)}=4.011, p=0.005$ ] and a stimulus type x visual area x clinical group [ $F_{(4,236)}=3.483, p=0.01$ ] interactions. Three way interactions involving stimulus type, visual area and groups were explored in subsequent repeated measures ANOVA.

Given that no effect of hemisphere or interaction between hemisphere and group was found we averaged the signal of both hemispheres and performed a repeated measures analysis for each stimulus type using visual areas (V1, V2d, V2v, V3d, V3v) as within subjects variables and clinical group (NF1 vs controls) and age group (children vs adults) as between subjects factors.

Concerning the stimulus with low spatial and high temporal frequency and low contrast (biasing the M pathway), differences between patients with NF1 and controls were evident as an overall significant effect of clinical group [ $F_{(1,63)}=9.914, p=0.003$ ] and a significant interaction between area and clinical group [ $F_{(3.5, 37)}=6.194, p<0.001$ ]. This interaction was attributable to significantly lower activations from patients with NF1 than controls in visual areas V2d ( $t_{(65)}=3.5, p=0.001$ ), V2v ( $t_{(65)}=2.5, p=0.017$ ) and

V3d ( $t_{(65)}=3.5, p=0.001$ ), but not in V1 and V3v, as shown in Figure 4. Differences between children and adults were indicated by a marginally significant effect of age group [ $F_{(1,63)}=3.850, p=0.054$ ] and a significant visual area x age group interaction [ $F_{(3.5, 37)}=6.194, p<0.001$ ]. This interaction was attributable to adults activating more than children in visual areas V2d ( $t_{(65)}=2.3, p=0.025$ ) and V3d ( $t_{(65)}=2.5, p=0.014$ ), Figure 4.

Regarding the stimulus with high contrast, higher spatial and lower temporal frequency (biasing the P pathway), we observed an overall clinical group effect [ $F_{(1,63)}=5.785, p=0.019$ ] but no visual area x clinical group interaction [ $F_{(3.8, 242.3)}=1.026, \text{NS}$ ], indicating that effects were comparable across visual areas (see Figure 4). Furthermore, for this stimulus type neither an age group effect [ $F_{(1,63)}=3.285, \text{NS}$ ], nor an interaction between visual area and age group [ $F_{(3.8, 242.3)}=1.321, \text{NS}$ ] were present, indicating that there is no

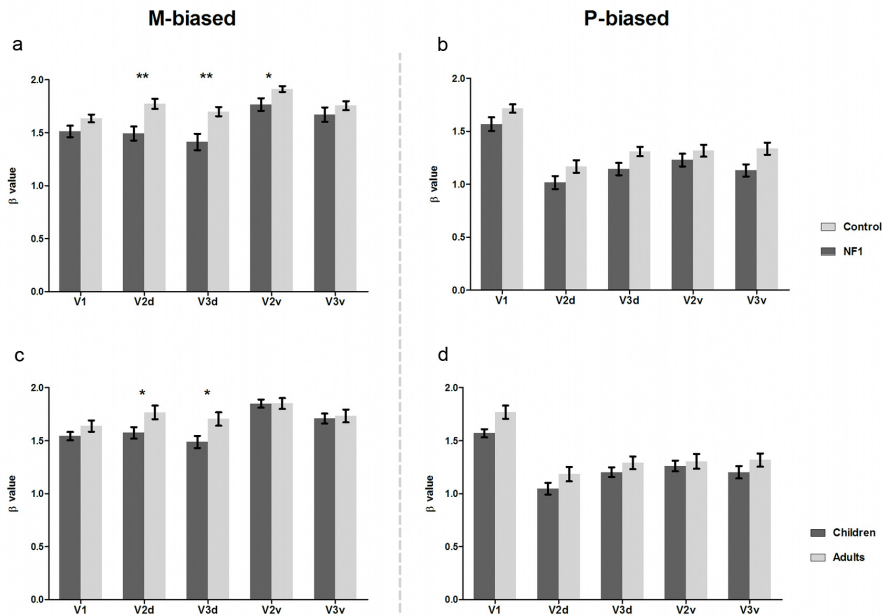


**Figure 4. BOLD activity in retinotopically defined areas for M- and P-biased stimuli. a.b.** depict mean beta values in retinotopically defined areas V1, V2d, V3d, V2v, V3v for patients with NF1 (dark grey;  $n = 28$ , 15 children and 13 adults) and controls (light grey;  $n = 39$ , 24 children and 15 adults) in the presence of M-biased stimulus (a) and P-biased stimulus (b). **c.d.** depict mean beta values in retinotopically defined areas for children (dark grey;  $n = 39$ , 15 with NF1 and 24 controls) and adults (light grey;  $n = 28$ , 13 with NF1 and 15 controls) in the presence of M-biased stimulus (c) and P-biased stimulus (d). Significant differences between groups are indicated by  $*p<0.05$ ,  $**p<0.01$ . Error bars represent SEM.

difference in activation between children and adults when responding to the stimulus biased for the P pathway, as shown in Figure 4.

### **Correspondence between low-level visual deficits in NF1 and cognitive abilities**

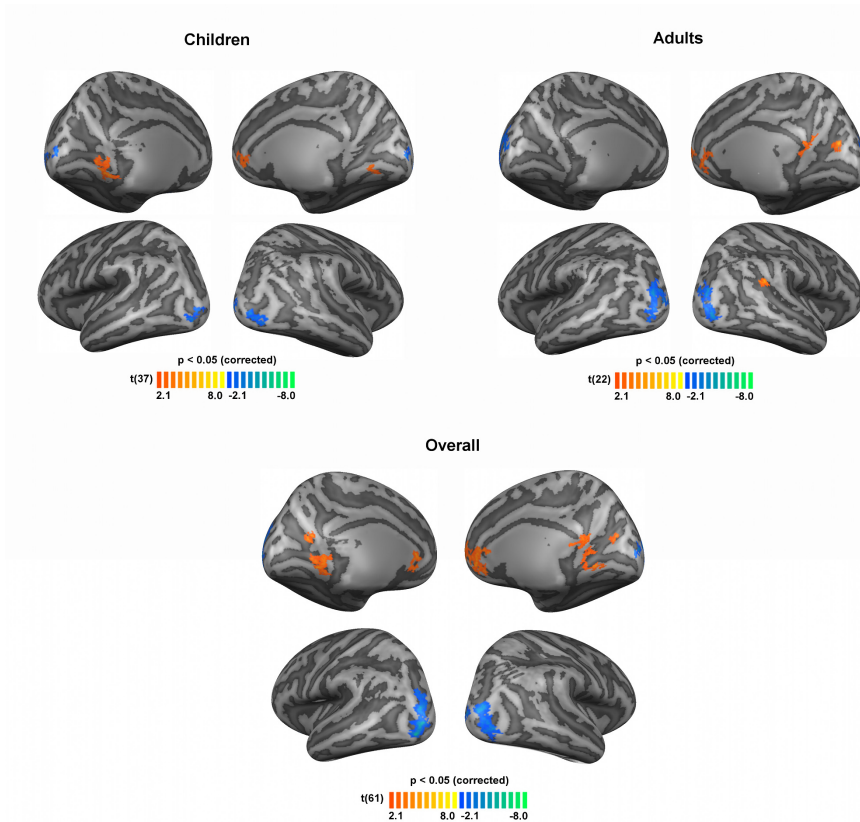
BOLD activation to each stimulus type in each visual area did not correlate with IQ for children and adolescents and Raven scores for adults. The lack of correspondence suggests that abnormal activation of low-level visual areas is not explained by low intellectual abilities.

### **Volume based analysis of cortical activation: random effects analysis**

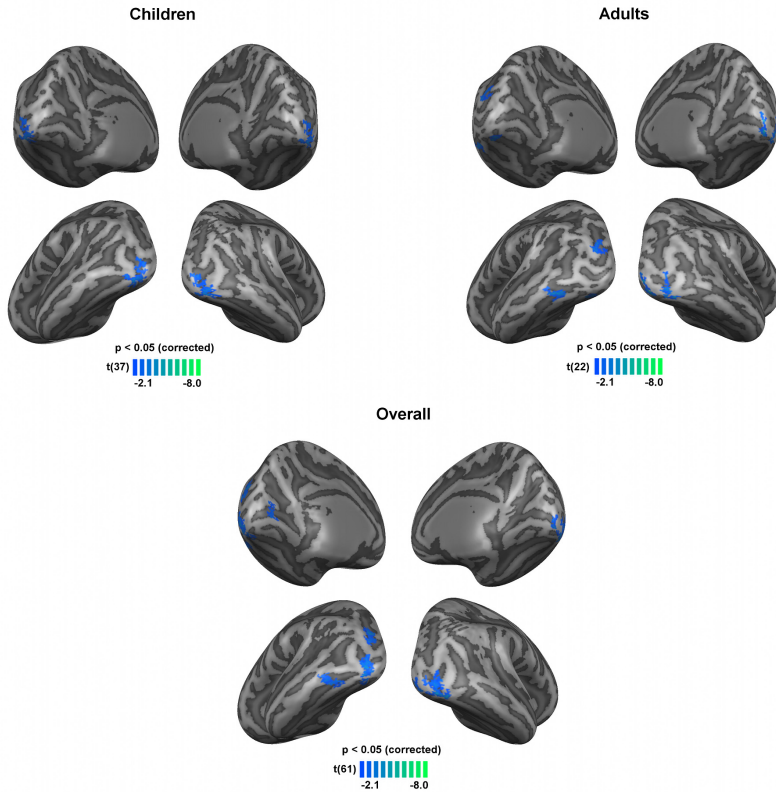
To further identify cortical regions showing group differences in brain activation evoked by each of the stimuli used we compared the BOLD activation between clinical groups (NF1  $n=28$  and controls  $n=35$ , 4 control adults were not included in this analysis, see Materials and Methods section). Figures 5 and 6 show differences in BOLD activation elicited by the M- and P-biased stimulation, respectively.

Figure 5 shows the differences in activation profiles between patients with NF1 and controls in the presence of the low contrast, low spatial, high temporal frequency stimulus (M-biased). Overall, individuals with NF1 showed significantly lower activations than controls in the middle and superior occipital gyri bilaterally, consistent with the locations for V2d and V3d, as observed in the ROI analysis; differences in V2v were probably not observed due to their lower statistical significance. Surprisingly, clusters of higher activation for patients with NF1 relative to controls were observed in the cingulate gyrus, retrosplenial cortex, medial prefrontal cortex, parieto-occipital sulcus and lingual gyrus. Table 2 summarizes the brain regions with significant differences between groups.

In the presence of the stimulus that biased, although not exclusively, the P pathway, patients with NF1 activated less than controls in regions within the occipital lobe, including the inferior occipital gyrus, occipital pole, the calcarine and occipito-temporal sulci, Figure 6, Table 3.



**Figure 5. Significant differences in brain activations between patients with NF1 and controls, regarding the M-biased stimulus for children, adults and overall (children and adults) groups.** Blue colours depict regions where activation was lower for individuals with NF1 than controls. Orange colours depict regions where activation was higher for individuals with NF1 than controls. Results are shown on views of the left and right hemispheres of cortex-based aligned three-dimensional reconstructions generated from the average anatomical data sets of the subjects in each group (children, adults, overall). Light grey represents gyri, dark grey represents sulci. T-maps thresholded at  $p < 0.05$  corrected using cortex-based cluster threshold estimation (cluster size  $41 \text{ mm}^3$ ).  $N = 15$  children with NF1, 24 control children, 13 adults with NF1 and 11 control adults.



**Figure 6. Significant differences in brain activations between patients with NF1 and controls, regarding the P-biased stimulus for children, adults and overall (children and adults) groups.** Blue colours depict regions where activation was lower for individuals with NF1 than controls. Results are shown on views of the left and right hemispheres of cortex-based aligned three-dimensional reconstructions generated from the average anatomical data sets of the subjects in each group (children, adults, overall). Light grey represents gyri, dark grey represents sulci. T-maps thresholded at  $p < 0.05$  corrected using cortex-based cluster threshold estimation (cluster size 41 mm<sup>2</sup>). N = 15 children with NF1, 24 control children, 13 adults with NF1 and 11 control adults.

**Table 2. Localization and cluster size of the regions with significant between-group differences in activation during M-biased stimulation for the overall (children and adults) group.**

Region	BA	Center of Mass (T. coord.)			Cluster size (mm <sup>2</sup> )
		X	Y	Z	
NF1 < Control					
RH middle and superior occipital gyri	17/18/19	32.29	-82.61	0.64	300
	18	11.98	-94.96	7.13	41
LH middle and superior occipital gyri	17/18/19	-30.25	-83.29	6.41	374
NF1 > Control					
RH anterior cingulate and medial prefrontal	10/32	6.72	41.61	6.68	373
LH anterior cingulate	32	-1.91	24.17	4.06	196
RH retrosplenial and lingual gyrus	17/29/30	11.40	-50.16	2.41	101
RH retrosplenial	30	2.87	-49.67	11.85	83
RH parieto-occipital fissure (cuneus)	18	15.72	-67.72	15.84	42
LH parieto-occipital fissure (cuneus)	17/18	-44.77	-59.94	17.88	59
LH lingual gyrus	17	-14.38	-45.16	-1.68	196

X, Y and Z indicate the center of mass in Talairach coordinates. BA, Brodmann areas. LH, left hemisphere. RH, right hemisphere. Regions were determined by t-test second level analysis corrected with cluster threshold estimation ( $p < 0.05$ , cluster size 41 mm<sup>2</sup>) performed after the group-based RFX GLM analysis. Talairach coordinates are derived from the clusters shown in Figure 5.

**Table 3. Localization and cluster size of the regions with significant between-group differences in activation during P-biased stimulation for the overall (children and adults) group.**

Region	BA	Center of Mass (T. coord.)			Cluster size (mm <sup>2</sup> )
		X	Y	Z	
NF1 < Control					
RH inferior occipital gyrus	17/18	33.41	-81.66	-11.19	138
LH inferior occipital gyrus	18	-31.95	-86.26	-8.20	152
	19	-25.59	-78.34	-17.18	41
LH superior occipital gyrus	18/19	-27.53	-79.18	14.97	144
RH occipital pole	17	-94.25	-10.73	2.09	47
LH calcarine sulcus	17	-8.89	-70.57	6.29	72
LH occipito-temporal sulcus	37	-43.85	-60.40	-10.17	109

X, Y and Z indicate the center of mass in Talairach coordinates. BA, Brodmann areas. LH, left hemisphere. RH, right hemisphere. Regions were determined by t-test second level analysis corrected with cluster threshold estimation ( $p < 0.05$ , cluster size 41 mm<sup>2</sup>) performed after the group-based RFX GLM analysis. Talairach coordinates are derived from the clusters shown in Figure 6.

We further examined the functional response profiles of regions showing significant statistical differences between groups. Brain regions where patients with NF1 presented lower activation than controls (blue clusters in Figures 5 and 6) were due to hypoactivation, i.e. less activation from the individuals with NF1 (timecourses not shown), as expected. However, the stimulus driving preferentially the M pathway resulted in a number of regions showing significantly higher BOLD signal in individuals with NF1 than controls, as mentioned above. Interestingly, in the retrosplenial cortex, the anterior cingulate cortex and the medial prefrontal cortex, the differences between groups emerged because individuals with NF1 presented positive BOLD activations while controls deactivated, Figure 7. Additionally, in the lingual gyrus, controls showed negative BOLD signals while patients with NF1 did not show activations in this area.

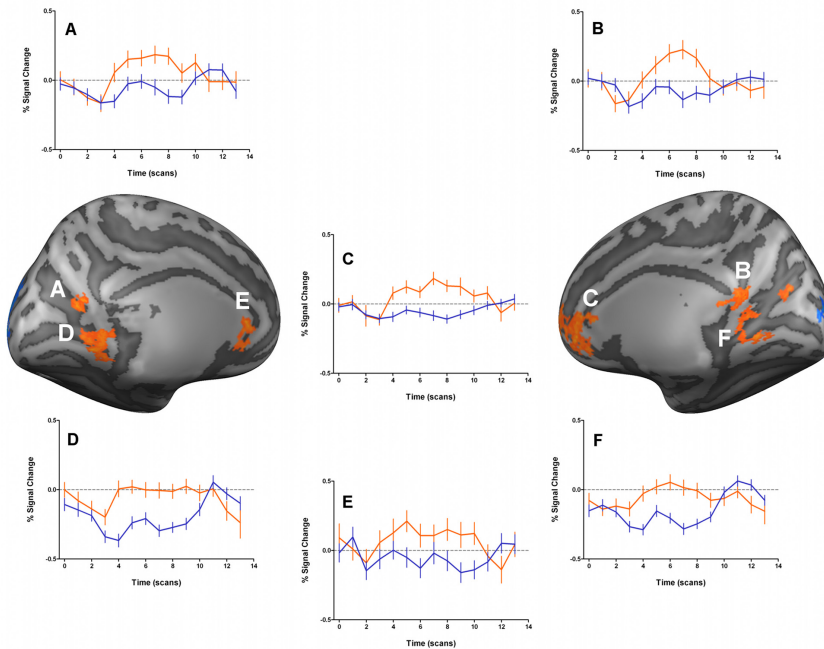


**Figure 7. Time course information of the clusters with significantly higher activations for patients with NF1 than controls, regarding the M-biased stimulus for the overall (children and adults) group.** Results are shown on lateral views of the left and right hemispheres of cortex-based aligned three-dimensional reconstructions generated from the average anatomical data sets of the subjects. T-maps are thresholded at  $p < 0.05$  corrected using cortex-based cluster threshold estimation (cluster size  $41 \text{ mm}^2$ ). Plots A to F correspond to the timecourse information for the clusters with the same letter in the cortex representations. Timecourse percent signal change is shown in orange lines for patients with NF1 and blue lines for controls. Error bars reflect mean SEs.  $N = 28$  patients with NF1 and 35 control subjects.



## DISCUSSION

The present work provides the first fMRI study on basic visual processing deficits in children, adolescents and adult patients with NF1. We used stimuli that were designed, based on functional properties, to preferentially activate the magnocellular or parvocellular pathways. Regions showing differences between controls and patients with NF1 were either visual or belonging to the default mode network.

Our findings indicate that individuals with NF1 have deficient activation of the visual cortex, as compared to their respective control group, for both types of low-level visual stimulation, in agreement with our previous report of impaired contrast sensitivity in the M and P pathways of patients with NF1 (Ribeiro et al., 2012). Accordingly, we observed a similar deficit in visual activation both in children and adults with NF1. Such similarity is also reflected in no significant effect in the interaction between clinical group and age group. This finding indicates that low-level visual processing deficits do not ameliorate with age.

In what concerns the stimulus with low contrast, low spatial and high temporal frequency (driving into a larger extent the M pathway), patients with NF1 manifested more pronounced deficits in activating early visual retinotopic areas, V2d, V2v and V3d. The fact that early visual deficits are mainly explained by extrastriate V2/V3 contributions suggests that early complex (intermediate vision) functional properties are mostly impaired in NF1. Furthermore, dorsal V2 and V3 areas showed larger extent of hypoactivation than ventral V2 and V3 regions, in accordance with the notion of functional asymmetries in early visual cortex (Liu et al., 2006b; Mendola et al., 2006; Eickhoff et al., 2008), and with the notion that M input dominates in dorsal regions (Bullier, 2001; Bullier et al., 2001).

Regarding the stimulus with high contrast, higher spatial frequency and low temporal frequency (more tuned to the P pathway), patients with NF1 showed an activation deficit that was equally distributed across retinotopically-defined visual areas, and also deficient neural activation in visual areas in the inferior occipital and occipito-temporal regions.

Altered visual processing in lower and higher levels of the dorsal and ventral streams may explain the visuospatial deficits that characterize the cognitive phenotype in NF1. Accordingly, Clements-Stephens *et al.* (2008) reported, en passage, hypoactivation of the occipital cortex in patients with NF1 while performing the judgement of line orientation test. This test recruits preferentially dorsal stream structures that build-up on information from low-level visual areas (Kesler et al., 2004; Tranel et al., 2009).

Another finding from the present study is the difference in activation between age groups observed for the M-biased stimulation in dorsal areas V2 and V3, with adults showing higher magnitude of activation than children. Recently, functional (Bucher et al., 2006; Klaver et al., 2008) and structural (Loenneker et al., 2010) studies focusing on the maturation of the dorsal and ventral streams suggested a slower maturation of the dorsal in relation to the ventral pathway. Our finding is an indication corroborating the late maturation of the dorsal pathway even for low-level visual areas, where ventral and dorsal pathways emerge and bifurcate.

Turning now to the differences between patients with NF1 and controls in the functional response profiles in brain regions outside visual areas, we were intrigued by the specific patterns observed for the M-biased stimulation. While P-biased stimulation did not cause differences outside visual regions, M tuned stimulus induced surprising positive BOLD activity in patients with NF1 while controls deactivated. This pattern was observed in posterior brain regions: parieto-occipital sulcus and retrosplenial cortex, as well as anterior brain regions: anterior cingulate and medial prefrontal cortex. Interestingly, these findings imply an anomalous activation pattern in patients with NF1 in regions belonging to the brain default mode network (DMN). Regions belonging to the DMN commonly include the medial prefrontal cortex extending to the anterior cingulate, posterior cingulate/retrosplenial cortex and the parietal cortices in the region of the angular gyri. In Figure 8 there is a side by side representation of the brain's DMN and the activity profile observed in patients with NF1 while being stimulated with the M-biased stimulus.

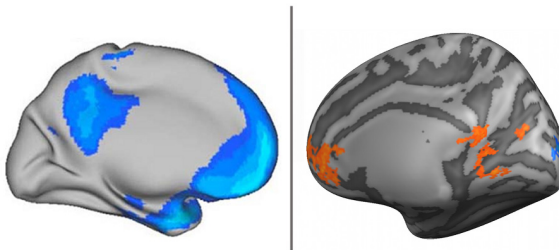


**Figure 8. Medial regions of the brain's default-mode-network.** The left side of the image is the brain's default network identified in a meta-analysis that included 132 participants mapping brain regions more active in passive as compared to active tasks using positron emission tomography (PET). Figure adapted from Buckner et al., 2008. On the right side of the image the map of significant differences in brain activations between patients with NF1 and controls, regarding the M-biased stimulus.

By definition, the DMN brain regions are active during task irrelevant thoughts (McKiernan et al., 2003), daydreaming (Mason et al., 2007) and self-referential thought (Gusnard et al., 2001) and deactivate during performance of cognitively demanding or engaging tasks (Shulman et al., 1997; Raichle et al., 2001; McKiernan et al., 2003). This set of brain regions comprises significant intrinsic correlations of functional activity with each other (Greicius et al., 2003; Fox et al., 2005).

During M-stimulation the NF1 group failed to deactivate the DMN suggesting that during these particular stimulation periods the participants with NF1 had a higher tendency to task-irrelevant thoughts than during the other task condition. The mechanisms behind this abnormal DMN activation could be related to the attentional deficits known to occur in children with NF1. In that sense, one may hypothesise that activity in the DMN is explained by greater incidence of ADHD related symptoms in patients with NF1, and thus an inability to stay on the task and tendency to daydream. In any case in order to understand the neural mechanisms contributing to DMN activation it is important to account its dependence on stimulus type, given it only occurred during M-biased stimulation. The “magnocellular advantage” theory proposed by Laycock et al. (Laycock et al., 2007; Laycock et al., 2008) suggests an important role for the M pathway in driving attentional mechanisms in higher-order cortical regions. How this relates to abnormal DMN activation is an intriguing aspect to be explored in future studies.

Although our data does not provide an ultimate explanation of this effect, our finding of paradoxical activation in midline DMN regions (medial prefrontal cortex, anterior cingulate and retrosplenial cortex) might give insightful information that can help in better understanding attentional deficits in patients with NF1 (Huijbregts et al., 2010), and their implications for abnormal cognitive processing. Taking into account that low level visual impairments can impact high-level cognitive functions, our results provide evidence for a specific and intriguing link between the magnocellular pathway and the default mode network. In fact, it has been observed that in clinical populations with impaired magnocellular processing, as schizophrenia (Martinez et al., 2008; Coleman et al., 2009), autism (Pellicano et al., 2005; Sutherland and Crewther, 2010), and Fragile X syndrome (Kogan et al., 2004), the midline DMN regions fail to deactivate (Menon et al., 2004; Kennedy et al., 2006; Pomarol-Clotet et al., 2008; Salgado-Pineda et al., 2011).

In summary, this study provides the first functional brain imaging indication that the early visual system is impaired in NF1, providing pathophysiological evidence for a potential impact in the high-level visual cognitive profile of patients with NF1. More-

over, our results provide an intriguing link between impaired magnocellular and default mode network processing, a finding that has been separately observed in autism and schizophrenia. Additional studies will be needed to further define the impact of these impairments in high-level cognitive functions of patients with NF1, particularly the abnormal allocation of neural resources observed in the midline regions of the default mode network.

## REFERENCES

- Bawden H, Dooley J, Buckley D, Camfield P, Gordon K, Riding M, Llewellyn G. MRI and nonverbal cognitive deficits in children with neurofibromatosis 1. *J Clin Exp Neuropsychol.* 18:6 (1996) 784-792.
- Billingsley RL, Jackson EF, Slopis JM, Swank PR, Mahankali S, Moore BD, 3rd. Functional magnetic resonance imaging of phonologic processing in neurofibromatosis 1. *J Child Neurol.* 18:11 (2003) 731-740.
- Boynton GM, Hegde J. Visual cortex: the continuing puzzle of area V2. *Curr Biol.* 14:13 (2004) R523-524.
- Brainard DH. The Psychophysics Toolbox. *Spat Vis.* 10:4 (1997) 433-436.
- Bucher K, Dietrich T, Marcar VL, Brem S, Halder P, Boujraf S, Summers P, Brandeis D, Martin E, Loenneker T. Maturation of luminance- and motion-defined form perception beyond adolescence: a combined ERP and fMRI study. *Neuroimage.* 31:4 (2006) 1625-1636.
- Buckner RL, Andrews-Hanna JR, Schacter DL. The brain's default network: anatomy, function, and relevance to disease. *Ann N Y Acad Sci.* 1124:(2008) 1-38.
- Bullier J. Integrated model of visual processing. *Brain Res Brain Res Rev.* 36:2-3 (2001) 96-107.
- Bullier J, Hupe JM, James AC, Girard P. The role of feedback connections in shaping the responses of visual cortical neurons. *Prog Brain Res.* 134:(2001) 193-204.
- Carandini M, Movshon JA, Ferster D. Pattern adaptation and cross-orientation interactions in the primary visual cortex. *Neuropharmacology.* 37:4-5 (1998) 501-511.
- Clements-Stephens AM, Rimrod SL, Gaur P, Cutting LE. Visuospatial processing in children with neurofibromatosis type 1. *Neuropsychologia.* 46:2 (2008) 690-697.
- Coleman MJ, Cestnick L, Krastoshevsky O, Krause V, Huang Z, Mendell NR, Levy DL. Schizophrenia patients show deficits in shifts of attention to different levels of global-local stimuli: evidence for magnocellular dysfunction. *Schizophr Bull.* 35:6 (2009) 1108-1116.
- Cumming BG, DeAngelis GC. The physiology of stereopsis. *Annu Rev Neurosci.* 24:(2001) 203-238.
- De Valois RL, De Valois KK. *Spatial vision.* New York: Oxford University Press 1988.
- Dillenburger B, Roe AW. Influence of parallel and orthogonal real lines on illusory contour perception. *J Neurophysiol.* 103:1 (2010) 55-64.
- Dilts CV, Carey JC, Kircher JC, Hoffman RO, Creel D, Ward K, Clark E, Leonard CO. Children and adolescents with neurofibromatosis 1: a behavioral phenotype. *J Dev Behav Pediatr.* 17:4 (1996) 229-239.

- Dougherty RF, Koch VM, Brewer AA, Fischer B, Modersitzki J, Wandell BA. Visual field representations and locations of visual areas V1/2/3 in human visual cortex. *J Vis.* 3:10 (2003) 586-598.
- Douglas RJ, Martin KAC. Neocortex. In: *The synaptic organization of the brain*, 4th ed. Edition (Shepherd GM, ed), pp 459-510. New York ; Oxford: Oxford University Press 1998.
- Eickhoff SB, Rottschy C, Kujovic M, Palomero-Gallagher N, Zilles K. Organizational principles of human visual cortex revealed by receptor mapping. *Cereb Cortex.* 18:11 (2008) 2637-2645.
- El-Shamayleh Y, Movshon JA. Neuronal responses to texture-defined form in macaque visual area V2. *J Neurosci.* 31:23 (2011) 8543-8555.
- Eldridge R, Denckla MB, Bien E, Myers S, Kaiser-Kupfer MI, Pikus A, Schlesinger SL, Parry DM, Dambrosia JM, Zasloff MA, et al. Neurofibromatosis type 1 (Recklinghausen's disease). Neurologic and cognitive assessment with sibling controls. *Am J Dis Child.* 143:7 (1989) 833-837.
- Eliason MJ. Neurofibromatosis: implications for learning and behavior. *J Dev Behav Pediatr.* 7:3 (1986) 175-179.
- Engel SA, Rumelhart DE, Wandell BA, Lee AT, Glover GH, Chichilnisky EJ, Shadlen MN. fMRI of human visual cortex. *Nature.* 369:6481 (1994) 525.
- Felleman DJ, Van Essen DC. Distributed hierarchical processing in the primate cerebral cortex. *Cereb Cortex.* 1:1 (1991) 1-47.
- Fischl B, Sereno MI, Tootell RB, Dale AM. High-resolution intersubject averaging and a coordinate system for the cortical surface. *Hum Brain Mapp.* 8:4 (1999) 272-284.
- Forman SD, Cohen JD, Fitzgerald M, Eddy WF, Mintun MA, Noll DC. Improved assessment of significant activation in functional magnetic resonance imaging (fMRI): use of a cluster-size threshold. *Magn Reson Med.* 33:5 (1995) 636-647.
- Formisano E, Esposito F, Di Salle F, Goebel R. Cortex-based independent component analysis of fMRI time series. *Magn Reson Imaging.* 22:10 (2004) 1493-1504.
- Fox MD, Snyder AZ, Vincent JL, Corbetta M, Van Essen DC, Raichle ME. The human brain is intrinsically organized into dynamic, anticorrelated functional networks. *Proc Natl Acad Sci U S A.* 102:27 (2005) 9673-9678.
- Friedman JM, Birch P, Greene C. National Neurofibromatosis Foundation International Database. *Am J Med Genet.* 45:1 (1993) 88-91.
- Friston KJ, Josephs O, Rees G, Turner R. Nonlinear event-related responses in fMRI. *Magn Reson Med.* 39:1 (1998) 41-52.
- Goebel R, Esposito F, Formisano E. Analysis of functional image analysis contest (FIAC) data with brainvoyager QX: From single-subject to cortically aligned group general linear model analysis and self-organizing group independent component analysis. *Hum Brain Mapp.* 27:5 (2006) 392-401.
- Greicius MD, Krasnow B, Reiss AL, Menon V. Functional connectivity in the resting brain: a network analysis of the default mode hypothesis. *Proc Natl Acad Sci U S A.* 100:1 (2003) 253-258.
- Grill-Spector K, Malach R. The human visual cortex. *Annu Rev Neurosci.* 27 (2004) 649-677.
- Gusnard DA, Akbudak E, Shulman GL, Raichle ME. Medial prefrontal cortex and self-referential mental activity: relation to a default mode of brain function. *Proc Natl Acad Sci U S A.* 98:7 (2001) 4259-4264.

- Hendry SH, Reid RC. The koniocellular pathway in primate vision. *Annu Rev Neurosci.* 23:(2000) 127-153.
- Hofman KJ, Harris EL, Bryan RN, Denckla MB. Neurofibromatosis type 1: the cognitive phenotype. *J Pediatr.* 124:4 (1994) S1-8.
- Horwitz GD, Hass CA. Nonlinear analysis of macaque V1 color tuning reveals cardinal directions for cortical color processing. *Nat Neurosci.* (2012) *in press.*
- Hubel DH, Wiesel TN. Receptive fields of single neurones in the cat's striate cortex. *J Physiol.* 148 (1959) 574-591.
- Hubel DH, Wiesel TN. Ferrier lecture. Functional architecture of macaque monkey visual cortex. *Proc R Soc Lond B Biol Sci.* 198:1130 (1977) 1-59.
- Hubel DH, Livingstone MS. Segregation of form, color, and stereopsis in primate area 18. *J Neurosci.* 7:11 (1987) 3378-3415.
- Huijbregts S, Swaab H, de Sonneville L. Cognitive and motor control in neurofibromatosis type I: influence of maturation and hyperactivity-inattention. *Dev Neuropsychol.* 35:6 (2010) 737-751.
- Hyman SL, Shores A, North KN. The nature and frequency of cognitive deficits in children with neurofibromatosis type 1. *Neurology.* 65:7 (2005) 1037-1044.
- Jo HJ, Lee JM, Kim JH, Shin YW, Kim IY, Kwon JS, Kim SI. Spatial accuracy of fMRI activation influenced by volume- and surface-based spatial smoothing techniques. *Neuroimage.* 34:2 (2007) 550-564.
- Kennedy DP, Redcay E, Courchesne E. Failing to deactivate: resting functional abnormalities in autism. *Proc Natl Acad Sci U S A.* 103:21 (2006) 8275-8280.
- Kesler SR, Haberecht MF, Menon V, Warsofsky IS, Dyer-Friedman J, Neely EK, Reiss AL. Functional neuroanatomy of spatial orientation processing in Turner syndrome. *Cereb Cortex.* 14:2 (2004) 174-180.
- Klaver P, Lichtensteiger J, Bucher K, Dietrich T, Loenneker T, Martin E. Dorsal stream development in motion and structure-from-motion perception. *Neuroimage.* 39:4 (2008) 1815-1823.
- Kogan CS, Boutet I, Cornish K, Zangenehpour S, Mullen KT, Holden JJ, Der Kaloustian VM, Andermann E, Chaudhuri A. Differential impact of the FMR1 gene on visual processing in fragile X syndrome. *Brain.* 127:Pt 3 (2004) 591-601.
- Kriegeskorte N, Goebel R. An efficient algorithm for topologically correct segmentation of the cortical sheet in anatomical mr volumes. *Neuroimage.* 14:2 (2001) 329-346.
- Laycock R, Crewther SG, Crewther DP. A role for the 'magnocellular advantage' in visual impairments in neurodevelopmental and psychiatric disorders. *Neurosci Biobehav Rev.* 31:3 (2007) 363-376.
- Laycock R, Crewther DP, Crewther SG. The advantage in being magnocellular: a few more remarks on attention and the magnocellular system. *Neurosci Biobehav Rev.* 32:8 (2008) 1409-1415.
- Leventhal AG. Vision and visual dysfunction. Vol 4, *The Neural basis of visual function*, edited by A. G. Leventhal: Macmillan 1991.
- Levine TM, Materek A, Abel J, O'Donnell M, Cutting LE. Cognitive profile of neurofibromatosis type 1. *Semin Pediatr Neurol.* 13:1 (2006) 8-20.
- Levitt JB, Lund JS, Yoshioka T. Anatomical substrates for early stages in cortical processing of visual information in the macaque monkey. *Behav Brain Res.* 76:1-2 (1996) 5-19.

- Liu CS, Bryan RN, Miki A, Woo JH, Liu GT, Elliott MA. Magnocellular and parvocellular visual pathways have different blood oxygen level-dependent signal time courses in human primary visual cortex. *AJNR Am J Neuroradiol.* 27:8 (2006a) 1628-1634.
- Liu T, Heeger DJ, Carrasco M. Neural correlates of the visual vertical meridian asymmetry. *J Vis.* 6:11 (2006b) 1294-1306.
- Livingstone M, Hubel D. Segregation of form, color, movement, and depth: anatomy, physiology, and perception. *Science.* 240:4853 (1988) 740-749.
- Loenneker T, Klaver P, Bucher K, Lichtensteiger J, Imfeld A, Martin E. Microstructural development: Organizational differences of the fiber architecture between children and adults in dorsal and ventral visual streams. *Hum Brain Mapp.* 32:6 (2010) 935-946.
- Lyon DC, Connolly JD. The case for primate V3. *Proc Biol Sci.* 279:1729 (2012) 625-633.
- Martinez A, Hillyard SA, Dias EC, Hagler DJ, Jr., Butler PD, Guilfoyle DN, Jalbrzikowski M, Silipo G, Javitt DC. Magnocellular pathway impairment in schizophrenia: evidence from functional magnetic resonance imaging. *J Neurosci.* 28:30 (2008) 7492-7500.
- Mason MF, Norton MI, Van Horn JD, Wegner DM, Grafton ST, Macrae CN. Wandering minds: the default network and stimulus-independent thought. *Science.* 315:5810 (2007) 393-395.
- McKiernan KA, Kaufman JN, Kucera-Thompson J, Binder JR. A parametric manipulation of factors affecting task-induced deactivation in functional neuroimaging. *J Cogn Neurosci.* 15:3 (2003) 394-408.
- Mendola JD, Conner IP, Sharma S, Bahekar A, Lemieux S. fMRI Measures of perceptual filling-in in the human visual cortex. *J Cogn Neurosci.* 18:3 (2006) 363-375.
- Menon V, Leroux J, White CD, Reiss AL. Frontostriatal deficits in fragile X syndrome: relation to FMR1 gene expression. *Proc Natl Acad Sci U S A.* 101:10 (2004) 3615-3620.
- Merigan WH, Nealey TA, Maunsell JH. Visual effects of lesions of cortical area V2 in macaques. *J Neurosci.* 13:7 (1993) 3180-3191.
- Nassi JJ, Callaway EM. Parallel processing strategies of the primate visual system. *Nat Rev Neurosci.* 10:5 (2009) 360-372.
- National Institutes of Health Consensus Development Conference Statement: neurofibromatosis. Bethesda, Md., USA, July 13-15 1987. *Neurofibromatosis.* 1:3 (1988) 172-178.
- North K. Neurofibromatosis type 1. *Am J Med Genet.* 97:2 (2000) 119-127.
- Payne JM, Moharir MD, Webster R, North KN. Brain structure and function in neurofibromatosis type 1: current concepts and future directions. *J Neurol Neurosurg Psychiatry.* 81:3 (2010) 304-309.
- Pellicano E, Gibson L, Maybery M, Durkin K, Badcock DR. Abnormal global processing along the dorsal visual pathway in autism: a possible mechanism for weak visuospatial coherence? *Neuropsychologia.* 43:7 (2005) 1044-1053.
- Penny W, Holmes, A., Friston, K. Random effects analysis. In: *Human Brain Function*, 2nd Edition (Frackowiak R FK, Frith C, Dolan R, Friston K, Price C, Zeki S, Ashburner J, Penny W.) Academic Press. 2003.
- Pomarol-Clotet E, Salvador R, Sarro S, Gomar J, Vila F, Martinez A, Guerrero A, Ortiz-Gil J, Sans-Sansa B, Capdevila A, Cebamanos JM, McKenna PJ. Failure to deactivate in the prefrontal cortex in schizophrenia: dysfunction of the default mode network? *Psychol Med.* 38:8 (2008) 1185-1193.

- Raichle ME, MacLeod AM, Snyder AZ, Powers WJ, Gusnard DA, Shulman GL. A default mode of brain function. *Proc Natl Acad Sci U S A.* 98:2 (2001) 676-682.
- Raven J, Raven JC, Court JH Manual for Raven's progressive matrices and vocabulary scales. Edition. Oxford: Oxford Psychologists 1993.
- Ribeiro MJ, Violante IR, Bernardino I, Ramos F, Saraiva J, Reviriego P, Upadhyaya M, Silva ED, Castelo-Branco M. Abnormal achromatic and chromatic contrast sensitivity in Neurofibromatosis type 1. *Invest Ophthalmol Vis Sci.* 53:1 (2012) 287-293.
- Riccardi V Neurofibromatosis: phenotype, natural history and pathogenesis, second Edition. Baltimore: Johns Hopkins University Press 1992.
- Rockel AJ, Hiorns RW, Powell TP. The basic uniformity in structure of the neocortex. *Brain.* 103:2 (1980) 221-244.
- Rowbotham I, Pit-ten Cate IM, Sonuga-Barke EJ, Huijbregts SC. Cognitive control in adolescents with neurofibromatosis type 1. *Neuropsychology.* 23:1 (2009) 50-60.
- Salgado-Pineda P, Fakra E, Delaveau P, McKenna PJ, Pomarol-Clotet E, Blin O. Correlated structural and functional brain abnormalities in the default mode network in schizophrenia patients. *Schizophr Res.* 125:2-3 (2011) 101-109.
- Schrimsher GW, Billingsley RL, Slopis JM, Moore BD, 3rd. Visual-spatial performance deficits in children with neurofibromatosis type-1. *Am J Med Genet A.* 120A:3 (2003) 326-330.
- Sereno MI, Dale AM, Reppas JB, Kwong KK, Belliveau JW, Brady TJ, Rosen BR, Tootell RB. Borders of multiple visual areas in humans revealed by functional magnetic resonance imaging. *Science.* 268:5212 (1995) 889-893.
- Shilyansky C, Karlsgodt KH, Cummings DM, Sidiropoulou K, Hardt M, James AS, Ehninger D, Bearden CE, Poirazi P, Jentsch JD, Cannon TD, Levine MS, Silva AJ. Neurofibromin regulates corticostriatal inhibitory networks during working memory performance. *Proc Natl Acad Sci U S A.* 107:29 (2010) 13141-13146.
- Shulman GL, Corbetta M, Buckner RL, Raichle ME, Fiez JA, Miezin FM, Petersen SE. Top-down modulation of early sensory cortex. *Cereb Cortex.* 7:3 (1997) 193-206.
- Sutherland A, Crewther DP. Magnocellular visual evoked potential delay with high autism spectrum quotient yields a neural mechanism for altered perception. *Brain.* 133:Pt 7 (2010) 2089-2097.
- Talairach J, Tournoux P Co-planar stereotaxic atlas of the human brain : 3-dimensional proportional system : an approach to cerebral imaging. Stuttgart: Georg Thieme 1988.
- Tranel D, Vianna E, Manzel K, Damasio H, Grabowski T. Neuroanatomical correlates of the Benton Facial Recognition Test and Judgment of Line Orientation Test. *J Clin Exp Neuropsychol.* 31:2 (2009) 219-233.
- Wandell BA, Dumoulin SO, Brewer AA. Visual field maps in human cortex. *Neuron.* 56:2 (2007) 366-383.
- Wechsler D Escala de Inteligência para Crianças - Terceira Edição (WISC-III): Manual. Lisboa: Cegoc-Tea 2003.
- Zeki S A vision of the brain. Oxford ; Boston: Blackwell Scientific Publications 1993.
- Zeki S, Shipp S. The functional logic of cortical connections. *Nature.* 335:6188 (1988) 311-317.
- Zeki SM. Uniformity and diversity of structure and function in rhesus monkey prestriate visual cortex. *J Physiol.* 277:(1978) 273-290.



## CHAPTER 5

GABA is reduced in the visual cortex of patients with Neurofibromatosis type 1: a new perspective on the disease mechanism

**ABSTRACT**

Alterations in the balance between excitatory and inhibitory neurotransmission have been implicated in several neurodevelopmental disorders. Neurofibromatosis type 1 (NF1) is one of the most common monogenic disorders causing cognitive deficits for which studies on a mouse model (*Nf1<sup>+/-</sup>*) proposed increased GABA-mediated inhibitory neurotransmission as the neural mechanism underlying these deficits. To test whether a similar mechanism translates to the human disorder, we used magnetic resonance spectroscopy (MRS) to measure GABA levels in the visual cortex of children and adolescents with NF1 and matched controls. We found that patients with NF1 have significantly lower GABA levels than controls and that NF1 mutation type significantly predicted cortical GABA. Moreover, functional imaging of the visual cortex indicated that blood-oxygen-level-dependent (BOLD) signal was correlated with GABA levels both in patients and controls. Our results provide *in vivo* evidence of GABAergic dysfunction in NF1 by showing a reduction of GABA levels in human patients. This constitutes a relevant finding to understand the physiological profile of the disorder with implications for the identification of targets for therapeutic strategies.

## INTRODUCTION

The balance between excitatory and inhibitory neurotransmission is tightly regulated in the human brain and largely dependent on the levels of glutamate, the major excitatory neurotransmitter, and  $\gamma$ -aminobutyric acid (GABA), the major inhibitory neurotransmitter. Alterations in this push-pull mechanism might underlie the cognitive deficits found in several neurodevelopmental disorders (Ramamoorthi and Lin, 2011).

In Neurofibromatosis type 1 (NF1), studies employing the *Nf1*<sup>+/-</sup> mice model suggested increased GABA-mediated inhibition as the cause underlying learning deficits (Costa et al., 2002). Furthermore, targeted deletion of the *Nf1* gene in specific brain cell types indicated that mice with reduced neurofibromin expression in GABAergic neurons had spatial learning and long-term potentiation (LTP) deficits (Cui et al., 2008). In order to understand the mechanism by which neurofibromin could regulate GABAergic neurotransmission Cui and colleagues performed a series of experiments in the *Nf1*<sup>+/-</sup> mice model, some of which are reviewed below:

### *Electrophysiological recordings in hippocampal slices from the Nf1<sup>+/-</sup> mice:*

Recordings of spontaneous inhibitory postsynaptic currents (sIPSCs) and miniature inhibitory postsynaptic currents (mIPSCs), which result from the spontaneous release of neurotransmitters, were measured in hippocampal slices. Those revealed not to be altered in the *Nf1*<sup>+/-</sup> mice, indicating normal GABA-mediated inhibition under baseline conditions. Inducing high frequency stimulation to mimic inhibitory neuronal firing during learning resulted in a larger increase in mIPSC frequency in *Nf1*<sup>+/-</sup> mice compared with the wild type (WT) mice, suggesting that neurofibromin regulates GABA release under periods of high frequency stimulation. On the other hand, recordings of miniature excitatory postsynaptic currents (mEPSCs) under baseline and depolarizing conditions showed no differences between WT and *Nf1*<sup>+/-</sup> mice.

### *Molecular mechanisms leading to altered GABAergic neurotransmission in the Nf1<sup>+/-</sup> mice:*

Neurofibromin is a negative regulator of the Ras signalling cascade (Ballester et al., 1990). Mutations in the *Nf1* gene result in hyperactivation of Ras downstream effectors, such as the kinase targets MEK and ERK. Those phosphorylate synapsin 1, a vesicle-associated phosphoprotein localized at presynaptic terminals that regulate vesicle dynamics and neurotransmitter release (Hilfiker et al., 1999; Chi et al., 2001).

To characterize ERK activation and ERK-dependent phosphorylation of synapsin 1 in *Nf1*<sup>+/-</sup> mutants, mice were trained with a fear condition paradigm known to trigger biochemical changes related to cognition in the hippocampus (Kushner et al., 2005). *Nf1*<sup>+/-</sup> mice showed higher ERK and synapsin 1 phosphorylation than WT mice, suggesting that neurofibromin regulates ERK signalling and synapsin 1 phosphorylation, Figure 1.

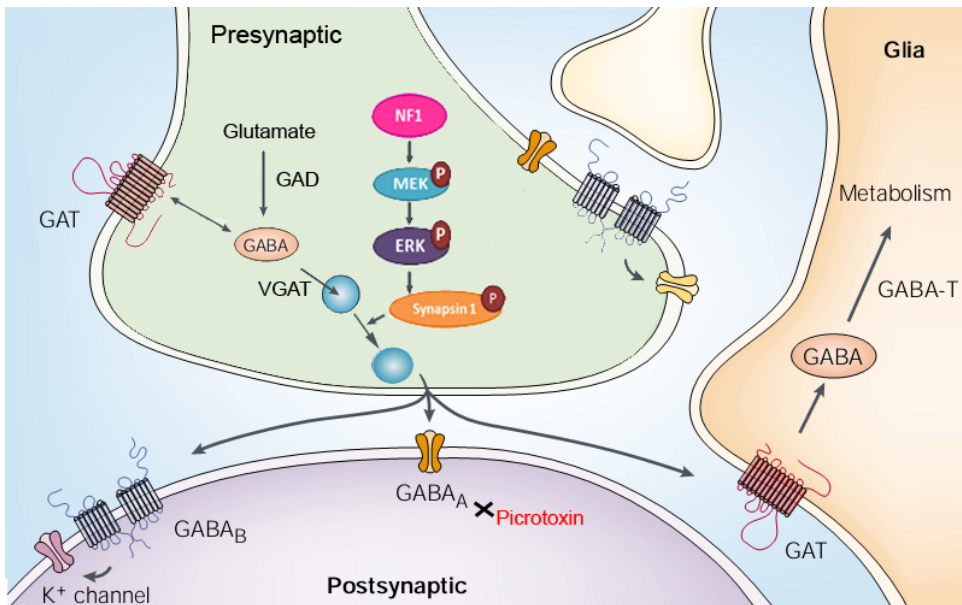


**Figure 1. Schematic diagram of transmitter release, transport and synthesis at a GABAergic synaptic terminal.** GABA is synthesized in inhibitory neurons from glutamate by the enzyme glutamic acid decarboxylase (GAD), and is transported into vesicles by a vesicular neurotransmitter transporter (VGAT). GABA can be released either vesicularly or non-vesicularly (by reverse transport). GABA receptors are located at pre- and postsynaptic sites. The effects of GABA can be mediated by the activation of metabotropic (GABA<sub>B</sub>) and ionotropic (GABA<sub>A</sub> and GABA<sub>C</sub>) receptors. Reuptake of GABA by surrounding neurons and glia occurs through the activity of GABA transporters (GAT). Subsequently, GABA is metabolized by a transamination reaction that is catalysed by GABA transaminase (GABA-T). The metabolism of GABA occurs in both neurons (not shown) and glia. At presynaptic locations neurofibromin (NF1) deficiency causes over activation of the Ras pathway, leading to phosphorylation (P) of the downstream kinase targets MEK and ERK. Activation of ERK leads to increased phosphorylation of synapsin 1, a protein that regulates vesicular packing and could facilitate GABA release from inhibitory neurons. Adapted from Owens and Kriegstein, 2002.

To assess visuospatial memory, mice were trained in the Morris water maze. The *Nf1*<sup>+/-</sup> mice performed worse than the WT mice in this test, indicating that they have spatial learning deficits. The investigators were able to rescue this phenotype using low doses of picrotoxin, a GABA<sub>A</sub> receptor antagonist. Picrotoxin administration to neurofibromin knockout and WT mice before training in the water maze rescued the performance of the *Nf1*<sup>+/-</sup> mice, at doses that did not affect learning in the WT mice.

Recently, these results were extended to the medial prefrontal cortex and striatum of *Nf1*<sup>+/-</sup> mice, by showing increased frequency of sIPSCs while sEPSCs were not affected (Shilyansky et al., 2010). This result indicates again that neurofibromin plays an important role in the physiology of inhibitory but not excitatory neurons and importantly, that the ratio of excitatory to inhibitory transmission is low in the *Nf1*<sup>+/-</sup> mice.

These results inspired us to measure GABA levels and their potential functional impact in patients with NF1. Before addressing the specific goals of our study it is helpful to review the role of GABA in the central nervous system and the processes contributing to regulation of GABA levels.

GABA-containing cells are distributed throughout the cortical lamina and GABAergic interneurons constitute 15-20% of the cortical neurons, being the rest essentially glutamatergic pyramidal cells (Hendry et al., 1987; DeFelipe, 1993; Markram et al., 2004). All mammalian neuronal circuits contain excitatory and inhibitory transmitter systems forming intense feed-forward and feedback connections.

In the adult mammalian brain, GABA has been associated primarily with the mediation of synaptic inhibition. However, inhibitory neurons do much more than just controlling the level of neuronal activity. They are critical for organizing the complex spatiotemporal patterns of network oscillations (Buzsaki et al., 2007; Mann and Paulsen, 2007), selectively gating inputs or outputs (Klausberger and Somogyi, 2008; Lee et al., 2012), suppression of background activity (Bahner et al., 2011), and timing of action potentials (Tukker et al., 2007). Regulation of inhibitory strength is a dynamic process that adapts to the changing patterns and degrees of network activity (Buzsaki et al., 2007). A particularly important regulatory system is the modulation of GABA content in inhibitory interneurons (Choi et al., 2012).

GABA is primarily synthesized from glutamate in a reaction catalysed by the enzyme glutamic acid decarboxylase (GAD). GABA is loaded into synaptic vesicles by a vesicular neurotransmitter transporter (VGAT). The effects of GABA are mediated by ionotropic (GABA<sub>A</sub> and GABA<sub>C</sub>) and metabotropic (GABA<sub>B</sub>) receptors which can be

localized either pre- or postsynaptically (Owens and Kriegstein, 2002; Choi et al., 2012), Figure 1.

Two general types of GABA-mediated postsynaptic potential have been described. Fast responses are mediated by ionotropic receptors and slow responses by metabotropic GABA<sub>B</sub> receptors. Both types of receptors are capable of regulating GABA release (Scanziani, 2000; Walker and Semyanov, 2008).

GABA signals are terminated by reuptake into nerve terminals and glial cells through plasma-membrane GABA transporters (GATs), thereafter GABA is metabolized in a reaction catalysed by GABA transaminase (GABA-T), where it contributes to energy metabolism in the tricarboxylic acid cycle (Choi et al., 2012), Figure 1.

The concentration of GABA in the living human brain is reported to be about 1 mM (Rothman et al., 1993; Terpstra et al., 2002; Jensen et al., 2005b). However, there is a significant regional variance in GABA contents (Banay-Schwartz et al., 1993), in accordance with the specific actions of GABAergic neurons. For example, GABA may reach 10 mmol/g in substantia nigra (Okada et al., 1971).

Although overall concentration is determined, the knowledge on local GABA concentrations in different compartments is far from satisfactory. The absolute concentrations of GABA in the presynaptic cytosol, in vesicles, and in the extrasynaptic space are not known. On the other hand, concentration in the synaptic cleft has been estimated in different types of neurons, with peak concentrations reaching values as high as 0.3 to 3mM (Mozrzymas et al., 1999; Perrais and Ropert, 1999; Barberis et al., 2004). The cytosolic GABA concentration is most difficult to estimate, since most of the neuronal GABA pool is used for energy metabolism rather than for synaptic inhibition.

GABA levels are dynamically modulated in response to increasing or decreasing network activity and in the context of brain disorders. For example, repetitive hyperactivity in the hippocampus of chronically epileptic rats causes upregulation of GADs (Escalapez and Houser, 1999), while expression of VGAT is altered following ischemia or excitotoxic stimulation (Gomes et al., 2011).

### **In vivo assessment of GABA levels in patients with NF1**

Despite the evidence of altered GABAergic inhibition in mice models, this hypothesis has never been tested in patients with NF1 and GABA levels have never been measured.

We applied magnetic resonance spectroscopy (MRS) to measure GABA levels in patients with NF1. This is the only *in vivo* tool capable of non-invasively measure brain metabolites. However, neurotransmitters can be difficult to detect *in vivo* because of complicated spectral patterns and overlap with other resonances, Figure 2a. To resolve the GABA signal we used an editing technique, which exploits the spin-spin or *J*-coupling of the GABA-C4 resonance at 3.0 ppm to the GABA-C3 resonance at 1.9 ppm, Figure 2b, as well as, the fact that the majority of the signals present in the brain spectra at 3.0 ppm are not coupled to signals at 1.9 ppm. *J*-difference editing requires two sets of experiments. In a given number of acquisitions a frequency selective pulse is applied at 1.9 ppm. This pulse will have an effect on the GABA signals at 3.0 ppm, but will not interfere with other signals at this location since they are not coupled with spins at 1.9 ppm. During another set of equivalent number of acquisitions the same pulse is applied to the opposite side of the spectrum (7.5 ppm), in order to reduce baseline artifacts. The difference between these two experiments will give a spectrum that only contains the signals that are affected by the pulse. This editing approach is widely used, and the method most commonly applied is the MEGA-PRESS method (Mescher et al., 1998). The reliability of GABA detection with an editing technique has been validated with *ex vivo* measurements (Bielicki et al., 2004).

A drawback of MRS is that it is only capable of detecting total concentration of a metabolite within a localized region; it cannot distinguish between separate functional pools of GABA. Nonetheless, given the relationships demonstrated in previous studies between behaviour and MRS measures of local GABA (Goddard et al., 2004; Northoff et al., 2007; Edden et al., 2009; Sumner et al., 2010; Gomez et al., 2011; Stagg et al., 2011), it seems likely that the MRS measure of GABA is at least, correlated with the neurotransmitter pools of GABA.

MRS measurements in patients with NF1 and controls were performed in early visual cortex, an area where the role of inhibition has been widely studied and where we previously found evidences of functional alterations (Ribeiro et al., 2012; Violante et al., 2012). Moreover, it has recently been shown that GABA measures in the human visual cortex can reflect perceptual and behavioural processes in a parametric manner (Edden et al., 2009; Yoon et al., 2010).

When studying the human disorder, the variability of mutations that give rise to the disease (Thomson et al., 2002) should be taken into account. Therefore, it is important to investigate whether genotypic differences lead to changes in GABA levels. We ad-

dressed this by testing the hypothesis that different types of mutations would impact neurofibromin function differently and consequently manifest in cortical GABA levels.

To assess the functional correlates of the MRS signal, participants underwent functional magnetic resonance imaging (fMRI) while performing a visual task. Importantly, the blood-oxygenation-level-dependent (BOLD) signal is sensitive to the balance between excitation and inhibition (Logothetis, 2008) and therefore sensitive to variations

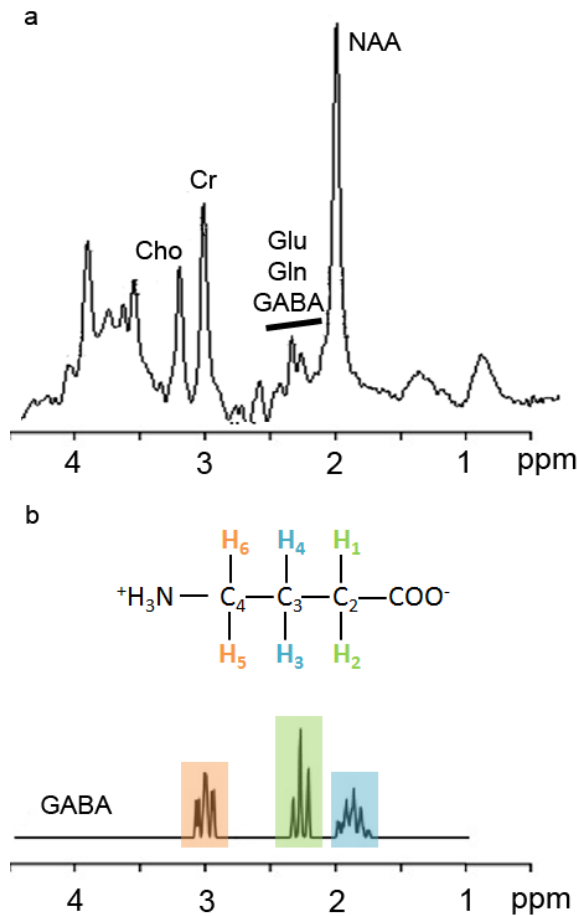


**Figure 2. Magnetic resonance spectra (MRS) of GABA. a.**  $^1\text{H}$ -MRS spectrum of the human brain acquired at 3T, showing peaks corresponding to N-acetyl aspartate (NAA), creatine-containing compounds (Cr), choline-containing compounds (Cho), glutamate (Glu), glutamine (Gln) and GABA. **b.** Chemical formula of GABA and the GABA spectrum at 3T, showing the assignments to the GABA  $\text{CH}_2$  spins. Adapted from Puts and Edden, 2012.



in GABA levels (Goddard et al., 2004). Consequently, it is physiologically relevant to determine whether the previously observed negative correlation between BOLD and GABA (Northoff et al., 2007; Edden et al., 2009; Muthukumaraswamy et al., 2011) is preserved in patients with NF1.

## MATERIALS AND METHODS

### Participants

We studied 20 patients with NF1 (mean age  $13.0 \pm 3.1$  SD, age range 7.76 – 19.49, 15 females) and 26 healthy control subjects (mean age  $13.1 \pm 2.9$  SD, age range 7.42 – 19.67, 16 females), matched for age and gender. Patients were diagnosed by NIH-criteria (National Institutes of Health Consensus Development Conference Statement: neurofibromatosis, 1988). Exclusion criteria for all participants were as follows: psychiatric disorder, neurological illness affecting brain function other than NF1, epilepsy, or a clinically significant intracranial abnormality detected on MRI. UBOs (Unidentified Bright Objects -  $T_2$ -hyperintensities commonly found in patients with NF1) located in the occipital cortex were considered exclusion criteria. Additionally, we excluded patients with intelligence quotient  $<70$ . The control group was recruited from a local school and informal advertising. Participants' academic records were in accordance with their chronological age, indicating adequate intellectual functioning. Children prescribed with stimulant medication (methylphenidate) were not medicated on the day of testing (4 NF1).

All participants had normal or corrected-to-normal visual acuity. To rule out eye disorders in the NF1 group, patients underwent an ophthalmological assessment including best-corrected visual acuity, stereopsis evaluation using Randot, slit lamp examination of anterior chamber structures and fundus examination. No anomalies that could affect vision were found. We assessed handedness using the Edinburgh Inventory (Oldfield, 1971); in the NF1 group 15 subjects were right-handed and 5 had mixed-handedness. In the control group 20 subjects were right-handed and 6 had mixed-handedness.

There were no between-group differences in age ( $t$ -test), gender or handedness (chi-square test).

Two participants with NF1 failed to perform the fMRI task as instructed, thus analysis involving fMRI data was carried out on 18 patients with NF1 and 26 control subjects. Participants underwent all imaging acquisitions on the same session.

### Genetic characterization

NF1 mutational profile was obtained by whole *NF1* gene sequencing. The mutation analysis of 19 of the 20 patients has been reported previously (Ribeiro et al., 2012). For the patient missing genetic testing, DNA was extracted from peripheral blood and standard procedures were used to perform whole-gene sequencing and multiplex ligation-dependent probe amplification analysis (Upadhyaya et al., 2009).

### fMRI paradigm

Visual stimuli were similar to those employed by Muthukumaraswamy *et al.* (2009) and consisted of a circular moving grating (80% contrast, spatial frequency 2 cycles/degree, 4° diameter, velocity 1 degree/second), equiluminant to the background. Stimuli were presented in the lower left visual field, subtended 4° horizontally and vertically, with the centre of the stimulus located 3.3° from a central fixation point, Figure 3. Stimulus duration was chosen randomly in an interval between 1.5–2 s followed by 10 s of fixation point only; 30 events were presented. Participants were instructed to maintain fixation on the central point for the entire experiment and to press a button, as fast as

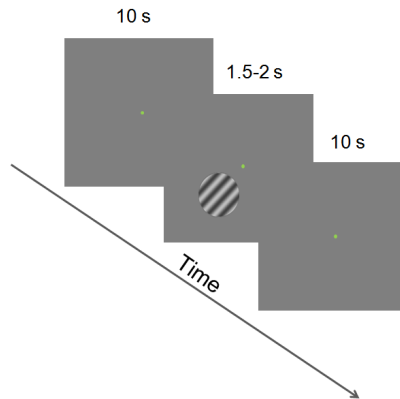


**Figure 3. A schematic diagram of the design for the fMRI visual stimulation.** Stimuli consisted of a circular moving grating (80% contrast, spatial frequency 2 cycles/degree, 4° diameter, velocity 1 degree/second), equiluminant to the background. Stimuli were presented in the lower left visual field, subtended 4° horizontally and vertically, with the centre of the stimulus located 3.3° from a central fixation point. Stimulus duration was chosen randomly in an interval between 1.5–2 s followed by 10 s of fixation point only; 30 events were presented. Participants were instructed to maintain fixation on the central green point for the entire experiment and to press a button, as fast as possible, when the grating disappeared.

possible, when the grating disappeared. Fixation was ensured by monitoring participants' eyes with a camera placed on the mirror system (Avotec Real Eye 5721, Florida, USA). All participants performed the task with a high-level of accuracy, >95 % correct responses.

### **MRI and MRS acquisitions**

Scanning was performed on a 3T Siemens scanner, using a 12-channel birdcage head coil. For each participant we acquired: i) a  $T_1$ -weighted ( $T_1w$ ) MPRAGE sequence, 1 mm<sup>3</sup> isotropic voxel, repetition time (TR) 2.3 s, echo time (TE) 2.98 ms, flip angle (FA) 9°, field of view (FOV) 256x256, 160 slices; ii) a  $T_2$ -weighted FLAIR sequence used to identify UBOs, 1 mm<sup>3</sup> isotropic voxel, TR 5 s, TE 2.98 ms, Inversion Time 1.8 s, FOV 250x250, 160 slices; iii) a single-shot echo-planar imaging (EPI) for the fMRI acquisition, 3 mm<sup>3</sup> isotropic voxel, TR 2 s, TE 39 ms, FA 90°, FOV 256x256, 23 slices; iv) a GABA-edited MR spectra using the MEGA-PRESS method (Mescher et al., 1998; Edden and Barker, 2007), 3 cm<sup>3</sup> isotropic voxel, TE 68 ms, TR 1.5 s, 196 averages, 1024 data points. During odd number acquisitions a frequency-selective inversion pulse was applied to the GABA-C3 resonance at 1.9 ppm ("On resonance"). During even number acquisitions the pulse was applied at 7.5 ppm ("Off resonance"). The voxel was positioned within the occipital cortex with its lower face aligned with the cerebellar tentorium. The sagittal sinus was avoided ensuring that the volume remained inside the occipital lobe, Figure 4a. During structural and spectroscopic acquisitions, participants were watching cartoons. This helped children to stay motionless during acquisitions. During the spectroscopic acquisition participants' eyes were monitored to ensure that none of the participants was at sleep.

### **MRI data analysis**

$T_1w$  images were used for MRS voxel placement and image segmentation. Segmentation was performed using in-house software written in Matlab7 (The MathWorks Inc., Massachusetts, USA) and the VBM8 toolbox in SPM8 (<http://www.fil.ion.ucl.ac.uk/spm>) and applied to determine the relative proportions of grey matter (GM), white matter (WM) and cerebrospinal fluid (CSF) in the voxel. FLAIR images were used to identify  $T_2$  hyperintensities, a common neuroradiological finding in patients with NF1. None of the control participants had UBOs and none of the UBOs found in patients were located in the occipital cortex.

### **fMRI data analysis**

Image processing and analysis were conducted using BrainVoyager QX2.3 (Brain Innovation, Maastricht, The Netherlands). We applied slice scan-time correction, linear trend removal, temporal high-pass filtering (2 cycles per run), spatial smoothing (FWHM 5mm) and motion correction. General linear model predictors were built by convolving a 2/10 s boxcar time course with a two-gamma function. Statistical thresholding was performed using false discovery rate,  $q(\text{FDR}) < 0.05$ .

### **MRS data analysis**

A difference spectrum was generated for each participant (“On resonance”-“Off resonance”). Using in-house software written in Matlab, we applied 4 Hz exponential line broadening to all spectra. Peak integration was used to quantify GABA (~3 ppm) and the combined glutamate plus glutamine (Glx) peaks (~3.75 ppm) in the difference spectra and total creatine (tCr) peak (3 ppm) in the summed spectra. Integrals of GABA, Glx and tCr peaks were automatically calculated using a linear fit of the baseline and Gaussian fits to the peaks.

### **Statistics**

Statistical analyses were performed with PAWS Statistics 18 (SPSS Inc., Chicago, USA). First, we verified the normality assumption for the different parameters using the Shapiro Wilk’s test. All data were normally distributed. For analysis, we used independent samples t-tests and Pearson’s correlation analyses.

To assess the effect of genotype on GABA levels, we first transformed GABA/tCr measurements of all participants to z-scores and performed a multiple regression analysis using a forced entry model, in which all predictors are forced into the model simultaneously. To construct the model we took into account the fact that age (Marenco et al., 2010), gender (O’Gorman et al., 2011) and GM content (Jensen et al., 2005a) may affect GABA concentration. Additional predictors were constructed from categorical variables relative to the type of *NF1* mutation (nonsense, missense, splice-site and mutation not found in the *NF1* gene).

## RESULTS

### MRS GABA levels

MRS measurements were performed in the visual cortex (Figure 4) of 20 children and adolescents with NF1 and 26 matched control subjects. GABA and glutamate + glutamine (Glx) peaks were well edited for all participants. Ratios of GABA/tCr and Glx/tCr were calculated for each subject. The tCr integrals were not statistically different between groups ( $t_{(44)} = -0.784, p = 0.437$ ). GABA/tCr provides reliable GABA concentration estimates and reduces inter-subject variance attributable to differences in signal-to-noise ratio and CSF fraction within the voxel (Bogner et al., 2009).

Patients with NF1 displayed significantly reduced GABA/tCr levels compared with controls, ( $t_{(44)} = -3.61, p = 0.001$ ), while Glx/tCr levels were not significantly different ( $t_{(44)} = -0.835, ns$ ), Figure 1c,d.

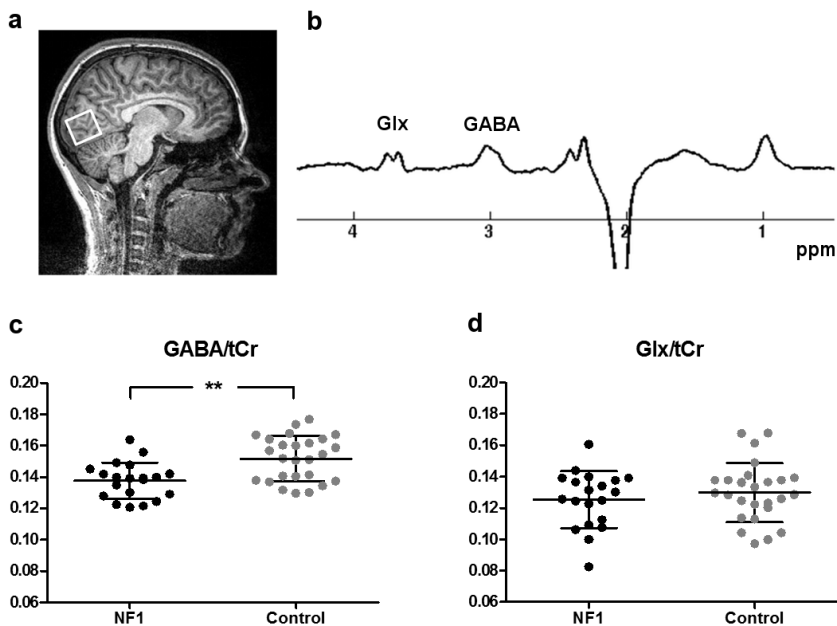


**Figure 4. GABA measurements.** a. Localization of the MRS voxel (white square) in the visual cortex of a representative participant. b. Edited MRS spectrum from a representative participant showing clearly resolved peaks for GABA and glutamine+glutamate (Glx). c,d. Cortical GABA/tCr levels and Glx/tCr levels for patients with NF1 (black, n=20) and controls (grey, n=26), respectively. Graphs depict individual values, mean and standard deviation.  $**p < 0.01$ .

The percentages of GM, WM and CSF in the spectroscopy voxel were assessed for each participant and were not significantly different between patients and controls ( $p = 0.196$ ,  $p = 0.074$ ,  $p = 0.604$ , respectively). This ensured that any difference in metabolite levels did not arise as a consequence of differences in tissue content between groups. Moreover, GABA/tCr was not correlated with GM ( $r = -0.066$ ,  $p = 0.782$  patients,  $r = 0.203$ ,  $p = 0.321$  controls), WM ( $r = -0.037$ ,  $p = 0.877$  patients,  $r = -0.302$ ,  $p = 0.134$  controls), or CSF ( $r = 0.023$ ,  $p = 0.924$  patients,  $r = 0.056$ ,  $p = 0.785$  controls). Additionally, differences in GABA levels cannot be explained by a different impact of age or gender in patients and control groups because neither age nor gender were associated with GABA/tCr (age:  $r = 0.267$ ,  $p = 0.255$  patients,  $r = -0.095$ ,  $p = 0.643$  controls; gender:  $r = 0.266$ ,  $p = 0.257$  patients,  $r = 0.142$ ,  $p = 0.490$  controls).

### Effect of genotype on GABA levels

**Table 1. Summary of the NF1 mutations identified in the patients with NF1**

Mutation Type	Mutation at cDNA level	Mutation at Protein Level
Nonsense	c. 2041C>T	p. Arg681X
	c. 3318C>G	p.Tyr1109X
	c. 3942G>A	p.Trp1314X
	c.5458C>T	p.Gln1828X
Frameshift	c.2500-2501 ins C	
Missense	c.2048T>C	p.Leu695Pro
	c.2786T>C	p.Leu929Pro
	c.5501T>G	p.Leu1834Arg*
Splice site	c.730+1G>A	IVS5
	c.1720+3A>G	IVS11 #
	c. 5944-6A>G	IVS31
	c.8097+1G>A	IVS47

\* Genetic characterization reported for the first time

# Mutation found in two related patients

The NF1 mutational profile of the patients is shown in Table 1. The mutational analysis of 19 of the 20 patients had been reported before (Ribeiro et al., 2012). For the new patient we found a novel missense mutation, which represents a change within the gene that has not been identified in > 1000 normal chromosomes studied for the entire *NF1* gene mutations. Disease-causing mutations were identified in 65% of the patients, in accordance with previous studies (Griffiths et al., 2007). Cases where the mutation was not identified might have a mutation missed by whole-gene sequencing but affecting gene expression, given that the criteria for diagnosis were fulfilled. A multiple regression model was applied to establish whether the type of mutation (nonsense, missense, splice site or mutation not found in the *NF1* gene) might explain the GABA levels in the occipital cortex. We used as predictors the type of mutation, age, gender and percentage of GM in the voxel. Given that only one frameshift mutation was present in our cohort, this type of mutation was not included as a predictor. The model obtained was significant for the predictor variables ( $F_{(7,37)} = 2.414, p = 0.039, R^2 = 0.31$ ).

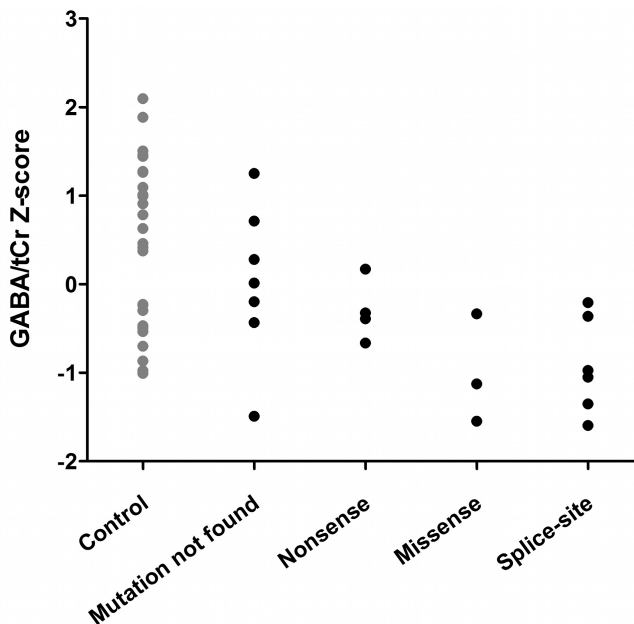


**Figure 5.** GABA/tCr z-scores for each participant grouped by genotype. GABA/tCr measurements from each participant were transformed to z-scores and plotted grouped according to the type of mutation found in our cohort of patients with NF1.

We found that splice-site or missense mutations are significant contributors to predict reduced GABA levels in the occipital cortex (Beta = -0.423,  $t = -3.005$ ,  $p = 0.005$  for splice-site mutations and Beta = -0.324,  $t = -2.104$ ,  $p = 0.042$  in the case of missense mutations). However, nonsense mutations or cases where the mutation is not found are insufficient to predict GABA levels below those of controls, Figure 5. Additionally, age, gender and GM content did not add predictive power to the model.

### Correlation between GABA and BOLD

We measured fMRI BOLD signal while participants performed a low-level visual task, Figure 3a. GABA/tCr levels were significantly correlated with peak BOLD amplitude in patients ( $n = 18$ ,  $r = -0.502$ ,  $p = 0.034$ ) and controls ( $n = 26$ ,  $r = -0.458$ ,  $p = 0.019$ ), Figure 3b. In contrast, no correlations were observed for the Glx/tCr levels in patients or control subjects, in agreement with previous findings (Edden et al., 2009; Stagg et al., 2011). Nevertheless, the regression slopes for the GABA-BOLD correlation were significantly different between groups ( $t_{(40)} = 15.5$ ,  $p < 0.001$ ), being steeper in patients with NF1. Given the reduced levels of GABA found in patients and the correlation between GABA and BOLD, one might expect higher BOLD in NF1. However, this is not necessarily the case and peak hemodynamic responses were not significantly different between groups, Figure 3c. In fact for the different average GABA/tCr in each group the BOLD signal presents the same mean activation.

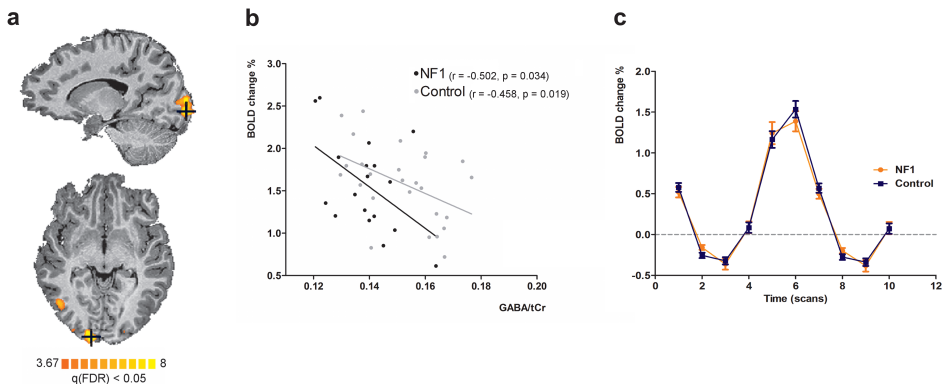


**Figure 6. Functional magnetic resonance imaging results.** **a.** BOLD activation in the visual cortex of a representative participant ( $p < 0.05$ , corrected for multiple comparisons using false discovery rate). A black crosshair indicates the peak voxel. **b.** GABA in the occipital cortex correlates with BOLD levels in patients (black,  $n = 18$ ) and controls (grey,  $n = 26$ ). **c.** BOLD response timecourses to the visual stimulation at the peak voxel for patients (orange) and controls (blue), error bars depict SEM.



## DISCUSSION

In this study, we report for the first time measurements of GABA levels in patients with NF1, which proved to be crucial to translate the hypothesis of altered inhibition in this condition. Our results point to lower GABA levels, while no alterations were observed in Glx/tCr levels, indicating an alteration in the balance between excitation and inhibition in the patients' visual cortex. An imbalance in the excitatory/inhibitory push-pull mechanism is in agreement with our previous findings of impaired visual contrast sensitivity in patients with NF1 (Ribeiro et al., 2012). Impaired contrast sensitivity was also found in pharmacological studies employing drugs that alter GABAergic transmission (Pearson and Timney, 1998). Furthermore, decreased GABA levels are in line with the evidence that lower GABA concentration is related to poorer visual orientation discrimination performance (Edden et al., 2009), a hallmark deficit of the cognitive impairments found in patients with NF1 (Schrimsher et al., 2003). Recently, it was shown that increased spiking of parvalbumin-positive (PV<sup>+</sup>) interneurons in the mouse primary visual cortex (V1) sharpens neuronal feature selectivity and improves perceptual discrimination (Lee et al., 2012). Additionally, application of bicuculine, a GABA<sub>A</sub> receptor antagonist, reversibly reduces orientation selectivity in animals (Sillito, 1975; Tsumoto et al., 1979; Sillito et al., 1980; Wolf et al., 1986). These results link GABAergic neurotransmission to a physiological impact of local manipulations of GABA concentration.

Previous studies conducted in animal models applied electrophysiological recordings in brain slices and provided evidences of increased IPSPs', an indication of augmented inhibitory neurotransmission. In an elegant study, Cui *et al.* (2008) used Cre-loxP mice to limit neurofibromin heterozygosity to specific cell types. They found that increased inhibition was related to a rise in miniature IPSPs' frequency as a result of *NF1* heterozygosity in inhibitory neurons, suggesting a role for neurofibromin in GABAergic neurotransmission. Accordingly, increased frequency of miniature IPSPs was attributable to higher levels of GABA release due to increased phosphorylation of synapsin 1, a protein with a critical role in the regulation of neurotransmitter storage and release (Hilfiker et al., 1999). Our results in human patients point to reduced GABA levels, which may at first sight look contradictory to the animal model. Whereas no alterations were observed in Glx/tCr levels, in accordance with the findings from the animal model showing that neurofibromin alterations do not affect excitatory transmission.

Reduced GABA levels in patients are not necessarily inconsistent with increased inhibitory activity observed in the (*Nf1*<sup>+/-</sup>) mouse model. It is important to highlight that

there is a distinction between total GABA *concentration* measured by MRS and GABA *neurotransmission* measured in the animal model, even though there is a close relationship between overall GABA concentration measured by MRS and the concentration at the vesicular pool (Golan et al., 1996). In fact, MRS measurements of healthy individuals under the influence of alcohol (Gomez et al., 2011) and benzodiazepines (Goddard et al., 2004) revealed decreased GABA levels in the visual cortex, while studies in animals reported increased IPSPs (Perrais and Ropert, 1999; Roberto et al., 2003).

Mechanistically, it is possible that in the human brain the activation of synapsin 1 is also increased, leading to a larger pool of releasable synaptic vesicles. The low GABA levels measured here might reflect a compensatory mechanism. Increased GABAergic neurotransmission can modulate GABA metabolism by down-regulating GABA synthesizing enzymes (GADs), limiting the GABA available for packaging and release (Sheikh and Martin, 1998). As mentioned earlier GABA levels are dynamically modulated in response to increasing or decreasing network activity and in the context of brain disorders (Esclapez and Houser, 1999; Gomes et al., 2011). Further studies are needed to evaluate these possibilities. In particular, studies in both patients and animal models employing  $^{13}\text{C}$ -MRS and molecular imaging using positron emission tomography (PET) would deepen our understanding of the disease mechanism.

Interestingly, other neurodevelopmental disorders have been related with GABAergic dysfunction, namely autism, Down syndrome, schizophrenia and Fragile X (Ramamoorthi and Lin, 2011). Similarly to the alterations proposed by the NF1 mouse model, a mouse model of Down syndrome (Ts65Dn) showed increased inhibition (Kleschevnikov et al., 2004), while decreased GABA levels have been reported in patients *in vivo* (Smigielska-Kuzia et al., 2010) as well as in biochemical measurements in foetuses (Whittle et al., 2007). To develop potential treatments, it is critical to understand how enhanced inhibitory neurotransmission in mice models might be reflected in decreased GABA levels in humans. For that, it will be crucial to apply to the mice models the analytical tools available to measure GABA levels in humans.

In this study, we also investigated the genotypic impact on GABA levels. The study of genotype-phenotype correlations in NF1 is hampered by the high mutation rate of the *NF1* gene, resulting in more than 1000 different disease-causing mutations reported (HGMD, <http://www.hgmd.cf.ac.uk>). Nonetheless, by grouping mutations by type and performing linear regression analysis, we found that individuals with missense and splice-site mutations have significantly less GABA/tCr levels than control subjects.

Our findings are consistent with the idea that abnormal neurofibromin proteins resulting from missense or splice-site mutations can act as dominant negatives disrupting the function of the healthy allele, given that patients with NF1 are heterozygous for the mutation (Jett and Friedman, 2009), and resulting in a more severe phenotype than nonsense mutations (Khajavi et al., 2006). These results should, however, be interpreted cautiously in terms of mutation type, due to the relatively reduced number of patients.

At last, we confirmed that BOLD and GABA levels are negatively correlated, in agreement with previous studies (Edden et al., 2009; Stagg et al., 2011). We performed a regression analysis for each group and although it indicated that we can predict equally well in both groups the effect of GABA in BOLD (similar correlation coefficients, showing similarly explained variance), the difference in slopes observed indicates that changes in BOLD activity are larger for the same unitary change in GABA levels in NF1, under matched activation conditions. This suggests a more sensitive inhibitory vs. excitatory push-pull mechanism in patients. Peak hemodynamic responses were not significantly different between groups, implying that other factors besides the physiological coupling between BOLD and inhibition also contribute to the BOLD signal variance (Logothetis, 2008).

Regarding methodological considerations, several studies have addressed the issue of sensitivity and validity of GABA measurements using MEGA-PRESS (Puts and Edden, 2012). Still, it is relevant to remind that the GABA peak may be contaminated by macromolecules (Rothman et al., 1993; Kegeles et al., 2007). However, it seems unlikely that differences between patients with NF1 and controls were explained by macromolecules, particularly taking into account the correlation found between GABA measurements and BOLD signal. Besides, there are mounting evidences of the biological relevance of GABA measurements using MRS, and its correlation with behavioural processes (Edden et al., 2009; Sumner et al., 2010; Stagg et al., 2011).

In summary, we reported GABA changes in patients with NF1. Our results show that the excitation/inhibition balance is altered in the visual cortex of patients, as a consequence of reduced GABA levels. Although our conclusions are derived from measurements of GABA in visual cortex, it is likely that analogous abnormalities generalize to other cortical areas, in agreement with the widespread GABAergic alterations observed in mice (Shilyansky et al., 2010). In addition, there is substantial evidence that the morphological subtypes of cortical neurons and their basic laminar and tangential connectivity are conserved across cortical areas (Douglas and Martin, 2004).

GABA concentration was related to the type of mutation, providing a link between neurofibromin function and regulation of GABA metabolism in humans. Importantly, our experimental and methodological approach provides an example that could be applied to monitor GABA changes as a consequence of therapeutic approaches in NF1 and other neurodevelopmental disorders where alterations in GABAergic neurotransmission were proposed to underlie cognitive deficits, namely autism, Fragile X syndrome and Down syndrome (Ramamoorthi and Lin, 2011).

## REFERENCES

- Bahner F, Weiss EK, Birke G, Maier N, Schmitz D, Rudolph U, Frotscher M, Traub RD, Both M, Draguhn A. Cellular correlate of assembly formation in oscillating hippocampal networks in vitro. *Proc Natl Acad Sci U S A*. 108:35 (2011) E607-616.
- Ballester R, Marchuk D, Boguski M, Saulino A, Letcher R, Wigler M, Collins F. The NF1 locus encodes a protein functionally related to mammalian GAP and yeast IRA proteins. *Cell*. 63:4 (1990) 851-859.
- Banay-Schwartz M, Palkovits M, Lajtha A. Heterogeneous distribution of functionally important amino acids in brain areas of adult and aging humans. *Neurochem Res*. 18:4 (1993) 417-423.
- Barberis A, Petrini EM, Cherubini E. Presynaptic source of quantal size variability at GABAergic synapses in rat hippocampal neurons in culture. *Eur J Neurosci*. 20:7 (2004) 1803-1810.
- Bielicki G, Chassain C, Renou JP, Farges MC, Vasson MP, Eschalier A, Durif F. Brain GABA editing by localized in vivo <sup>1</sup>H magnetic resonance spectroscopy. *NMR Biomed*. 17:2 (2004) 60-68.
- Bogner W, Gruber S, Doelken M, Stadlbauer A, Ganslandt O, Boettcher U, Trattng S, Doerfler A, Stefan H, Hammen T. In vivo quantification of intracerebral GABA by single-voxel <sup>1</sup>H-MRS-How reproducible are the results? *Eur J Radiol*. 73:3 (2009) 526-531.
- Buzsaki G, Kaila K, Raichle M. Inhibition and brain work. *Neuron*. 56:5 (2007) 771-783.
- Chi P, Greengard P, Ryan TA. Synapsin dispersion and recluster during synaptic activity. *Nat Neurosci*. 4:12 (2001) 1187-1193.
- Choi I-Y, Shen J, Gruetter R. In Vivo GABA Metabolism. In: *Neural Metabolism In Vivo* (Lajtha A, ed), pp 1095-1116: Springer US 2012.
- Costa RM, Federov NB, Kogan JH, Murphy GG, Stern J, Ohno M, Kucherlapati R, Jacks T, Silva AJ. Mechanism for the learning deficits in a mouse model of neurofibromatosis type 1. *Nature*. 415:6871 (2002) 526-530.
- Cui Y, Costa RM, Murphy GG, Elgersma Y, Zhu Y, Gutmann DH, Parada LF, Mody I, Silva AJ. Neurofibromin regulation of ERK signaling modulates GABA release and learning. *Cell*. 135:3 (2008) 549-560.
- DeFelipe J. Neocortical neuronal diversity: chemical heterogeneity revealed by colocalization studies of classic neurotransmitters, neuropeptides, calcium-binding proteins, and cell surface molecules. *Cereb Cortex*.

- 3:4 (1993) 273-289.
- Douglas RJ, Martin KA. Neuronal circuits of the neocortex. *Annu Rev Neurosci.* 27:(2004) 419-451.
- Edden RA, Barker PB. Spatial effects in the detection of gamma-aminobutyric acid: improved sensitivity at high fields using inner volume saturation. *Magn Reson Med.* 58:6 (2007) 1276-1282.
- Edden RA, Muthukumaraswamy SD, Freeman TC, Singh KD. Orientation discrimination performance is predicted by GABA concentration and gamma oscillation frequency in human primary visual cortex. *J Neurosci.* 29:50 (2009) 15721-15726.
- Esclapez M, Houser CR. Up-regulation of GAD65 and GAD67 in remaining hippocampal GABA neurons in a model of temporal lobe epilepsy. *J Comp Neurol.* 412:3 (1999) 488-505.
- Goddard AW, Mason GF, Appel M, Rothman DL, Gueorguieva R, Behar KL, Krystal JH. Impaired GABA neuronal response to acute benzodiazepine administration in panic disorder. *Am J Psychiatry.* 161:12 (2004) 2186-2193.
- Golan H, Talpalar AE, Schleifstein-Attias D, Grossman Y. GABA metabolism controls inhibition efficacy in the mammalian CNS. *Neurosci Lett.* 217:1 (1996) 25-28.
- Gomes JR, Lobo AC, Melo CV, Inacio AR, Takano J, Iwata N, Saido TC, de Almeida LP, Wieloch T, Duarte CB. Cleavage of the vesicular GABA transporter under excitotoxic conditions is followed by accumulation of the truncated transporter in nonsynaptic sites. *J Neurosci.* 31:12 (2011) 4622-4635.
- Gomez R, Behar KL, Watzl J, Weinzimer SA, Gulanski B, Sanacora G, Koretski J, Guidone E, Jiang L, Petrakis IL, Pittman B, Krystal JH, Mason GF. Intravenous ethanol infusion decreases human cortical gamma-aminobutyric acid and N-acetylaspartate as measured with proton magnetic resonance spectroscopy at 4 tesla. *Biol Psychiatry.* 71:3 (2011) 239-246.
- Griffiths S, Thompson P, Frayling I, Upadhyaya M. Molecular diagnosis of neurofibromatosis type 1: 2 years experience. *Fam Cancer.* 6:1 (2007) 21-34.
- Hendry SH, Schwark HD, Jones EG, Yan J. Numbers and proportions of GABA-immunoreactive neurons in different areas of monkey cerebral cortex. *J Neurosci.* 7:5 (1987) 1503-1519.
- Hilfiker S, Pieribone VA, Czernik AJ, Kao HT, Augustine GJ, Greengard P. Synapsins as regulators of neurotransmitter release. *Philos Trans R Soc Lond B Biol Sci.* 354:1381 (1999) 269-279.
- Jensen JE, Frederick Bde B, Renshaw PF. Grey and white matter GABA level differences in the human brain using two-dimensional, J-resolved spectroscopic imaging. *NMR Biomed.* 18:8 (2005a) 570-576.
- Jensen JE, Frederick BD, Wang L, Brown J, Renshaw PF. Two-dimensional, J-resolved spectroscopic imaging of GABA at 4 Tesla in the human brain. *Magn Reson Med.* 54:4 (2005b) 783-788.
- Jett K, Friedman JM. Clinical and genetic aspects of neurofibromatosis 1. *Genet Med.* 12:1 (2009) 1-11.
- Kegeles L, Mao X, Gonzalez R, Shungu DC. Evaluation of anatomic variation in macromolecule contribution to the GABA signal using metabolite nulling and the J-editing technique at 3T. In: 15th Annual Meeting of ISMRM, p p. abstract 391. Berlin, Germany 2007.
- Khajavi M, Inoue K, Lupski JR. Nonsense-mediated mRNA decay modulates clinical outcome of genetic disease. *Eur J Hum Genet.* 14:10 (2006) 1074-1081.
- Klausberger T, Somogyi P. Neuronal diversity and temporal dynamics: the unity of hippocampal circuit operations. *Science.* 321:5885 (2008) 53-57.

- Kleschevnikov AM, Belichenko PV, Villar AJ, Epstein CJ, Malenka RC, Mobley WC. Hippocampal long-term potentiation suppressed by increased inhibition in the Ts65Dn mouse, a genetic model of Down syndrome. *J Neurosci.* 24:37 (2004) 8153-8160.
- Kushner SA, Elgersma Y, Murphy GG, Jaarsma D, van Woerden GM, Hojjati MR, Cui Y, LeBoutillier JC, Marrone DF, Choi ES, De Zeeuw CI, Petit TL, Pozzo-Miller L, Silva AJ. Modulation of presynaptic plasticity and learning by the H-ras/extracellular signal-regulated kinase/synapsin I signaling pathway. *J Neurosci.* 25:42 (2005) 9721-9734.
- Lee S-H, Kwan AC, Zhang S, Phoumthipphavong V, Flannery JG, Masmanidis SC, Taniguchi H, Huang ZJ, Zhang F, Boyden ES, Deisseroth K, Dan Y. Activation of specific interneurons improves V1 feature selectivity and visual perception. *Nature.* 488:7411 (2012) 379-383.
- Logothetis NK. What we can do and what we cannot do with fMRI. *Nature.* 453:7197 (2008) 869-878.
- Mann EO, Paulsen O. Role of GABAergic inhibition in hippocampal network oscillations. *Trends Neurosci.* 30:7 (2007) 343-349.
- Marengo S, Savostyanova AA, van der Veen JW, Geramita M, Stern A, Barnett AS, Kolachana B, Radulescu E, Zhang F, Callicott JH, Straub RE, Shen J, Weinberger DR. Genetic modulation of GABA levels in the anterior cingulate cortex by GAD1 and COMT. *Neuropsychopharmacology.* 35:8 (2010) 1708-1717.
- Markram H, Toledo-Rodriguez M, Wang Y, Gupta A, Silberberg G, Wu C. Interneurons of the neocortical inhibitory system. *Nat Rev Neurosci.* 5:10 (2004) 793-807.
- Mescher M, Merkle H, Kirsch J, Garwood M, Gruetter R. Simultaneous in vivo spectral editing and water suppression. *NMR Biomed.* 11:6 (1998) 266-272.
- Mozrzymas JW, Barberis A, Michalak K, Cherubini E. Chlorpromazine inhibits miniature GABAergic currents by reducing the binding and by increasing the unbinding rate of GABAA receptors. *J Neurosci.* 19:7 (1999) 2474-2488.
- Muthukumaraswamy SD, Evans CJ, Edden RA, Wise RG, Singh KD. Individual variability in the shape and amplitude of the BOLD-HRF correlates with endogenous GABAergic inhibition. *Hum Brain Mapp.* 33:2 (2011) 455-465.
- National Institutes of Health Consensus Development Conference Statement: neurofibromatosis. Bethesda, Md., USA, July 13-15 1987. *Neurofibromatosis.* 1:3 (1988) 172-178.
- Northoff G, Walter M, Schulte RF, Beck J, Dydak U, Henning A, Boeker H, Grimm S, Boesiger P. GABA concentrations in the human anterior cingulate cortex predict negative BOLD responses in fMRI. *Nat Neurosci.* 10:12 (2007) 1515-1517.
- O'Gorman RL, Michels L, Edden RA, Murdoch JB, Martin E. In vivo detection of GABA and glutamate with MEGA-PRESS: reproducibility and gender effects. *J Magn Reson Imaging.* 33:5 (2011) 1262-1267.
- Okada Y, Nitsch-Hassler C, Kim JS, Bak JJ, Hassler R. Role of  $\gamma$ -aminobutyric acid (GABA) in the extrapyramidal motor system. 1. Regional distribution of GABA in rabbit, rat, guinea pig and baboon CNS. *Exp Brain Res.* 13:5 (1971) 514-518.
- Oldfield RC. The assessment and analysis of handedness: the Edinburgh inventory. *Neuropsychologia.* 9:1 (1971) 97-113.
- Owens DF, Kriegstein AR. Is there more to GABA than synaptic inhibition? *Nat Rev Neurosci.* 3:9 (2002)

715-727.

- Pearson P, Timney B. Effects of moderate blood alcohol concentrations on spatial and temporal contrast sensitivity. *J Stud Alcohol.* 59:2 (1998) 163-173.
- Perrais D, Ropert N. Effect of zolpidem on miniature IPSCs and occupancy of postsynaptic GABAA receptors in central synapses. *J Neurosci.* 19:2 (1999) 578-588.
- Puts NA, Edden RA. In vivo magnetic resonance spectroscopy of GABA: a methodological review. *Prog Nucl Magn Reson Spectrosc.* 60:(2012) 29-41.
- Ramamoorthi K, Lin Y. The contribution of GABAergic dysfunction to neurodevelopmental disorders. *Trends Mol Med.* 17:8 (2011) 452-462.
- Ribeiro MJ, Violante IR, Bernardino I, Ramos F, Saraiva J, Reviriego P, Upadhyaya M, Silva ED, Castelo-Branco M. Abnormal achromatic and chromatic contrast sensitivity in neurofibromatosis type 1. *Invest Ophthalmol Vis Sci.* 53:1 (2012) 287-293.
- Roberto M, Madamba SG, Moore SD, Tallent MK, Siggins GR. Ethanol increases GABAergic transmission at both pre- and postsynaptic sites in rat central amygdala neurons. *Proc Natl Acad Sci U S A.* 100:4 (2003) 2053-2058.
- Rothman DL, Petroff OA, Behar KL, Mattson RH. Localized <sup>1</sup>H NMR measurements of gamma-aminobutyric acid in human brain in vivo. *Proc Natl Acad Sci U S A.* 90:12 (1993) 5662-5666.
- Scanziani M. GABA spillover activates postsynaptic GABA(B) receptors to control rhythmic hippocampal activity. *Neuron.* 25:3 (2000) 673-681.
- Schrimsher GW, Billingsley RL, Slopis JM, Moore BD, 3rd. Visual-spatial performance deficits in children with neurofibromatosis type-1. *Am J Med Genet A.* 120A:3 (2003) 326-330.
- Sheikh SN, Martin DL. Elevation of brain GABA levels with vigabatrin (gamma-vinylGABA) differentially affects GAD65 and GAD67 expression in various regions of rat brain. *J Neurosci Res.* 52:6 (1998) 736-741.
- Shilyansky C, Karlsgodt KH, Cummings DM, Sidiropoulou K, Hardt M, James AS, Ehninger D, Bearden CE, Poirazi P, Jentsch JD, Cannon TD, Levine MS, Silva AJ. Neurofibromin regulates corticostriatal inhibitory networks during working memory performance. *Proc Natl Acad Sci U S A.* 107:29 (2010) 13141-13146.
- Sillito AM. The contribution of inhibitory mechanisms to the receptive field properties of neurones in the striate cortex of the cat. *J Physiol.* 250:2 (1975) 305-329.
- Sillito AM, Kemp JA, Milson JA, Berardi N. A re-evaluation of the mechanisms underlying simple cell orientation selectivity. *Brain Res.* 194:2 (1980) 517-520.
- Smigielska-Kuzia J, Bockowski L, Sobaniec W, Kulak W, Sendrowski K. Amino acid metabolic processes in the temporal lobes assessed by proton magnetic resonance spectroscopy (1H MRS) in children with Down syndrome. *Pharmacol Rep.* 62:6 (2010) 1070-1077.
- Stagg CJ, Bachtiar V, Johansen-Berg H. The role of GABA in human motor learning. *Curr Biol.* 21:6 (2011) 480-484.
- Sumner P, Edden RA, Bompas A, Evans CJ, Singh KD. More GABA, less distraction: a neurochemical predictor of motor decision speed. *Nat Neurosci.* 13:7 (2010) 825-827.

- Terpstra M, Ugurbil K, Gruetter R. Direct in vivo measurement of human cerebral GABA concentration using MEGA-editing at 7 Tesla. *Magn Reson Med.* 47:5 (2002) 1009-1012.
- Thomson SA, Fishbein L, Wallace MR. NF1 mutations and molecular testing. *J Child Neurol.* 17:8 (2002) 555-561; discussion 571-552, 646-551.
- Tsumoto T, Eckart W, Creutzfeldt OD. Modification of orientation sensitivity of cat visual cortex neurons by removal of GABA-mediated inhibition. *Exp Brain Res.* 34:2 (1979) 351-363.
- Tukker JJ, Fuentealba P, Hartwich K, Somogyi P, Klausberger T. Cell type-specific tuning of hippocampal interneuron firing during gamma oscillations in vivo. *J Neurosci.* 27:31 (2007) 8184-8189.
- Upadhyaya M, Spurlock G, Kluwe L, Chuzhanova N, Bennett E, Thomas N, Guha A, Mautner V. The spectrum of somatic and germline NF1 mutations in NF1 patients with spinal neurofibromas. *Neurogenetics.* 10:3 (2009) 251-263.
- Violante IR, Ribeiro MJ, Cunha G, Bernardino I, Duarte JV, Ramos F, Saraiva J, Silva E, Castelo-Branco M. Abnormal Brain Activation in Neurofibromatosis Type 1: A Link between Visual Processing and the Default Mode Network. *PLoS One.* 7:6 (2012) e38785.
- Walker MC, Semyanov A. Regulation of excitability by extrasynaptic GABA(A) receptors. *Results Probl Cell Differ.* 44:(2008) 29-48.
- Whittle N, Sartori SB, Dierssen M, Lubec G, Singewald N. Fetal Down syndrome brains exhibit aberrant levels of neurotransmitters critical for normal brain development. *Pediatrics.* 120:6 (2007) e1465-1471.
- Wolf W, Hicks TP, Albus K. The contribution of GABA-mediated inhibitory mechanisms to visual response properties of neurons in the kitten's striate cortex. *J Neurosci.* 6:10 (1986) 2779-2795.
- Yoon JH, Maddock RJ, Rokem A, Silver MA, Minzenberg MJ, Ragland JD, Carter CS. GABA concentration is reduced in visual cortex in schizophrenia and correlates with orientation-specific surround suppression. *J Neurosci.* 30:10 (2010) 3777-3781.



## CHAPTER 6

Gyrification, cortical and  
subcortical morphometry in  
Neurofibromatosis type 1:  
an uneven profile of  
developmental abnormalities

**ABSTRACT**

Neurofibromatosis type 1 (NF1) is a monogenic disorder associated with cognitive impairments. In order to understand how mutations in the *NF1* gene impact brain structure it is essential to characterize in detail the brain structural abnormalities in patients with NF1. Previous studies have reported contradictory findings and have focused only on volumetric measurements. In here we investigated the volumes of subcortical structures and the composite dimensions of the cortex, through the analysis of cortical volume, cortical thickness, cortical surface area and gyrification.

We studied 14 children with NF1 and 14 typically developing children matched for age, gender, IQ and handedness. Regional subcortical volumes and cortical gyrification measurements were obtained using FreeSurfer. Between-group differences were evaluated while controlling for the increase in total intracranial volume observed in NF1. Subcortical analysis revealed disproportionately larger thalami, right caudate and middle corpus callosum in patients with NF1. Cortical analyses on volume, thickness and surface area were however not indicative of significant alterations in patients. Interestingly, patients with NF1 had significant lower gyrification indices than typically developing children primarily in frontal and temporal lobes, but also affecting the insula, cingulate cortex, parietal and occipital regions.

The neuroanatomic abnormalities observed were localized to specific brain regions indicating that particular areas might constitute selective targets for *NF1* gene mutation. Furthermore, the lower gyrification indices were accompanied by a disproportionate increase in brain size without the corresponding increase in folding in patients with NF1. Taken together these findings suggest that specific neurodevelopmental processes, such as gyrification, are more vulnerable to *NF1* dysfunction than others. The identified changes in brain organization are consistent with the patterns of cognitive dysfunction in the NF1 phenotype.

## INTRODUCTION

Brain development is dependent on a series of complex events including cellular proliferation, growth, differentiation and migration, programmed cell death and synaptic elimination. These events largely determine brain morphology (Rakic and Kornack, 2007). Since brain structure is under significant genetic influence (Thompson et al., 2001) it is important to use genetic models to understand its ontogeny.

Neurofibromatosis type 1 (NF1) is a good model in this respect, because it is a monogenic disorder caused by mutations in the *NF1* gene. In the brain, neurofibromin, the protein product of the *NF1* gene, is expressed in both neurons and glial cells (Daston and Ratner, 1992; Zhu et al., 2005) and is required for neural development (Hegedus et al., 2007; Lush et al., 2008). Loss of neurofibromin results in increased cellular growth (Yunoue et al., 2003), while it is also involved in learning and memory (Fernandez-Medarde and Santos, 2011). Thus, this disease provides a unique window into gene-brain-behavior relationships. The role of neurofibromin in cellular growth and its ubiquitous expression in the brain suggest that brain structure might be affected in patients. In fact, there is a high incidence of macrocephaly, optic gliomas and T<sub>2</sub>-weighted hyperintensities (Payne et al., 2010). Nevertheless, the gross brain anatomy appears normal and it has been difficult to determine if brain structure is altered independent of focal lesions.

Recent advances in neuroimaging allow an increasingly detailed delineation of developmental anomalies. Previous studies focusing on NF1 brain structure have examined the relative contributions of grey matter (GM) and white matter (WM) to increased brain size, with contradictory results (Payne et al., 2010). The majority of studies points to macrocephaly being caused by increases in WM (Said et al., 1996; Steen et al., 2001) or a combination of WM and GM (Cutting et al., 2002a; Greenwood et al., 2005). Only one study pointed to increases in GM (Moore et al., 2000). However, few reports attempted to delineate specific regions with abnormal morphometry. Cutting *et al.* (2002a) focused on frontal and parietal lobe subdivisions and found they presented increased WM volume. Greenwood and colleagues (Greenwood et al., 2005) divided the brain in 16 parcellations and besides a total increase in GM and WM volumes in patients with NF1, they reported increased GM in occipital and parietal regions and increased WM in anterior regions. Other brain structure anomalies observed included increased brainstem growth rate, suggestive of abnormal cell proliferation (DiMario et al., 1999), smaller surface area and GM volume of the left *planum temporal* of NF1 boys compared with controls (Billingsley et al., 2002) and abnormal thalamic metabolic patterns observed

with positron emission tomography (Kaplan et al., 1997) and magnetic resonance spectroscopy (Wang et al., 2000). Furthermore, in a previous study from our laboratory, support vector machines were able to reveal the existence of brain structural differences in GM and WM tissue that could accurately discriminate individuals with NF1 from controls (Duarte et al., 2012).

However, no previous study performed morphometric measurements of subcortical and cortical structures across the whole brain. Moreover, we extended our investigation beyond the volumetric dimension as alterations in neurofibromin expression might be differently reflected across the brain and manifest in distinct structures and morphological traits.

In this study, our aim was to provide a multidimensional morphometric analysis to clarify how brain structure is affected by NF1. For that we measured subcortical and cortical volumes, cortical thickness, cortical surface area and gyrification across the entire brain. The importance of assessing multiple morphometric traits is explained by the fact that they underlie distinctive evolutionary (Rakic, 1995), genetic (Panizzon et al., 2009) and developmental (Armstrong et al., 1995; Raznahan et al., 2011) processes. A crucial point in our study was a careful matching of the control group, as several factors are known to influence the results, including age (Raznahan et al., 2011), gender (Luders et al., 2006), intelligence (Shaw et al., 2006; Luders et al., 2008) and handedness (Narr et al., 2007). Previous studies focusing on structural alterations in NF1 were often biased by gender (Cutting et al., 2002a) or included patients with brain tumors (Moore et al., 2000; Greenwood et al., 2005). Moreover, the majority of studies lacked matching for the intelligence quotient (IQ). Therefore, in the present study we selected both patients and controls to ensure matching for age, sex, handedness and IQ.

We hypothesized that children with NF1 would present a pattern of morphological alterations that it is not limited to one brain region given the range of neuropsychological deficits observed in patients and the wide expression of neurofibromin in the brain. Nevertheless, we also expected that brain abnormalities would be most prominent in frontal and parietal neocortical regions in agreement with the consistent impairments observed across studies in executive and visuospatial domains (Levine et al., 2006).

## METHODS

### Subjects

The participants in this study belong to a larger cohort from our previous studies (Duarte et al., 2012; Violante et al., 2012) and were selected so that the groups were matched for age, gender, IQ and handedness. We studied 14 patients with NF1 (mean age:  $11.34 \pm 2.51$  SD; age range: 7.83 – 16.08 years; 6 males, 8 females) and 14 matched typically developing (TD) subjects (mean age:  $11.89 \pm 2.06$  SD; age range: 7.83 – 15.33 years; 5 males, 9 females). All participants were right-handed.

**Table 1.** Demographic and Neuropsychological characterization

	NF1 (n = 14)	TD (n = 14)
Age	11.34 (2.51) Range: 7.83 – 16.08	11.89 (2.06) Range: 7.83 – 15.33
Gender (M:F)	6M : 8F	5M : 9F
Handedness (right:left)	14:0	14:0
FSIQ	104.36 (13.41) Range: 90 - 126	110.00 (10.97) Range: 90 - 124
VIQ	107.28 (11.38) Range: 94 - 126	109.86 (11.90) Range: 93 - 129
PIQ	99.43 (12.43) Range: 80 - 119	109.07 (12.86) Range: 87 - 136

NF1 = Neurofibromatosis type 1; TD = typically developing; M = male; F = female; FSIQ = full-scale intelligence quotient; VIQ = verbal intelligence quotient; PIQ = performance intelligence quotient. Data are mean (SD).

Patients were recruited and diagnosed in collaboration with the Clinical Genetics Department of the Paediatric Hospital of Coimbra according to the NIH defined diagnostic criteria (National Institutes of Health Consensus Development Conference Statement: neurofibromatosis, 1988). The TD group was recruited from a local school. Exclusion criteria for all participants were as follows: psychiatric disorder, neurological illness affecting brain function other than NF1, epilepsy, tumors or other clinically significant intracranial abnormality detected on MRI. UBOs (Unidentified Bright Objects -  $T_2$ -hyperintensities commonly found in patients with NF1) were not considered exclusion criteria when present in patients. Additionally, we only included patients with intelligence quotient  $\geq 90$  in order to be able to match to typically developing children. Children prescribed with stimulant medication (methylphenidate) were not medicated on the day of MRI acquisition and neuropsychological assessment (3 NF1).

Neuropsychological assessment was performed using the Portuguese adapted version of the Wechsler Intelligence Scale for Children (WISC-III) (Wechsler, 2003). Demographic and neuropsychological characterization of both groups is shown in Table 1.

### **MRI acquisition**

Scanning was performed on a 3T Siemens TimTrio scanner, using a 12-channel birdcage head coil. In this study we analyzed acquired data with the following parameters: i) two  $T_1$ -weighted ( $T_1w$ ) MPRAGE sequences, 1x1x1 mm voxel size, repetition time (TR) 2.3 s, echo time (TE) 2.98 ms, flip angle (FA) 9°, field of view (FOV) 256x256, 160 slices; ii) a  $T_2$ -weighted ( $T_2w$ ) FLAIR sequence, 1x1x1 mm voxel size, TR 5 s, TE 2.98 ms, Inversion Time (TI) 1.8 s, FOV 250x250, 160 slices. FLAIR images were used to identify  $T_2$  hyperintensities. A neuroradiologist, blind to the participants' clinical history observed the MR structural scans and reported on the distribution and number of UBOs.

### **MRI data analyses**

Cortical reconstruction and volumetric segmentation were performed with the FreeSurfer image analysis suite (FreeSurfer v5.1.0, <http://surfer.nmr.mgh.harvard.edu>), as described in prior publications (Dale et al., 1999; Fischl and Dale, 2000; Fischl et al., 2002). Briefly the processing included, motion correction, averaging of the two  $T_1w$  images, registration to Talairach space, segmentation of the subcortical WM and deep GM

volumetric structures (Fischl et al., 2002; Fischl et al., 2004), intensity normalization, tessellation of the GM/WM boundary, automated topology correction (Fischl et al., 2001; Segonne et al., 2007), and surface deformation following intensity gradients to optimally place the GM/WM and GM/CSF borders (Dale et al., 1999). Image outputs were visually inspected and inaccuracies corrected when required. Registration was performed to a spherical atlas (Fischl et al., 1999), Figure 1.

Cortical thickness was calculated as the closest distance from the GM/WM boundary to the GM/CSF boundary at each vertex on the tessellated surface (Fischl and Dale, 2000). Surface area assigned to each vertex on the GM/WM matter surface was calculated as the average area of all triangles that surround the vertex. Local gyrification indices (LGI) were computed using local measurements of gyrification over the whole cortical surface using the method developed by Schaer *et al.* (2008). The LGI reflects the amount of cortex buried within the sulcal folds.

Cortical volume, surface area, cortical thickness and the local gyrification indices were estimated for 34 gyral regions per hemisphere as defined by the atlas developed by Desikan *et al.* (2006), Figure 2, recently modified to include the insula as a region of interest. GM volume was estimated for subcortical structures. WM and GM brain volumes, WM and GM cerebellar volumes, WM and GM lobar volumes and total intracranial volumes (TIV) were also estimated for each participant.

### Statistical analyses

Statistical analyses were performed with PAWS Statistics 18 (SPSS Inc., Chicago, USA). First, we verified the normality assumption for the different parameters using the Shapiro Wilk's test. All data were normally distributed. Group differences in demographic and neuropsychological data were evaluated with independent samples t-tests. Gender differences were evaluated using Chi-square tests.

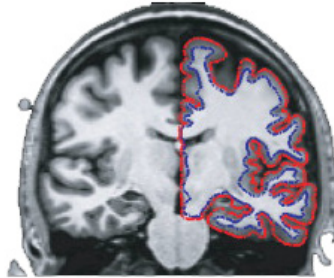
Group differences in overall volumetric measurements were assessed using independent samples t-tests. For lobar regions and cerebellar WM and GM we used repeated measures ANCOVA with group (NF1 vs typically developing) as the between-subjects factor and hemispheres (left vs right) and brain regions (lobes/cerebellar WM/cerebellar GM) as the within-subjects factors and total intracranial volume (TIV) as covariate.

Analyses of subcortical volumetric differences were assessed using multivariate ANOVA. To determine whether the results were mediated by overall intracranial volume we performed an ANCOVA with TIV as covariate. We did not apply a repeated

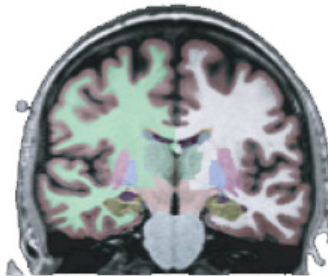
measurement analysis with hemisphere as between-subjects factor because some regions investigated could not be split by hemisphere.

Cortical differences between groups were investigated using repeated measures ANCOVA with group (NF1 vs typically developing) as the between-subjects factor and hemispheres (left vs right) and brain regions (34 gyral regions) as the within-subjects factors and TIV as covariate. Follow-up tests were performed using multivariate ANCOVAs with TIV as covariate.

T1-weighted MPAGE images averaged and cortical reconstruction performed - definition of white matter and pial boundaries

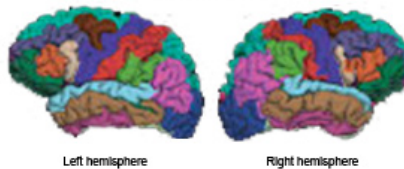


Automated probabilistic segmentation of subcortical grey matter



Surface models are created and automated parcellation of gyral regions is performed using curvature information

Folded Surfaces



Left hemisphere

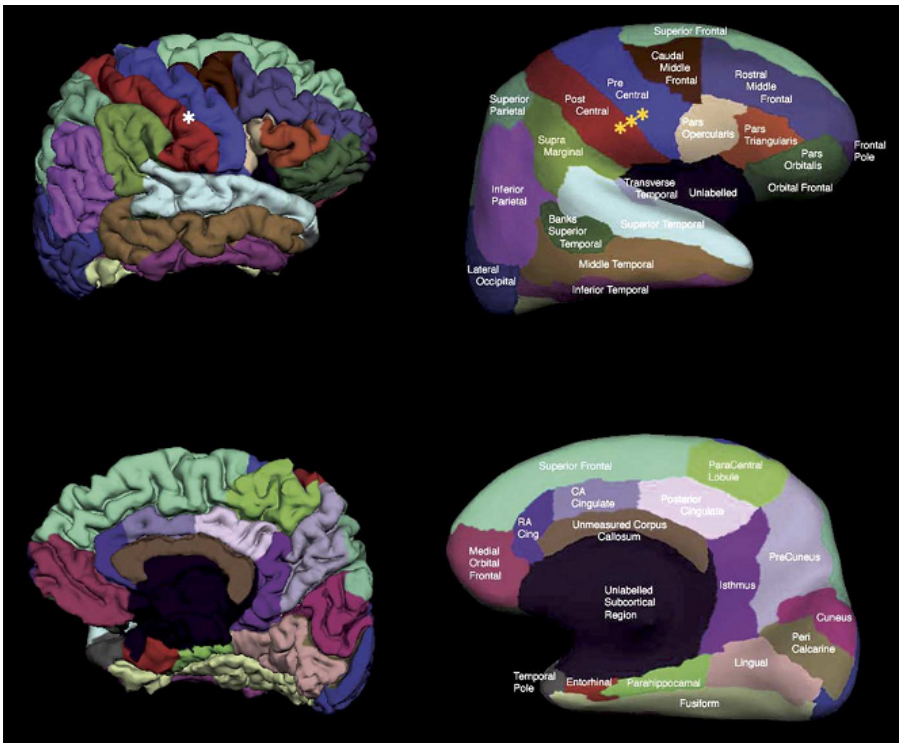
Right hemisphere

Figure 1. Schematic representation of FreeSurfer cortical reconstruction (top), segmentation (middle) and parcellation procedure (bottom). Adapted from Salat et al., 2009.



Relationships between brain measurements and age were studied using Pearson's correlations.

To control for type I errors we used the Benjamini & Hochberg (Benjamini and Hochberg, 1995) false discovery rate (FDR) method. We set  $q = 0.05$  or  $0.1$  (i.e., 5% or 10% false positives). Multiple ROI-based analyses survived FDR control at  $q = 0.1$  and several survived FDR control at  $q = 0.05$ . Although FDR at  $q = 0.1$  can be considered a liberal correction for multiple comparisons, it should be taken into account the exploratory nature of the present study.



**Figure 2.** Gyral based regions defined by the atlas developed by Desikan et al. Pial (left) and inflated (right) cortical representations of the regions of interest in one hemisphere. The top row illustrates the lateral view of the hemisphere while the bottom row shows the medial view of the hemisphere. The white asterisk on the pial surface (left) indicates the cortex around the perimeter of the central sulcus that is buried within the gyri and thus not visible. The yellow asterisks on the inflated surface (right) indicate the cortex around the perimeter of the central sulcus that has been inflated and is now visible. Reproduced from Desikan et al., 2006.

## RESULTS

### Demographic and neuropsychological

Demographic and neuropsychological data are described in Table 1. Children with NF1 and typically developing (TD) children did not differ significantly in age [ $t_{(26)} = -0.632, p = 0.533$ ], IQ [ $t_{(26)} = -1.219, p = 0.234$ ], verbal IQ [ $t_{(26)} = -0.584, p = 0.564$ ], or gender [ $\chi^2 = 0.150, p = 0.699$ ]. Performance IQ was marginally significant [ $t_{(26)} = -2.016, p = 0.054$ ], with larger scores observed in TD children.

One or more UBOs were present in 85.7% (12 out of 14) of the children with NF1 distributed as follows: 85.7% (n=12) of the patients had UBOs in the globus pallidus, 21.4% (n=3) in the thalami, 14.3% (n=2) in the corpus callosum, 7.1% (n=1) in the putamen, 14.3% (n=2) in the cerebellum and 28.6% (n=4) had UBOs in the WM. The frequency and distribution of UBOs is in accordance with published data (Payne et al., 2010). None of the TD participants had UBOs.

### Overall volumetric measurements

Children with NF1 showed a 10% increase in total intracranial volume (TIV) as compared with the TD group [NF1:  $1658 \pm 127 \text{ cm}^3$ ; TD:  $1505 \pm 138 \text{ cm}^3$ ;  $t_{(26)} = 3.041, p = 0.005$ ]. This overall increase was more attributable to an increase in WM [NF1:  $517 \pm 61 \text{ cm}^3$ ; TD:  $428 \pm 46 \text{ cm}^3$ ;  $t_{(26)} = 4.340, p < 0.001$ ] than GM, including cortical and subcortical GM [NF1:  $789 \pm 78 \text{ cm}^3$ ; TD:  $728 \pm 74 \text{ cm}^3$ ;  $t_{(26)} = 2.104, p = 0.045$ ]. Age was not significantly correlated with TIV for our subjects [ $r = 0.067, p = 0.736$ ].

We next examined overall volumetric differences at the lobar level. Results for WM are displayed in Figure 3. Group differences in WM were reflected by a main effect of group [ $F_{(1,25)} = 8.028, p = 0.009$ ], two-way interactions between hemisphere and group [ $F_{(1,25)} = 5.287, p = 0.030$ ] and lobe and group [ $F_{(3,75)} = 6.758, p < 0.001$ ]. Follow-up multivariate ANCOVA controlling for TIV, revealed that left and right frontal lobes were significantly larger in patients [left frontal lobe:  $F_{(1,25)} = 10.456, p = 0.003$ ; right frontal lobe:  $F_{(1,25)} = 5.786, p = 0.026$ ], as well as left and right temporal lobes [left temporal lobe:  $F_{(1,25)} = 10.930, p = 0.003$ ; right temporal lobe:  $F_{(1,25)} = 12.125, p = 0.002$ ]. However only the left hemisphere parietal lobe was significantly larger [left parietal lobe:  $F_{(1,25)} = 7.980, p = 0.009$ ; right parietal lobe:  $F_{(1,25)} = 3.295, p = 0.081$ ] and no differences were observed for the occipital lobe [left occipital lobe:  $F_{(1,25)} = 0.078, p = 0.782$ ; right occipital lobe:  $F_{(1,25)} = 0.713, p = 0.406$ ].

Results for GM are displayed in Figure 3. The lobar GM volumes included only cortical volumes and resulted in no significant effect of group and no interaction between group and lobe. Nonetheless, we found a significant two-way interaction between hemisphere and group [ $F_{(1,25)} = 8.468, p = 0.007$ ].

At the cerebellar level, neither the cerebellar white matter [left hemisphere:  $F_{(1,25)} = 0.042, p = 0.840$ ; right hemisphere:  $F_{(1,25)} = 1.908, p = 0.179$ ], nor the grey matter volumes [left hemisphere:  $F_{(1,25)} = 0.331, p = 0.570$ ; right hemisphere:  $F_{(1,25)} = 0.612, p = 0.441$ ] were statistically different between patients and TD children.

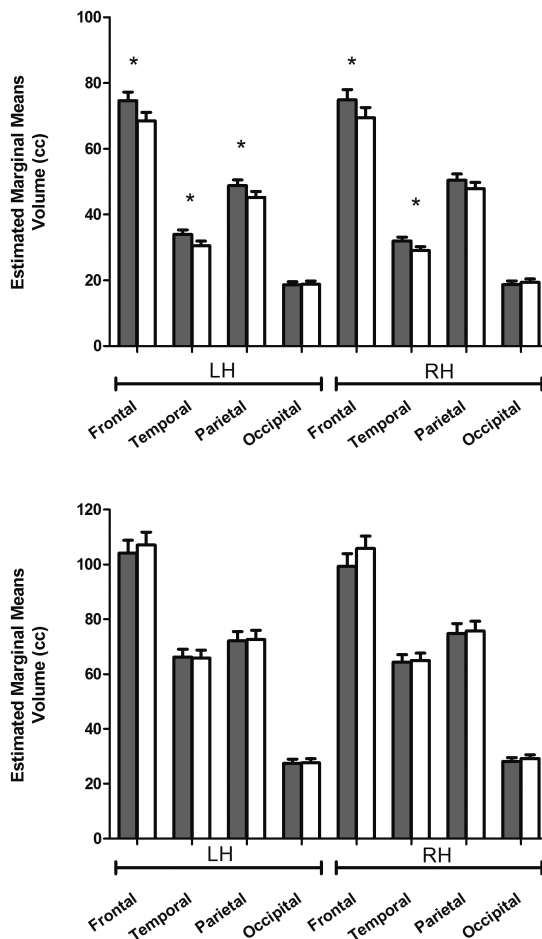
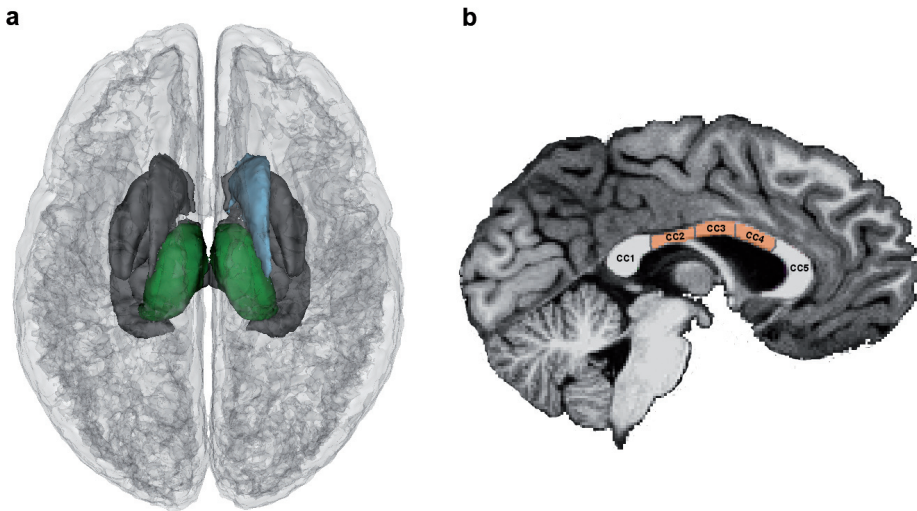


Figure 3. Lobar volumes in patients with NF1 (grey bars) and typically developing children (white bars). Lobar volumes are displayed by hemisphere after controlling for total intracranial volume for lobar white matter (top) and lobar grey matter (bottom). Graphs depict mean and SEM, \* $p < 0.05$ . LH = left hemisphere; RH = right hemisphere.

### Subcortical regional brain volumes

Children with NF1 showed increased volumes when compared to TD children in almost all subcortical brain regions evaluated, Table 2. Using a FDR ( $q = 0.05$ ) correction for multiple comparisons the majority of regions remained significant with the exception of the left putamen and the right pallidum. We next conducted an ANCOVA with TIV as covariate to determine whether these regional brain volume differences remained significant beyond overall increase in brain size in children with NF1. After controlling for TIV the thalami, the right caudate and the mid regions of the corpus callosum (mid posterior, central, mid anterior) remained significantly different between patients with NF1 and TD, Figure 4. Furthermore, these regions remained significant after correcting for multiple comparisons (FDR,  $q = 0.1$ ). After the more stringent control for multiple comparisons (FDR,  $q = 0.05$ ), only, the right thalamus and the mid anterior region of the corpus callosum remained significantly different, Table 2. Adding age or IQ as a covariates to the ANCOVA did not change the results.



**Figure 4. Group differences in subcortical regional brain volumes; superior view (a) and sagittal view showing the divisions for the corpus callosum (b).** Larger volume in patients with NF1 was observed in the left and right thalamus (green) and right caudate nucleus (blue) after controlling for total intracranial volume (TIV) and multiple comparisons using FDR, areas in grey correspond to regions where group differences were no longer significant after controlling for total intracranial volume. In the corpus callosum, patients with NF1 showed larger volumes of the mid regions (mid posterior, mid anterior and central). CC = corpus callosum; CC1 = posterior, CC2 = mid-posterior; CC3 = central; CC4 = mid-anterior; CC5 = anterior.

**Table 2. Results of ANCOVA analyses in subcortical regions**

Region	Hemisphere	Volume		Volume (TIV as a covariate)	
		F	p	F	p
Thalamus	L	<b>17.746</b>	<b>&lt;0.001<sup>a</sup></b> ↑	<b>6.106</b>	<b>0.021<sup>b</sup></b> ↑
	R	<b>19.924</b>	<b>&lt;0.001<sup>a</sup></b> ↑	<b>9.415</b>	<b>0.005<sup>a</sup></b> ↑
Caudate	L	<b>11.454</b>	<b>0.002<sup>a</sup></b> ↑	3.468	0.074
	R	<b>16.898</b>	<b>&lt;0.001<sup>a</sup></b> ↑	<b>6.861</b>	<b>0.015<sup>b</sup></b> ↑
Putamen	L	<b>6.005</b>	<b>0.021</b> ↑	0.610	0.442
	R	3.564	0.070 ↑	0.335	0.568
Pallidum	L	<b>5.422</b>	<b>0.028<sup>a</sup></b> ↑	0.344	0.563
	R	<b>4.398</b>	<b>0.046</b> ↑	0.023	0.880
Hippocampus	L	<b>14.112</b>	<b>0.001<sup>a</sup></b> ↑	3.942	0.058
	R	4.225	0.050	0.108	0.746
Amygdala	L	<b>7.578</b>	<b>0.011<sup>a</sup></b> ↑	0.235	0.632
	R	<b>9.841</b>	<b>0.004<sup>a</sup></b> ↑	1.358	0.255
Accumbens area	L	<b>6.534</b>	<b>0.017<sup>a</sup></b> ↑	1.525	0.228
	R	<b>8.865</b>	<b>0.006<sup>a</sup></b> ↑	3.140	0.089
Ventral Diencephalon	L	<b>14.808</b>	<b>0.001<sup>a</sup></b> ↑	4.242	0.050
	R	<b>12.403</b>	<b>0.002<sup>a</sup></b> ↑	2.748	0.110
CC Posterior		<b>8.107</b>	<b>0.008<sup>a</sup></b> ↑	3.676	0.067
CC Mid Posterior		<b>9.303</b>	<b>0.005<sup>a</sup></b> ↑	<b>5.587</b>	<b>0.026<sup>b</sup></b> ↑
CC Central		<b>10.893</b>	<b>0.003<sup>a</sup></b> ↑	<b>6.004</b>	<b>0.022<sup>b</sup></b> ↑
CC Mid Anterior		<b>12.729</b>	<b>0.001<sup>a</sup></b> ↑	<b>8.919</b>	<b>0.006<sup>a</sup></b> ↑
CC Anterior		<b>6.712</b>	<b>0.015<sup>a</sup></b> ↑	2.902	0.101
Brainstem		<b>12.859</b>	<b>0.001<sup>a</sup></b> ↑	2.563	0.122

Bold font represents significant results ( $p < 0.05$ ). <sup>a</sup> Represents significant results after correction for multiple comparisons with FDR ( $q = 0.05$  or  $0.1$ ) and <sup>b</sup> after with FDR ( $q = 0.1$ ). Arrows indicate the direction of the group difference, ↑ = NF1 > Typically developing subjects. CC = corpus callosum; L = left; R = right; TIV = total intracranial volume.

### Cortical volume, cortical thickness and cortical surface area

Cortical volume group differences, investigated using repeated measures ANCOVA with TIV as covariate, resulted in no main effect of group [ $F_{(1,25)} = 0.690, p = 0.414$ ], but statistically significant two-way interactions between region and group [ $F_{(33,825)} = 1.651, p = 0.013$ ] and hemisphere and group [ $F_{(1,25)} = 8.058, p = 0.009$ ].

Repeated measures ANCOVA of cortical thickness measurements resulted in no statistically significant effect of group [ $F_{(1,25)} = 1.084, p = 0.308$ ], but a significant effect of brain region [ $F_{(33,825)} = 5.870, p < 0.001$ ], a two-way interaction between region and group [ $F_{(33,825)} = 1.522, p = 0.031$ ] and a three-way interaction between hemisphere, region and group [ $F_{(33,825)} = 1.455, p = 0.049$ ].

The results for cortical surface area resemble those found for cortical volume and cortical thickness, with no significant effect of group [ $F_{(1,25)} = 0.378, p = 0.544$ ]. Nevertheless, we observed a significant two-way interaction between hemisphere and group [ $F_{(1,25)} = 6.061, p = 0.021$ ].

Because there was no group effect in any of the cortical variables explored above, we did not perform post-hoc tests.

### Gyrification Index

The gyrification index showed a significant effect of group [ $F_{(1,25)} = 10.400, p = 0.003$ ], an effect of region [ $F_{(33,825)} = 3.263, p < 0.001$ ] and a two-way interaction between region and group [ $F_{(33,825)} = 2.591, p < 0.001$ ]. Follow-up multivariate ANCOVA showed that patients with NF1 have reduced gyrification mainly in frontal and temporal lobar regions, but also in insula, parietal, occipital and cingulate gyri, Table 3 and Figure 5. After correction for multiple comparisons several gyral-regions remained statistically significant: left and right superior frontal, left and right superior temporal, right middle temporal and right transverse temporal (FDR,  $q = 0.05$ ). The majority of gyral-regions remained significant at FDR,  $q = 0.1$  (Table 3). Adding age or IQ as covariates to the repeated measures ANCOVA and follow-up ANCOVAs did not change the results.

**Table 3. Results of ANCOVA analyses for local gyrification index in gyral regions**

Gyral region	Hemisphere	Local Gyrification index		
		F	p	
Superior frontal	L	<b>12.315</b>	<b>0.002<sup>a</sup></b>	↓
	R	<b>11.938</b>	<b>0.002<sup>a</sup></b>	↓
Caudal middle frontal	L	1.074	0.310	
	R	<b>5.046</b>	<b>0.034<sup>b</sup></b>	↓
Rostral middle frontal	L	4.036	0.055	
	R	1.870	0.184	
Pars opercularis	L	<b>7.575</b>	<b>0.011<sup>b</sup></b>	↓
	R	4.071	0.054	
Pars triangularis	L	3.860	0.061	
	R	2.009	0.169	
Pars orbitalis	L	<b>8.324</b>	<b>0.008<sup>b</sup></b>	↓
	R	<b>4.869</b>	<b>0.037<sup>b</sup></b>	↓
Lateral orbitofrontal	L	<b>7.702</b>	<b>0.010<sup>b</sup></b>	↓
	R	1.797	0.192	
Medial orbitofrontal	L	<b>6.298</b>	<b>0.019<sup>b</sup></b>	↓
	R	<b>4.472</b>	<b>0.045</b>	↓
Precentral	L	<b>5.693</b>	<b>0.025<sup>b</sup></b>	↓
	R	<b>6.354</b>	<b>0.018<sup>b</sup></b>	↓
Paracentral	L	<b>5.165</b>	<b>0.032<sup>b</sup></b>	↓
	R	2.847	0.104	
Frontal pole	L	<b>6.768</b>	<b>0.015<sup>b</sup></b>	↓
	R	1.366	0.253	
Superior temporal	L	<b>11.052</b>	<b>0.003<sup>a</sup></b>	↓
	R	<b>24.242</b>	<b>&lt;0.001<sup>a</sup></b>	↓
Middle temporal	L	<b>5.876</b>	<b>0.023<sup>b</sup></b>	↓
	R	<b>18.742</b>	<b>&lt;0.001<sup>a</sup></b>	↓
	L	0.312	0.582	

Inferior temporal	R	<b>4.855</b>	<b>0.037<sup>b</sup></b>	↓
	L	2.504	0.126	
Entorhinal	R	<b>6.935</b>	<b>0.014<sup>b</sup></b>	↓
	L	0.044	0.836	
Fusiform	R	1.095	0.305	
	L	0.013	0.911	
Parahippocampal	R	0.529	0.474	
	L	3.399	0.077	
Temporal pole	R	<b>5.442</b>	<b>0.028<sup>b</sup></b>	↓
	L	3.517	0.072	
Transverse temporal	R	<b>14.003</b>	<b>0.001<sup>a</sup></b>	↓
	L	0.190	0.667	
Banks superior temporal sulcus	R	<b>5.689</b>	<b>0.025<sup>b</sup></b>	↓
	L	1.640	0.212	
Superior parietal	R	0.125	0.727	
	L	0.220	0.643	
Inferior parietal	R	1.463	0.238	
	L	2.117	0.158	
Supramarginal	R	<b>5.233</b>	<b>0.031<sup>b</sup></b>	↓
	L	<b>6.597</b>	<b>0.017<sup>b</sup></b>	↓
Postcentral	R	<b>9.344</b>	<b>0.005<sup>b</sup></b>	↓
	L	3.117	0.090	
Precuneus	R	3.762	0.064	
	L	0.719	0.405	
Lateral occipital	R	0.498	0.487	
	L	0.253	0.620	
Lingual	R	2.862	0.103	
	L	3.589	0.070	
Cuneus	R	<b>4.317</b>	<b>0.048</b>	↓
	L	1.915	0.179	
Pericalcarine	R	<b>5.044</b>	<b>0.034<sup>b</sup></b>	↓
	L	<b>4.848</b>	<b>0.037<sup>b</sup></b>	↓



Rostral anterior cingulate	R	<b>5.487</b>	<b>0.027<sup>b</sup></b>	↓
Caudal anterior cingulate	L	<b>6.789</b>	<b>0.015<sup>b</sup></b>	↓
	R	3.213	0.085	
Posterior cingulate	L	2.052	0.164	
	R	3.165	0.087	
Isthmus cingulate	L	0.213	0.648	
	R	2.808	0.106	
Insula	L	<b>7.013</b>	<b>0.014<sup>b</sup></b>	↓
	R	<b>5.616</b>	<b>0.026<sup>b</sup></b>	↓

Bold font represents significant results ( $p < 0.05$ ). <sup>a</sup> Represents significant results after correction for multiple comparisons with FDR ( $q = 0.05$  or  $0.1$ ) and <sup>b</sup> after with FDR ( $q = 0.1$ ). Arrows indicate the direction of the group difference, ↓ = NF1 < Typically developing subjects. L = left; R = right

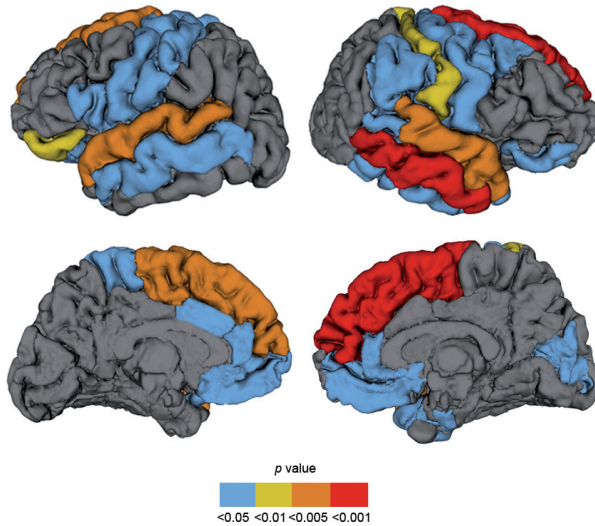


**Figure 5. Graphical illustration of significant reductions in gyrification in patients with NF1.** This figure shows an overlay of F-test statistics (with  $p$  values indicated by the color bar) where patients with NF1 have lower local gyrification index than typically developing children. Between-group comparisons were performed controlling for intracranial volume. Blue colour depict gyri with significant group differences at  $p < 0.05$ , not corrected; Yellow  $p < 0.01$  and Orange  $p < 0.005$ , both surviving correction for multiple comparisons with FDR  $q = 0.1$ ; Red gyri  $p < 0.001$ , survives correction for multiple comparisons with FDR  $q < 0.05$ .

### Brain size and folding relationships

In humans, the volume of the brain and the area of its cortical surface are strongly correlated (Toro et al., 2008). This relation is such that larger brains are normally accompanied by a higher increase in surface area than it would be expected by mere scaling of the brain. Furthermore, increase in folding is necessary for compactness of connections (Ruppin et al., 1993; Murre and Sturdy, 1995). Indeed, when brain volume and surface area are plotted in a logarithmic scale the slope of the regression line obtained indicates a disproportionate expansion of the cerebral cortex in relation to brain volume related to an increase in gyrification.

Given the group differences observed in IGI, we investigated whether the increase in brain size in NF1 is related to an increase in gyrification.

Figure 6a shows the relationship between cortical surface area and intracranial volume for patients with NF1 and TD children plotted in a log-log graph. TIV is correlated with surface area in both groups [NF1:  $r = 0.806$ ,  $p < 0.001$ ; TD:  $r = 0.925$ ,  $p < 0.001$ ]. The slope of the regression line is 0.941 for NF1 and 1.069 for TD children, higher than the value expected for an isometric scaling ( $2/3$ ) as observed in the human brain (Toro et al., 2008). Interestingly, the slopes are significantly different between groups [ $t_{(24)} = 4.044$ ,  $p < 0.001$ ], being steeper for TDs.

To investigate whether the degree of cortical folding is related with measurements of TIV, surface area and cortical thickness we performed Pearson's correlations between these variables. LGI was only positively correlated with TIV for TD subjects [NF1:  $r = 0.458$ ,  $p = 0.099$ ; TD:  $r = 0.744$ ,  $p = 0.002$ ], Figure 6b. The cortical surface area was correlated with IGI for both groups [NF1:  $r = 0.788$ ,  $p = 0.001$ ; TD:  $r = 0.875$ ,  $p < 0.001$ ], Figure 6c; while IGI and cortical thickness were not correlated for any of the groups (not shown), consistent with prior studies (Thompson et al., 2005; Lin et al., 2007; Bearden et al., 2009).

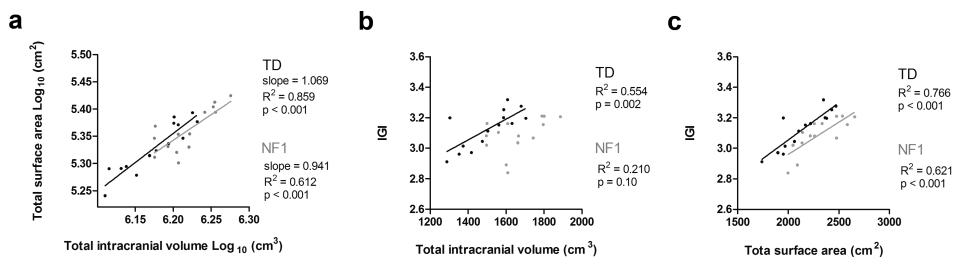


**Figure 6. Brain size and folding relationships in NF1 (grey) and typically developing children (TD), (black).** a. Cortical surface area versus intracranial volume (log-log graph). b. IGI versus intracranial volume. c. IGI versus surface area.

## DISCUSSION

In this study, we used computational methods to examine the impact of NF1, a single gene disorder, on multidimensional morphological brain traits. This is the first study to examine measurements of cortical thickness, cortical surface area and gyrification in this common neurodevelopmental genetic condition. We confirmed that children with NF1 have larger intracranial volumes than typically developing children (~10%) and our findings indicate that this enlargement is mainly a result of increased WM volume. At lobar level, our results indicate that patients with NF1 have larger WM volumes in the frontal lobe, consistent with prior studies (Cutting et al., 2002a; Greenwood et al., 2005; Duarte et al., 2012), temporal lobe, in agreement with voxel-based morphometry findings using a partly overlapping cohort of subjects (Duarte et al., 2012), and also right parietal lobe, as previously observed (Cutting et al., 2002b). We did not find alterations in the occipital lobe. Our lobar data is in agreement with the notion that WM alterations are predominant in anterior brain regions. We also observed a parallel increase in GM volume in patients with NF1, a result attributable to larger subcortical rather than cortical volumes.

Measurements of subcortical regional volumes indicated enlargements in patients with a dependence on overall brain volume for the majority of regions. After controlling for the effect of intracranial volume, the thalami, the right caudate nucleus and the mid portions of the corpus callosum remained significantly larger in patients with NF1 than TD children.

This study was the first, to our knowledge, to report a volumetric alteration of the thalami in children with NF1. Moreover, we have previously identified this structure as belonging to a spatial pattern that significantly contributes to discriminate between brains from patients with NF1 and brains from controls (Duarte et al., 2012). Other studies reported thalamic hypometabolism (Kaplan et al., 1997),  $T_1$  reduction (Steen et al., 2001) and abnormal choline and N-acetylaspartate content content (Wang et al., 2000), possibly reflecting altered myelination and neuronal loss or neuronal dysfunction.

The thalamus is a highly interactive structure, with widespread connections to multiple cortical regions, that provides selection and transformation of different sensory inputs to the cortex. The various nuclei of the thalamus are involved in the integration of sensory and motor information, memory and executive functions (Schmahmann and Pandya, 2008), competences in which NF1 patients show disabilities (Hyman et al., 2005; Levine et al., 2006; Roy et al.).

The right caudate nucleus was also found to be larger in patients and it was previously identified as a relevant structure to discriminate between NF1 and control subjects (Duarte et al., 2012). The caudate is a nucleus of the basal ganglia and therefore plays a role in sensorimotor coordination, while there is also cumulating evidences indicating an involvement in goal-directed behaviour (Grahn et al., 2008). It is widely connected with the frontal lobe and particularly with dorsolateral prefrontal cortex (Kemp and Powell, 1970; Yeterian and Van Hoesen, 1978), which is involved in working memory and executive function. A recent functional magnetic resonance imaging (fMRI) study showed abnormal right caudate activation in NF1 in a spatial working memory task (Shilyansky et al., 2010). Moreover, Schrimsher et al. (Schrimsher et al., 2002) observed that children with a greater degree of right to left caudate volume asymmetry show subclinical inattentive behaviours that define ADHD. Interestingly, there is a high incidence of ADHD in NF1 (Hyman et al., 2005).

Finally, the enlargement observed in the midline portion of the corpus callosum corroborates previous reports from our group, in a partly overlapping cohort, using an independent method (Duarte et al., 2012) and others (Kayl et al., 2000; Dubovsky et al., 2001; Steen et al., 2001; Cutting et al., 2002b; Pride et al., 2010). Besides morphometric abnormalities, there is evidence of altered microstructure of the corpus callous in NF1 (Zamboni et al., 2007; Wignall et al., 2010). Behaviourally, higher volumes of corpus callosum were previously related to low IQ, impaired visuospatial and motor skills and learning problems in children with NF1 (Moore et al., 2000; Pride et al., 2010). Interestingly, we observed that the volume of the corpus callosum remains abnormal even for normal IQs.

Unlike the specific observations concerning subcortical structures, examination of cortical measurements indicated that alterations in cortical volume, cortical surface area and cortical thickness are not significant. Gyrification index was the only changed measure in cortex.

One of the most evident features of human evolution is the increase in brain size (Passingham, 1973). In response to evolutionary demands, a high level of gyrification occurred in parallel with an increase in cortical GM in order to maximize cortical surface while maintaining a smaller intracranial size (Zilles et al., 1988). The increase in folding in bigger brains seems to be necessary for the formation of efficient cortico-cortical connections in larger volumes (Ruppin et al., 1993; Murre and Sturdy, 1995). This evolutionary trait appears disrupted in NF1, with an increase in brain size without

a corresponding adaptive increase in folding. Accordingly, the correlation observed in TD children between IGI and intracranial volume is absent in NF1. Moreover, although both TD and NF1 children presented an allometric scaling between surface area and volume, showing more surface area than predicted by a homothetic relationship (Toro et al., 2008), the difference in slopes indicates that NF1 have less surface area than what would be expected for their brain volume.

The phylogenetic development of gyral and sulcal folds likely optimizes compaction of neuronal fibers while keeping neuronal signalling at efficient transit time (Ruppin et al., 1993; Murre and Sturdy, 1995). Given that abnormal cortical folding may reflect deficits in structural and, consequently, functional cortical connectivity, we will speculate on potential links between cortical folding abnormalities and the patterns of cognitive dysfunction that characterize the NF1 phenotype.

Concerning the cognitive phenotype related to cortical functions, executive functions have been reported to be impaired in children with NF1 (Roy et al., 2010; Payne et al., 2011), even when controlling for IQ (Roy et al., 2010). In here, we observed lower IGI in several frontal lobe regions that could underlie executive impairments, namely the superior frontal gyri (du Boisgueheneuc et al., 2006), right frontal pole (Tsujimoto et al., 2011) and orbitofrontal regions (Elliott et al., 2000; Zald and Andreotti, 2010). Moreover, the anterior cingulate cortex was also found to have lower IGI values in NF1 and it plays a role in attention and error detection (Bush et al., 2000). Interestingly, we have previously found an abnormal activity pattern in this region using an overlapping cohort of subjects (Violante et al., 2012), possibly related with a deficit in default-mode network function.

Patients with NF1 have deficits in expressive and receptive language, vocabulary and phonologic awareness (Levine et al., 2006). Previously, a correlation has been reported between verbal skills in NF1 and the inferior frontal gyrus morphology, such that individuals with “typical” gyral patterns in the right hemisphere performed worse across language measures than those showing “atypical” gyrus (Billingsley et al., 2003). In here, we observed a deficit in gyrification in regions involved with language functions, namely in regions belonging to the Broca’s complex (pars opercularis, pars orbitalis, pars triangularis) (Hagoort, 2005; Xiang et al., 2010), superior temporal gyrus and middle temporal gyrus (Chao et al., 1999; Cabeza and Nyberg, 2000) and supramarginal gyrus (Gough et al., 2005; Hartwigsen et al., 2010). Moreover, right transverse temporal gyrus, known as the Heschl’s gyrus also presented lower IGI in patients. Abnormalities in the inferior

frontal gyrus and Heschl's gyrus were associated with performance across language and neuropsychological measures in individuals with NF1 (Billingsley et al., 2003).

Motor deficits for both simple and complex motor tasks have been reported in NF1 (Feldmann et al., 2003; Levine et al., 2006; Rowbotham et al., 2009) consistent with the observed bilateral deficits in IGI in both precentral and paracentral gyri, underlying motor functions (Purves and Williams, 2001).

In spite of our identification of altered patterns of gyrification in regions underlying cognitive deficits typically observed in children with NF1, this was not the case for the posterior parietal lobe. This is rather surprising given that visuospatial deficits are considered a hallmark of the NF1 cognitive phenotype. This might be explained by the suggestion that other brain regions such as fronto-executive regions contribute to the pattern of impairment observed in specific visuospatial tests (i.e judgement of line orientation test).

In agreement with the notion of impaired low-level visual processing in NF1 (Clements-Stephens et al., 2008; Violante et al., 2012), we observed lower IGI in the right cuneus and pericalcarine regions.

It is estimated that around 30% of phenotypic variance in gyrification is attributed to genetic variation (Rogers et al., 2010). Therefore, the observed reductions in IGI point towards early abnormalities in control over neuronal migration or proliferation. Deeper fissures develop earlier and are more strongly influenced by genetic processes and thus might be less susceptible to environmental perturbations. Insular sulci and the central sulcus are among the first macroscopical structures identified on the human fetal brain (Afif et al., 2007) (Rajagopalan et al., 2011), and both the insula and the gyri surrounding the central sulcus presented less gyrification in NF1 than TD individuals.

The mechanisms that drive cortical folding remain poorly understood and there are different possible explanations for the observed abnormalities of cortical gyrification in NF1. The two most widely accepted hypothesis to explain gyrification are: 1) folding is caused by differential growth of the cortex and 2) folding is caused by mechanical tension generated in axons. The first model proposes that differential growth rates of cortical layers directly affect the degree of cortical convolutions (Caviness, 1975). An alternate theory to this hypothesis suggests that changes in subcortical connections can lead to altered cortical folding patterns without changing the area of the cortical surface (Kostovic and Rakic, 1990). The second model, based on tension-based cortical morphogenesis, proposes that the mechanical tension along axons is the driving force for

cortical folding (Van Essen, 1997). In line with this theory, we observed a significant increase in WM in the anterior NF1 brain accompanied by an enlargement of the corpus callosum. Moreover, diffusion tensor imaging studies showed altered microstructure in several white matter regions (Zamboni et al., 2007). Both models are not necessarily contradictory and could jointly explain the gyral abnormalities in NF1.

The present study has several limitations that need to be acknowledged when interpreting our findings. First, we studied a large age range and we were limited to a relatively small number of participants. In that sense, longitudinal studies are clearly warranted to disentangle the complex genetic and nongenetic influences that contribute to the neuroanatomic and cognitive abnormalities in NF1. Secondly, 12 of the 14 (85.7%) patients in this study have UBOs. These hyperintensities are the most common identified abnormality observed on MRI in patients with NF1 (Lopes Ferraz Filho et al., 2008) and might be associated with other clinical features (Szudek and Friedman, 2002). However, the location of the UBOs does not seem to indicate a regional causal link between structure volume and the presence of UBOs, given that hyperintensities were more frequent in the globus pallidus and this structure did not differ in terms of volume in relation to TD children.

In summary, we found that the overall increase in intracranial volume in patients with NF1, is explained by an enlarged WM volume in anterior brain regions and subcortical GM volumes, with a disproportionate increase in the volumes of the thalami, right caudate nucleus and corpus callosum. At the cortical level we observed abnormalities of gyrification, which could reflect developmental abnormalities in both cortical architecture and cortico-cortical connectivity. This newly identified pattern of gyral malformation, required quantitative tools such as IGI to be detected. Given the emphasis on a careful matching between patients and TD children we believe that the brain alterations observed in here are shaped primarily by genetically programmed anomalous neurodevelopment. The fact that neuroanatomic abnormalities in patients with NF1 are localized to particular brain regions adds to the growing body of evidence that specific genes independently control the morphometry of specific cytoarchitectonic areas.

## REFERENCES

- Afif A, Bouvier R, Buenerd A, Trouillas J, Mertens P. Development of the human fetal insular cortex: study of the gyration from 13 to 28 gestational weeks. *Brain Struct Funct.* 212:3-4 (2007) 335-346.

- Armstrong E, Schleicher A, Omran H, Curtis M, Zilles K. The ontogeny of human gyrification. *Cereb Cortex*. 5:1 (1995) 56-63.
- Bearden CE, van Erp TG, Dutton RA, Lee AD, Simon TJ, Cannon TD, Emanuel BS, McDonald-McGinn D, Zackai EH, Thompson PM. Alterations in midline cortical thickness and gyrification patterns mapped in children with 22q11.2 deletions. *Cereb Cortex*. 19:1 (2009) 115-126.
- Benjamini Y, Hochberg Y. Controlling the False Discovery Rate - a Practical and Powerful Approach to Multiple Testing. *Journal of the Royal Statistical Society Series B-Methodological*. 57:1 (1995) 289-300.
- Billingsley RL, Schrimsher GW, Jackson EF, Slopis JM, Moore BD, 3rd. Significance of planum temporale and planum parietale morphologic features in neurofibromatosis type 1. *Arch Neurol*. 59:4 (2002) 616-622.
- Billingsley RL, Slopis JM, Swank PR, Jackson EF, Moore BD, 3rd. Cortical morphology associated with language function in neurofibromatosis, type I. *Brain Lang*. 85:1 (2003) 125-139.
- Bush G, Luu P, Posner MI. Cognitive and emotional influences in anterior cingulate cortex. *Trends Cogn Sci*. 4:6 (2000) 215-222.
- Cabeza R, Nyberg L. Imaging cognition II: An empirical review of 275 PET and fMRI studies. *J Cogn Neurosci*. 12:1 (2000) 1-47.
- Caviness VS, Jr. Mechanical model of brain convolutional development. *Science*. 189:4196 (1975) 18-21.
- Chao LL, Haxby JV, Martin A. Attribute-based neural substrates in temporal cortex for perceiving and knowing about objects. *Nat Neurosci*. 2:10 (1999) 913-919.
- Clements-Stephens AM, Rimrod SL, Gaur P, Cutting LE. Visuospatial processing in children with neurofibromatosis type 1. *Neuropsychologia*. 46:2 (2008) 690-697.
- Cutting LE, Huang GH, Zeger S, Koth CW, Thompson RE, Denckl MB. Growth curve analyses of neuropsychological profiles in children with neurofibromatosis type 1: specific cognitive tests remain “spared” and “impaired” over time. *J Int Neuropsychol Soc*. 8:6 (2002a) 838-846.
- Cutting LE, Cooper KL, Koth CW, Mostofsky SH, Kates WR, Denckla MB, Kaufmann WE. Megalencephaly in NF1: predominantly white matter contribution and mitigation by ADHD. *Neurology*. 59:9 (2002b) 1388-1394.
- Dale AM, Fischl B, Sereno MI. Cortical surface-based analysis. I. Segmentation and surface reconstruction. *Neuroimage*. 9:2 (1999) 179-194.
- Daston MM, Ratner N. Neurofibromin, a predominantly neuronal GTPase activating protein in the adult, is ubiquitously expressed during development. *Dev Dyn*. 195:3 (1992) 216-226.
- Desikan RS, Segonne F, Fischl B, Quinn BT, Dickerson BC, Blacker D, Buckner RL, Dale AM, Maguire RP, Hyman BT, Albert MS, Killiany RJ. An automated labeling system for subdividing the human cerebral cortex on MRI scans into gyral based regions of interest. *Neuroimage*. 31:3 (2006) 968-980.
- DiMario FJ, Jr., Ramsby GR, Burleson JA. Brain morphometric analysis in neurofibromatosis 1. *Arch Neurol*. 56:11 (1999) 1343-1346.
- du Boisgueheneuc F, Levy R, Volle E, Seassau M, Duffau H, Kinkingnehun S, Samson Y, Zhang S, Dubois B. Functions of the left superior frontal gyrus in humans: a lesion study. *Brain*. 129:Pt 12 (2006) 3315-3328.



- Duarte JV, Ribeiro MJ, Violante IR, Cunha G, Silva E, Castelo-Branco M. Multivariate pattern analysis reveals subtle brain anomalies relevant to the cognitive phenotype in Neurofibromatosis type 1. *Hum Brain Mapp.* (2012) *in press.*
- Dubovsky EC, Booth TN, Vezina G, Samango-Sprouse CA, Palmer KM, Brasseux CO. MR imaging of the corpus callosum in pediatric patients with neurofibromatosis type 1. *AJNR Am J Neuroradiol.* 22:1 (2001) 190-195.
- Elliott R, Dolan RJ, Frith CD. Dissociable functions in the medial and lateral orbitofrontal cortex: evidence from human neuroimaging studies. *Cereb Cortex.* 10:3 (2000) 308-317.
- Feldmann R, Denecke J, Grenzebach M, Schuierer G, Weglage J. Neurofibromatosis type 1: motor and cognitive function and T2-weighted MRI hyperintensities. *Neurology.* 61:12 (2003) 1725-1728.
- Fernandez-Medarde A, Santos E. The RasGrf family of mammalian guanine nucleotide exchange factors. *Biochim Biophys Acta.* 1815:2 (2011) 170-188.
- Fischl B, Dale AM. Measuring the thickness of the human cerebral cortex from magnetic resonance images. *Proc Natl Acad Sci U S A.* 97:20 (2000) 11050-11055.
- Fischl B, Liu A, Dale AM. Automated manifold surgery: constructing geometrically accurate and topologically correct models of the human cerebral cortex. *IEEE Trans Med Imaging.* 20:1 (2001) 70-80.
- Fischl B, Sereno MI, Tootell RB, Dale AM. High-resolution intersubject averaging and a coordinate system for the cortical surface. *Hum Brain Mapp.* 8:4 (1999) 272-284.
- Fischl B, Salat DH, van der Kouwe AJ, Makris N, Segonne F, Quinn BT, Dale AM. Sequence-independent segmentation of magnetic resonance images. *Neuroimage.* 23 Suppl 1:(2004) S69-84.
- Fischl B, Salat DH, Busa E, Albert M, Dieterich M, Haselgrove C, van der Kouwe A, Killiany R, Kennedy D, Klaveness S, Montillo A, Makris N, Rosen B, Dale AM. Whole brain segmentation: automated labeling of neuroanatomical structures in the human brain. *Neuron.* 33:3 (2002) 341-355.
- Gough PM, Nobre AC, Devlin JT. Dissociating linguistic processes in the left inferior frontal cortex with transcranial magnetic stimulation. *J Neurosci.* 25:35 (2005) 8010-8016.
- Grahn JA, Parkinson JA, Owen AM. The cognitive functions of the caudate nucleus. *Prog Neurobiol.* 86:3 (2008) 141-155.
- Greenwood RS, Tupler LA, Whitt JK, Buu A, Dombeck CB, Harp AG, Payne ME, Eastwood JD, Krishnan KR, MacFall JR. Brain morphometry, T2-weighted hyperintensities, and IQ in children with neurofibromatosis type 1. *Arch Neurol.* 62:12 (2005) 1904-1908.
- Hagoort P. On Broca, brain, and binding: a new framework. *Trends Cogn Sci.* 9:9 (2005) 416-423.
- Hartwigsen G, Baumgaertner A, Price CJ, Koehnke M, Ulmer S, Siebner HR. Phonological decisions require both the left and right supramarginal gyri. *Proc Natl Acad Sci U S A.* 107:38 (2010) 16494-16499.
- Hegedus B, Dasgupta B, Shin JE, Emmett RJ, Hart-Mahon EK, Elghazi L, Bernal-Mizrachi E, Gutmann DH. Neurofibromatosis-1 regulates neuronal and glial cell differentiation from neuroglial progenitors in vivo by both cAMP- and Ras-dependent mechanisms. *Cell Stem Cell.* 1:4 (2007) 443-457.
- Hyman SL, Shores A, North KN. The nature and frequency of cognitive deficits in children with neurofibromatosis type 1. *Neurology.* 65:7 (2005) 1037-1044.

- Kaplan AM, Chen K, Lawson MA, Wodrich DL, Bonstelle CT, Reiman EM. Positron emission tomography in children with neurofibromatosis-1. *J Child Neurol.* 12:8 (1997) 499-506.
- Kayl AE, Moore BD, 3rd, Slopis JM, Jackson EF, Leeds NE. Quantitative morphology of the corpus callosum in children with neurofibromatosis and attention-deficit hyperactivity disorder. *J Child Neurol.* 15:2 (2000) 90-96.
- Kemp JM, Powell TP. The cortico-striate projection in the monkey. *Brain.* 93:3 (1970) 525-546.
- Kostovic I, Rakic P. Developmental history of the transient subplate zone in the visual and somatosensory cortex of the macaque monkey and human brain. *J Comp Neurol.* 297:3 (1990) 441-470.
- Levine TM, Materek A, Abel J, O'Donnell M, Cutting LE. Cognitive profile of neurofibromatosis type 1. *Semin Pediatr Neurol.* 13:1 (2006) 8-20.
- Lin JJ, Salamon N, Lee AD, Dutton RA, Geaga JA, Hayashi KM, Luders E, Toga AW, Engel J, Jr., Thompson PM. Reduced neocortical thickness and complexity mapped in mesial temporal lobe epilepsy with hippocampal sclerosis. *Cereb Cortex.* 17:9 (2007) 2007-2018.
- Lopes Ferraz Filho JR, Munis MP, Soares Souza A, Sanches RA, Goloni-Bertollo EM, Pavarino-Bertelli EC. Unidentified bright objects on brain MRI in children as a diagnostic criterion for neurofibromatosis type 1. *Pediatr Radiol.* 38:3 (2008) 305-310.
- Luders E, Narr KL, Thompson PM, Rex DE, Woods RP, Deluca H, Jancke L, Toga AW. Gender effects on cortical thickness and the influence of scaling. *Hum Brain Mapp.* 27:4 (2006) 314-324.
- Luders E, Narr KL, Bilder RM, Szeszko PR, Gurbani MN, Hamilton L, Toga AW, Gaser C. Mapping the relationship between cortical convolution and intelligence: effects of gender. *Cereb Cortex.* 18:9 (2008) 2019-2026.
- Lush ME, Li Y, Kwon CH, Chen J, Parada LF. Neurofibromin is required for barrel formation in the mouse somatosensory cortex. *J Neurosci.* 28:7 (2008) 1580-1587.
- Moore BD, 3rd, Slopis JM, Jackson EF, De Winter AE, Leeds NE. Brain volume in children with neurofibromatosis type 1: relation to neuropsychological status. *Neurology.* 54:4 (2000) 914-920.
- Murre JM, Sturdy DP. The connectivity of the brain: multi-level quantitative analysis. *Biol Cybern.* 73:6 (1995) 529-545.
- Narr KL, Bilder RM, Luders E, Thompson PM, Woods RP, Robinson D, Szeszko PR, Dimtcheva T, Gurbani M, Toga AW. Asymmetries of cortical shape: Effects of handedness, sex and schizophrenia. *Neuroimage.* 34:3 (2007) 939-948.
- National Institutes of Health Consensus Development Conference Statement: neurofibromatosis. Bethesda, Md., USA, July 13-15 1987. *Neurofibromatosis.* 1:3 (1988) 172-178.
- Panizzon MS, Fennema-Notestine C, Eyler LT, Jernigan TL, Prom-Wormley E, Neale M, Jacobson K, Lyons MJ, Grant MD, Franz CE, Xian H, Tsuang M, Fischl B, Seidman L, Dale A, Kremen WS. Distinct genetic influences on cortical surface area and cortical thickness. *Cereb Cortex.* 19:11 (2009) 2728-2735.
- Passingham RE. Anatomical differences between the neocortex of man and other primates. *Brain Behav Evol.* 7:5 (1973) 337-359.
- Payne JM, Moharir MD, Webster R, North KN. Brain structure and function in neurofibromatosis type 1: current concepts and future directions. *J Neurol Neurosurg Psychiatry.* 81:3 (2010) 304-309.

- Payne JM, Hyman SL, Shores EA, North KN. Assessment of executive function and attention in children with neurofibromatosis type 1: relationships between cognitive measures and real-world behavior. *Child Neuropsychol.* 17:4 (2011) 313-329.
- Pride N, Payne JM, Webster R, Shores EA, Rae C, North KN. Corpus callosum morphology and its relationship to cognitive function in neurofibromatosis type 1. *J Child Neurol.* 25:7 (2010) 834-841.
- Purves D, Williams SM. *Neuroscience*, 2nd Edition. Sunderland, Mass.: Sinauer Associates 2001.
- Rajagopalan V, Scott J, Habas PA, Kim K, Corbett-Detig J, Rousseau F, Barkovich AJ, Glenn OA, Studholme C. Local tissue growth patterns underlying normal fetal human brain gyrification quantified in utero. *J Neurosci.* 31:8 (2011) 2878-2887.
- Rakic P. A small step for the cell, a giant leap for mankind: a hypothesis of neocortical expansion during evolution. *Trends Neurosci.* 18:9 (1995) 383-388.
- Rakic P, Kornack DR. The Development and Evolutionary Expansion of the Cerebral Cortex in Primates. In: *Evolution of Nervous Systems* (Kaas JH, ed), pp 243-259. Oxford: Academic Press. 2007
- Raznahan A, Shaw P, Lalonde F, Stockman M, Wallace GL, Greenstein D, Clasen L, Gogtay N, Giedd JN. How does your cortex grow? *J Neurosci.* 31:19 (2011) 7174-7177.
- Rogers J, Kochunov P, Zilles K, Shelledy W, Lancaster J, Thompson P, Duggirala R, Blangero J, Fox PT, Glahn DC. On the genetic architecture of cortical folding and brain volume in primates. *Neuroimage.* 53:3 (2010) 1103-1108.
- Rowbotham I, Pit-ten Cate IM, Sonuga-Barke EJ, Huijbregts SC. Cognitive control in adolescents with neurofibromatosis type 1. *Neuropsychology.* 23:1 (2009) 50-60.
- Roy A, Roulin JL, Charbonnier V, Allain P, Fasotti L, Barbarot S, Stalder JF, Terrien A, Le Gall D. Executive dysfunction in children with neurofibromatosis type 1: a study of action planning. *J Int Neuropsychol Soc.* 16:6 (2010) 1056-1063.
- Ruppin E, Schwartz EL, Yeshurun Y. Examining the volume efficiency of the cortical architecture in a multi-processor network model. *Biol Cybern.* 70:1 (1993) 89-94.
- Said SM, Yeh TL, Greenwood RS, Whitt JK, Tupler LA, Krishnan KR. MRI morphometric analysis and neuropsychological function in patients with neurofibromatosis. *Neuroreport.* 7:12 (1996) 1941-1944.
- Salat DH, Greve DN, Pacheco JL, Quinn BT, Helmer KG, Buckner RL, Fischl B. Regional white matter volume differences in nondemented aging and Alzheimer's disease. *Neuroimage.* 44:4 (2009) 1247-1258.
- Schaer M, Cuadra MB, Tamarit L, Lazeyras F, Eliez S, Thiran JP. A surface-based approach to quantify local cortical gyrification. *IEEE Trans Med Imaging.* 27:2 (2008) 161-170.
- Schmahmann JD, Pandya DN. Disconnection syndromes of basal ganglia, thalamus, and cerebrotocerebellar systems. *Cortex.* 44:8 (2008) 1037-1066.
- Schrimsher GW, Billingsley RL, Jackson EF, Moore BD, 3rd. Caudate nucleus volume asymmetry predicts attention-deficit hyperactivity disorder (ADHD) symptomatology in children. *J Child Neurol.* 17:12 (2002) 877-884.
- Segonne F, Pacheco J, Fischl B. Geometrically accurate topology-correction of cortical surfaces using non-separating loops. *IEEE Trans Med Imaging.* 26:4 (2007) 518-529.
- Shaw P, Greenstein D, Lerch J, Clasen L, Lenroot R, Gogtay N, Evans A, Rapoport J, Giedd J. Intellectual

- ability and cortical development in children and adolescents. *Nature*. 440:7084 (2006) 676-679.
- Shilyansky C, Karlsgodt KH, Cummings DM, Sidiropoulou K, Hardt M, James AS, Ehninger D, Bearden CE, Poirazi P, Jentsch JD, Cannon TD, Levine MS, Silva AJ. Neurofibromin regulates corticostriatal inhibitory networks during working memory performance. *Proc Natl Acad Sci U S A*. 107:29 (2010) 13141-13146.
- Steen RG, Taylor JS, Langston JW, Glass JO, Brewer VR, Reddick WE, Mages R, Pivnick EK. Prospective evaluation of the brain in asymptomatic children with neurofibromatosis type 1: relationship of macrocephaly to T1 relaxation changes and structural brain abnormalities. *AJNR Am J Neuroradiol*. 22:5 (2001) 810-817.
- Szudek J, Friedman JM. Unidentified bright objects associated with features of neurofibromatosis 1. *Pediatr Neurol*. 27:2 (2002) 123-127.
- Thompson PM, Lee AD, Dutton RA, Geaga JA, Hayashi KM, Eckert MA, Bellugi U, Galaburda AM, Korenberg JR, Mills DL, Toga AW, Reiss AL. Abnormal cortical complexity and thickness profiles mapped in Williams syndrome. *J Neurosci*. 25:16 (2005) 4146-4158.
- Thompson PM, Cannon TD, Narr KL, van Erp T, Poutanen VP, Huttunen M, Lonnqvist J, Standertskjold-Nordenstam CG, Kaprio J, Khaledy M, Dail R, Zoumalan CI, Toga AW. Genetic influences on brain structure. *Nat Neurosci*. 4:12 (2001) 1253-1258.
- Toro R, Perron M, Pike B, Richer L, Veillette S, Pausova Z, Paus T. Brain size and folding of the human cerebral cortex. *Cereb Cortex*. 18:10 (2008) 2352-2357.
- Tsujimoto S, Genovesio A, Wise SP. Frontal pole cortex: encoding ends at the end of the endbrain. *Trends Cogn Sci*. 15:4 (2011) 169-176.
- Van Essen DC. A tension-based theory of morphogenesis and compact wiring in the central nervous system. *Nature*. 385:6614 (1997) 313-318.
- Violante IR, Ribeiro MJ, Cunha G, Bernardino I, Duarte JV, Ramos F, Saraiva J, Silva E, Castelo-Branco M. Abnormal Brain Activation in Neurofibromatosis Type 1: A Link between Visual Processing and the Default Mode Network. *PLoS One*. 7:6 (2012) e38785.
- Wang PY, Kaufmann WE, Koth CW, Denckla MB, Barker PB. Thalamic involvement in neurofibromatosis type 1: evaluation with proton magnetic resonance spectroscopic imaging. *Ann Neurol*. 47:4 (2000) 477-484.
- Wechsler D. *Escala de Inteligência para Crianças - Terceira Edição (WISC-III): Manual*. Lisboa: Cegoc-Tea. (2003).
- Wignall EL, Griffiths PD, Papadakis NG, Wilkinson ID, Wallis LJ, Bandmann O, Cowell PE, Hoggard N. Corpus callosum morphology and microstructure assessed using structural MR imaging and diffusion tensor imaging: initial findings in adults with neurofibromatosis type 1. *AJNR Am J Neuroradiol*. 31:5 (2010) 856-861.
- Xiang HD, Fonteijn HM, Norris DG, Hagoort P. Topographical functional connectivity pattern in the perisylvian language networks. *Cereb Cortex*. 20:3 (2010) 549-560.
- Yeterian EH, Van Hoesen GW. Cortico-striate projections in the rhesus monkey: the organization of certain cortico-caudate connections. *Brain Res*. 139:1 (1978) 43-63.

- Yunoue S, Tokuo H, Fukunaga K, Feng L, Ozawa T, Nishi T, Kikuchi A, Hattori S, Kuratsu J, Saya H, Araki N. Neurofibromatosis type I tumor suppressor neurofibromin regulates neuronal differentiation via its GTPase-activating protein function toward Ras. *J Biol Chem.* 278:29 (2003) 26958-26969.
- Zald DH, Andreotti C. Neuropsychological assessment of the orbital and ventromedial prefrontal cortex. *Neuropsychologia.* 48:12 (2010) 3377-3391.
- Zamboni SL, Loenneker T, Boltshauser E, Martin E, Il'yasov KA. Contribution of diffusion tensor MR imaging in detecting cerebral microstructural changes in adults with neurofibromatosis type 1. *AJNR Am J Neuroradiol.* 28:4 (2007) 773-776.
- Zhu Y, Guignard F, Zhao D, Liu L, Burns DK, Mason RP, Messing A, Parada LF. Early inactivation of p53 tumor suppressor gene cooperating with NF1 loss induces malignant astrocytoma. *Cancer Cell.* 8:2 (2005) 119-130.
- Zilles K, Armstrong E, Schleicher A, Kretschmann HJ. The human pattern of gyrification in the cerebral cortex. *Anat Embryol (Berl).* 179:2 (1988) 173-179.



# CONCLUDING REMARKS





# CHAPTER 7

Discussion  
and  
Conclusions

## DISCUSSION

The present thesis entails a tripartite methodology, employed to study the neurobiological basis underlying the cognitive deficits observed in patients with neurofibromatosis type 1 (NF1). Those involve visuospatial, executive function, motor, language and memory domains (Levine et al., 2006). Although these deficits have been extensively examined at the behavioural level, there is much to disentangle about the biological mechanisms contributing to the observed phenotype. Only by exploring these mechanisms one can truly understand pathogenesis and find adequate treatments that target disease mechanisms.

To gain access into the living human brain, we used magnetic resonance imaging and spectroscopy to acquire functional information on neural activity, and structural and neurochemical profiles of patients with NF1. In this final chapter I integrate these findings with reference to the results from other studies and provide suggestions for future studies. In addition, I propose a general mechanism to integrate functional, structural and neurochemical findings in NF1 based on our results and contributions from others.

### **Functional and neurochemical profiles in NF1: a focus on the visual cortex**

The first two research questions investigated in this thesis focused on the visual cortex (*Chapters 4 and 5*). Our group has recently shown a pattern of psychophysiological impairment in visual sensory processing in NF1 (Ribeiro et al., 2012). In *Chapter 4*, we explore this pattern further by using functional Magnetic Resonance Imaging (fMRI) to assess neural activation at the level of primary sensory visual cortex. fMRI has the advantage of probing neural activity and is able to provide spatial information within hierarchically defined early brain regions. We measured neural activation to stimuli that preferentially drive the activity of the two main pathways conducting information from the retina to the cortex: magnocellular (M) and parvocellular (P). Patients with NF1 showed deficient activation of the low-level visual cortex to both stimulus types, in agreement with our previous report of impaired contrast sensitivity in patients with NF1 (Ribeiro et al., 2012) and with deficient activation of the early visual cortex observed during performance of the judgment of line orientation task (Clements-Stephens et al., 2008). Importantly, impaired magno- and parvocellular activation was observed for children and adults with NF1, indicating that low-level visual processing deficits do not

ameliorate with age.

Altered visual processing at lower and higher levels of the dorsal and ventral streams may explain the visuospatial deficits that characterize the cognitive phenotype in patients with NF1. Moreover, impaired sensory processing can contribute to higher order cognitive deficits such as working memory and executive processing. In fact, besides the early visual cortex impairment, the NF1 group also presented a failure to deactivate regions belonging to the default mode network (DMN) during M-stimulation, particularly anterior medial prefrontal cortex/anterior cingulate cortex and the posterior cingulate and retrosplenial cortices. The mechanisms behind this abnormal DMN activation could be related to the attentional deficits known to occur in children with NF1. In that sense, one may hypothesise that activity in the DMN is explained by greater incidence of attention deficit hyperactive disorder (ADHD) related symptoms in patients with NF1, and thus an inability to stay on the task and tendency to daydream. In any case, in order to understand the neural mechanisms contributing to DMN activation it is important to account its dependence on stimulus type, given it only occurred during M-biased stimulation. The “magnocellular advantage” theory proposed by Laycock et al (Laycock et al., 2007; Laycock et al., 2008) suggests an important role for the M pathway in driving attentional mechanisms in higher-order cortical regions. According to Laycock, the M system plays a key role in guiding P processing by providing a general low-resolution “frame” for the visual environment, which is then “filled in” by details from the slower P system. How this relates to abnormal DMN activation is an intriguing aspect to be explored in future studies. Interestingly, it was recently shown that the pattern of connectivity of the DMN is altered in children with NF1, particularly the connections between the posterior cingulate cortex and the anterior medial prefrontal cortex (Chabernaud et al., 2012), regions with abnormal activity in our study. A normal connectivity pattern could be restored using lovastatin although it remains to be proven whether this rescues attentional deficits.

Our findings associated for the first time a visual sensory deficit to the NF1 cognitive profile. In other clinical populations there is already increasing appreciation of the contribution of early sensory dysfunction to higher order cognitive functions, particularly in autism (Sutherland and Crewther, 2010), Fragile X syndrome (Kogan et al., 2004) and schizophrenia (Martinez et al., 2008; Dias et al., 2011). This phenomenon is accompanied by an increasing comprehension of the complexity of early visual cortex involvement in many levels of visual computation (Alonso, 2002; Lee, 2003).

A deeper understanding of the processes that are capable of driving abnormal neural activation of the early visual cortex can be achieved by inspecting the neurotransmitters that shape visual responses. Information processing in the visual cortex relies on interactions between excitatory and inhibitory circuits, where excitatory outputs are shaped by the action of GABAergic interneurons (Dykes et al., 1984; Nelson et al., 1994; Swadlow, 2003; Atallah et al., 2012). For that reason, measurements of GABA levels can provide relevant information on the function of neuronal responses and subsequent behavioural processes. Therefore, the second research question explored in this thesis relied on measuring GABA in the early visual cortex to determine whether inhibition might be altered in NF1.

In *Chapter 5* we showed that GABA levels were reduced in patients with NF1 and that they could be predicted by the type of NF1 mutation. Reduced GABA levels are in line with the evidence that lower GABA concentration is related to poorer visual orientation discrimination performance (Edden et al., 2009), a hallmark deficit of the cognitive impairments found in patients with NF1 (Schrimsher et al., 2003). Correspondingly, the role of GABA in defining selectivity for stimulus orientation and direction of motion in the primary visual cortex has been well established in animals (Rose and Blakemore, 1974; Sillito, 1979; Tsumoto et al., 1979; Katzner et al., 2011). These results link GABAergic neurotransmission to local manipulations of GABA concentration. In that sense, it will be important to study orientation discrimination in NF1 and determine whether GABA levels are correlated with behavioural measurements.

Another point worth mentioning is the possible link between altered GABA concentration and psychophysical measurements of impaired contrast sensitivity in NF1. Contrast gain control operates in the retina (Shapley and Victor, 1981; Brown and Masland, 2001; Chander and Chichilnisky, 2001; Baccus and Meister, 2002) and is strengthened in the thalamus and visual cortex (Kaplan et al., 1987; Sclar et al., 1990; Cheng et al., 1995). However, the role of GABAergic inhibition in this process is subject to great controversy (Carandini and Heeger, 1994; Carandini et al., 1997; Freeman et al., 2002; Katzner et al., 2011). Furthermore, while measurements of GABA levels in the human visual cortex were correlated with surround suppression the same was not observed for contrast discrimination performance (Yoon et al., 2010). In future studies it will be interesting to assess surround suppression and overlay suppression in NF1. These two psychophysical approaches should constitute a good model to probe the extension of GABA abnormalities in NF1 and to further explain contrast

sensitivity deficits, given that they are thought to arise from two distinct suppressive neurophysiological mechanisms within the visual system. While surround suppression is thought to originate within the primary visual cortex (Walker et al., 2000; Akasaki et al., 2002; Osaki et al., 2011) and involves GABA mediated inhibition (Fu et al., 2010; Yoon et al., 2010), overlay suppression is thought to originate within the lateral geniculate nucleus (Freeman et al., 2002; Bonin et al., 2005; Li et al., 2006; Priebe and Ferster, 2006) and is not dependent upon GABA mediated inhibition within the visual cortex (Katzner et al., 2011).

Although our conclusions are derived from measurements of GABA in visual cortex, it is likely that analogous abnormalities generalize to other cortical areas, in agreement with the widespread GABAergic alterations observed in mice (Shilyansky et al., 2010). In fact, we performed GABA measurements in the dorsal anterior cingulate cortex of the same group of patients and observed reduced levels of GABA in this region. Given the substantial evidence that the morphological subtypes of cortical neurons and their basic laminar and tangential connectivity are conserved across cortical areas (Douglas and Martin, 2004) it is quite probable that the concentration of GABA is generally reduced in patients with NF1. If that is the case, this could contribute to explain the complex ocular motor pattern observed in children with NF1 (Lasker et al., 2003), where GABA is known to play a key role in saccadic behaviour (Schiller and Tehovnik, 2005; Hikosaka, 2007; Keller et al., 2008; Pouget et al., 2009).

Finally, our results should be conciliated with increased GABAergic neurotransmission measured in the *Nf1<sup>+/-</sup>* mice model. In that sense, the low GABA levels observed in patients might reflect a compensatory mechanism, since there is a dynamic modulation of GABA levels in response to increasing or decreasing network activity and in the context of brain disorders (Esclapez and Houser, 1999; Gomes et al., 2011). However, it remains an open possibility that the animal model does not recapitulate the neurochemical phenotype of the human disorder. Further studies are needed to evaluate these hypotheses. In particular, studies in both patients and animal models employing <sup>13</sup>C-Magnetic Resonance Spectroscopy (MRS) and molecular imaging using positron emission tomography (PET) to map GABA receptors, would deepen our understanding of the disease mechanism.

### **Brain regions involved in NF1**

Our studies would not be complete without investigating the neuroanatomy of NF1. In

order to understand how mutations in the NF1 gene impact brain structure it is essential to characterize in detail the brain structural abnormalities in patients. Therefore, in *Chapter 6* we assessed for the first time simultaneously, the variety of traits and brain regions that could be altered by the disorder in carefully matched patient and control groups. Our findings indicate that overall brain volume is increased in NF1 as a consequence of larger white matter and subcortical grey matter volumes. Moreover, patients with NF1 presented disproportionately larger thalami, right caudate and middle corpus callosum than typically developing children. In agreement with our findings, previous studies have identified the thalamus and the corpus callosum as structures involved in the neuroanatomy of NF1. In fact, the most consistent structural finding across studies is an enlargement of the corpus callosum in patients with NF1 (Kayl et al., 2000; Moore et al., 2000; Dubovsky et al., 2001; Steen et al., 2001; Cutting et al., 2002; Wignall et al., 2010). The corpus callosum is the major commissural structure in the human brain and it connects the left and right cerebral hemispheres. The principal function of the corpus callosum is to facilitate interhemispheric communication and transfer motor, sensory, and cognitive information between the hemispheres. Thalamic involvement in NF1 also pops out from the neuroanatomical findings reported. Diffusion-tensor imaging studies consistently reported alterations in the white matter microstructure of the thalamus (Zamboni et al., 2007; van Engelen et al., 2008; Ferraz-Filho et al., 2012). Moreover, PET studies employing radiotracers of glucose observed altered metabolism of the thalamus in patients with NF1 (Kaplan et al., 1997; Buchert et al., 2008). Interestingly, reports employing both the glucose radiotracer  $^{18}\text{F}$ -fluoro-deoxy-glucose (FDG), and the GABA<sub>A</sub> receptor antagonist  $^{11}\text{C}$ -flumazenil to quantify the density of GABA<sub>A</sub> receptors in epileptic patients, indicate that the hypometabolism documented by FDG-PET is co-localized with regional reduction of GABA<sub>A</sub> receptors (Ryvlin et al., 1998; Arnold et al., 2000). Future studies should investigate whether this evidence holds true for the NF1 thalamus. On the other hand, abnormal choline and N-acetylaspartate content in the thalamus of NF1 patients was observed using  $^1\text{H}$ -MRS (Wang et al., 2000), possibly reflecting altered myelination and neuronal loss or neuronal dysfunction. The thalamus is a highly interactive structure, with widespread connections to multiple cortical regions, that provides selection and transformation of different sensory inputs to the cortex. The various nuclei of the thalamus are involved in the integration of sensory and motor information, memory and executive functions (Schmahmann and Pandya, 2008), competences in which NF1 patients show disabilities (Hyman et al., 2005; Levine et al.,

2006; Roy et al.).

Unlike the specific observations concerning subcortical structures, examination of cortical measurements indicated that alterations in cortical volume, cortical surface area and cortical thickness were not significantly different from controls. Gyrification index was the only changed measure in cortex. Patients with NF1 showed lower gyrification indices than typically developing children primarily in frontal and temporal lobes, but also affecting the insula, cingulate cortex, parietal and occipital regions.

One of the most evident features of human evolution is the increase in brain size (Passingham, 1973). In response to evolutionary demands, a high level of gyrification occurred in parallel with an increase in cortical grey matter in order to maximize cortical surface while maintaining a smaller intracranial size (Zilles et al., 1988). The increase in folding in bigger brains seems to be necessary for the formation of efficient cortico-cortical connections in larger volumes (Ruppín et al., 1993; Murre and Sturdy, 1995). This evolutionary trait appears disrupted in NF1, with an increase in brain size without a corresponding adaptive increase in folding. The phylogenetic development of gyral and sulcal folds likely optimizes compaction of neuronal fibers while keeping neuronal signaling at efficient transit time (Ruppín et al., 1993; Murre and Sturdy, 1995). In that sense, abnormal cortical folding may reflect deficits in structural and, consequently, functional cortical connectivity. Lower gyrification indices were particularly evident in the frontal cortex, a region that has been successively associated to functional impairments (Billingsley et al., 2003, 2004; Shilyansky et al., 2010; Chabernaud et al., 2012; Violante et al., 2012).

Despite the pervasive expression of neurofibromin in the brain, the neuroanatomic abnormalities observed were dominantly localized to specific brain regions indicating that particular areas and specific neurodevelopmental processes, such as gyrification, might constitute selective targets for the NF1 gene mutation.

### **Integration of functional, structural and neurochemical findings**

Collectively, our data obtained in the same group of patients and convergent evidence from other functional and structural neuroimaging studies suggest the involvement of the visual cortex, the thalamus, the striatum (particularly the caudate), the corpus callosum, and the frontal cortex including the anterior cingulate cortex in NF1 disease mechanisms. It is therefore plausible that alterations in the circuitry interconnecting the cortex, basal ganglia, and thalamus are affected. The canonical connections forming these

cortico-striato-thalamo-cortical loops are shown in a simplified diagram here, Figure 1. Projections in this circuit use both the excitatory neurotransmitter glutamate and the inhibitory neurotransmitter GABA, as shown. The diagram is focused on the alterations observed in the visual cortex and thalamus, displayed as increased or reduced variables in comparison with controls. The role of the striatum in NF1 is less explored. However, it is certainly influenced by thalamo-cortical alterations. Furthermore, studies focusing on the functional consequences of increased volume and altered microstructure of the corpus callosum function in NF1 are warranted.

Interestingly, there is an absence of collective sustained findings involving the parietal cortex. This is rather surprising given that visuospatial deficits are considered a hallmark of the NF1 cognitive phenotype. This might be explained if the pattern of impairment observed in specific visuospatial tests (i.e judgement of line orientation test) is caused instead by impaired function of other brain regions such as fronto-executive regions. Evidence for this hypothesis can be found in visuospatial studies in NF1 (Billingsley et al., 2004; Clements-Stephens et al., 2008).

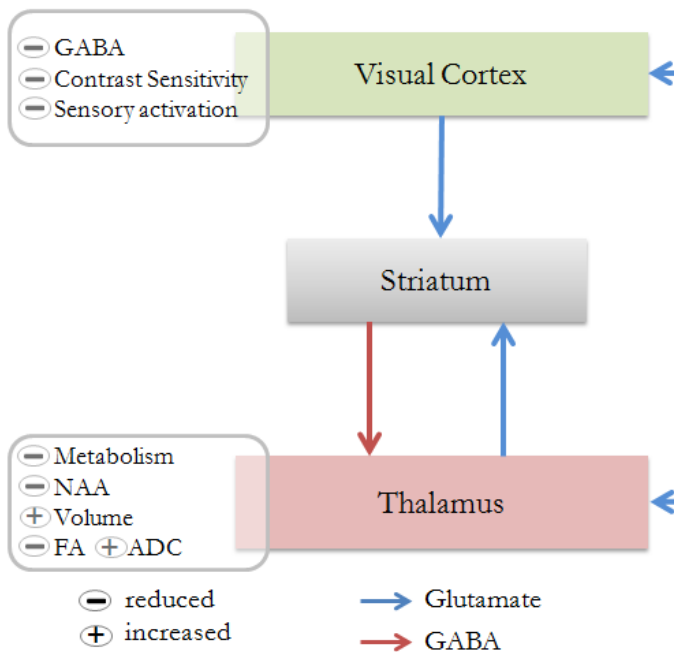


Figure 1. Simplified diagram of the cortico-striato-thalamo-cortical connections indicating alterations observed in NF1.



Finally, it remains to be referred the lack of correlations between our neuroimaging findings and IQ. Although, it is tempting to relate to relate neuropsychological performance directly with brain activity and structure, this is not entirely realistic. The majority of cognitive functions involve distributed processes in the brain and IQ certainly belongs to this category.

## CONCLUSIONS

As a single gene disorder, NF1 has a larger potential for elucidating gene–brain–behaviour connections than multigenic disorders, such as ADHD, autism, and schizophrenia. To further understand these connections we investigated the neurobiological basis underlying the cognitive deficits in patients with NF1. Although the studies presented in this thesis were not designed to yield knowledge directly applicable in clinical practice, our conclusions provide several aspects with relevance in clinical neuroscience:

- *Patients with NF1 have impaired visual sensory processing.* Impairments in downstream perception can contribute to higher order cognitive deficits that build up the information gathered from sensory areas.
- *GABA is reduced in the visual cortex of patients with NF1,* a pattern that possibly extends to other cortical regions. A distributed imbalance between excitatory and inhibitory systems is the most probable cause for the multiple cognitive deficits observed in NF1.
- *Subcortical structures are enlarged in NF1, while the cortical mantle has lower gyrification,* a pattern that indicates abnormal neuroanatomical development. The increase in folding in bigger brains enables efficient cortico-cortical connections. This evolutionary trait appears disrupted in NF1, with an increase in brain size without a corresponding adaptive increase in folding.

The work presented in this thesis identified novel neurobiological mechanisms and markers of NF1, which open new frontiers to comprehend the pathophysiology of the cognitive deficits and find adequate treatments for patients.

## REFERENCES

- Akasaki T, Sato H, Yoshimura Y, Ozeki H, Shimegi S. Suppressive effects of receptive field surround on neuronal activity in the cat primary visual cortex. *Neurosci Res.* 43:3 (2002) 207-220.
- Alonso JM. Neural connections and receptive field properties in the primary visual cortex. *Neuroscientist.* 8:5 (2002) 443-456.
- Arnold S, Berthele A, Drzezga A, Tolle TR, Weis S, Werhahn KJ, Henkel A, Yousry TA, Winkler PA, Bartenstein P, Noachtar S. Reduction of benzodiazepine receptor binding is related to the seizure onset zone in extratemporal focal cortical dysplasia. *Epilepsia.* 41:7 (2000) 818-824.
- Atallah BV, Bruns W, Carandini M, Scanziani M. Parvalbumin-expressing interneurons linearly transform cortical responses to visual stimuli. *Neuron.* 73:1 (2012) 159-170.
- Baccus SA, Meister M. Fast and slow contrast adaptation in retinal circuitry. *Neuron.* 36:5 (2002) 909-919.
- Billingsley RL, Jackson EF, Slopis JM, Swank PR, Mahankali S, Moore BD, 3rd. Functional magnetic resonance imaging of phonologic processing in neurofibromatosis 1. *J Child Neurol.* 18:11 (2003) 731-740.
- Billingsley RL, Jackson EF, Slopis JM, Swank PR, Mahankali S, Moore BD. Functional MRI of visual-spatial processing in neurofibromatosis, type 1. *Neuropsychologia.* 42:3 (2004) 395-404.
- Bonin V, Mante V, Carandini M. The suppressive field of neurons in lateral geniculate nucleus. *J Neurosci.* 25:47 (2005) 10844-10856.
- Brown SP, Masland RH. Spatial scale and cellular substrate of contrast adaptation by retinal ganglion cells. *Nat Neurosci.* 4:1 (2001) 44-51.
- Buchert R, von Borczyskowski D, Wilke F, Gronowsky M, Friedrich RE, Brenner W, Mester J, Clausen M, Mautner VF. Reduced thalamic 18F-fluorodeoxyglucose retention in adults with neurofibromatosis type 1. *Nucl Med Commun.* 29:1 (2008) 17-26.
- Carandini M, Heeger DJ. Summation and division by neurons in primate visual cortex. *Science.* 264:5163 (1994) 1333-1336.
- Carandini M, Heeger DJ, Movshon JA. Linearity and normalization in simple cells of the macaque primary visual cortex. *J Neurosci.* 17:21 (1997) 8621-8644.
- Chabernaud C, Mennes M, Kardel PG, Gaillard WD, Kalbfleisch ML, Vanmeter JW, Packer RJ, Milham MP, Castellanos FX, Acosta MT. Lovastatin regulates brain spontaneous low-frequency brain activity in Neurofibromatosis type 1. *Neurosci Lett.* 515:1 (2012) 28-33.
- Chander D, Chichilnisky EJ. Adaptation to temporal contrast in primate and salamander retina. *J Neurosci.* 21:24 (2001) 9904-9916.
- Cheng H, Chino YM, Smith EL, 3rd, Hamamoto J, Yoshida K. Transfer characteristics of lateral geniculate nucleus X neurons in the cat: effects of spatial frequency and contrast. *J Neurophysiol.* 74:6 (1995) 2548-2557.
- Clements-Stephens AM, Rimrod SL, Gaur P, Cutting LE. Visuospatial processing in children with neurofibromatosis type 1. *Neuropsychologia.* 46:2 (2008) 690-697.
- Cutting LE, Cooper KL, Koth CW, Mostofsky SH, Kates WR, Denckla MB, Kaufmann WE. Megalencephaly

- in NF1: predominantly white matter contribution and mitigation by ADHD. *Neurology*. 59:9 (2002) 1388-1394.
- Dias EC, Butler PD, Hoptman MJ, Javitt DC. Early sensory contributions to contextual encoding deficits in schizophrenia. *Arch Gen Psychiatry*. 68:7 (2011) 654-664.
- Douglas RJ, Martin KA. Neuronal circuits of the neocortex. *Annu Rev Neurosci*. 27:(2004) 419-451.
- Dubovsky EC, Booth TN, Vezina G, Samango-Sprouse CA, Palmer KM, Brasseux CO. MR imaging of the corpus callosum in pediatric patients with neurofibromatosis type 1. *AJNR Am J Neuroradiol*. 22:1 (2001) 190-195.
- Dykes RW, Landry P, Metherate R, Hicks TP. Functional role of GABA in cat primary somatosensory cortex: shaping receptive fields of cortical neurons. *J Neurophysiol*. 52:6 (1984) 1066-1093.
- Esclapez M, Houser CR. Up-regulation of GAD65 and GAD67 in remaining hippocampal GABA neurons in a model of temporal lobe epilepsy. *J Comp Neurol*. 412:3 (1999) 488-505.
- Ferraz-Filho JR, da Rocha AJ, Muniz MP, Souza AS, Goloni-Bertollo EM, Pavarino-Bertelli EC. Diffusion tensor MR imaging in neurofibromatosis type 1: expanding the knowledge of microstructural brain abnormalities. *Pediatr Radiol*. 42:4 (2012) 449-454.
- Freeman TC, Durand S, Kiper DC, Carandini M. Suppression without inhibition in visual cortex. *Neuron*. 35:4 (2002) 759-771.
- Fu Y, Wang XS, Wang YC, Zhang J, Liang Z, Zhou YF, Ma YY. The effects of aging on the strength of surround suppression of receptive field of V1 cells in monkeys. *Neuroscience*. 169:2 (2010) 874-881.
- Gomes JR, Lobo AC, Melo CV, Inacio AR, Takano J, Iwata N, Saido TC, de Almeida LP, Wieloch T, Duarte CB. Cleavage of the vesicular GABA transporter under excitotoxic conditions is followed by accumulation of the truncated transporter in nonsynaptic sites. *J Neurosci*. 31:12 (2011) 4622-4635.
- Hikosaka O. Basal ganglia mechanisms of reward-oriented eye movement. *Ann N Y Acad Sci*. 1104:(2007) 229-249.
- Hyman SL, Shores A, North KN. The nature and frequency of cognitive deficits in children with neurofibromatosis type 1. *Neurology*. 65:7 (2005) 1037-1044.
- Kaplan AM, Chen K, Lawson MA, Wodrich DL, Bonstelle CT, Reiman EM. Positron emission tomography in children with neurofibromatosis-1. *J Child Neurol*. 12:8 (1997) 499-506.
- Kaplan E, Purpura K, Shapley RM. Contrast affects the transmission of visual information through the mammalian lateral geniculate nucleus. *J Physiol*. 391:(1987) 267-288.
- Katzner S, Busse L, Carandini M. GABAA inhibition controls response gain in visual cortex. *J Neurosci*. 31:16 (2011) 5931-5941.
- Kayl AE, Moore BD, 3rd, Slopis JM, Jackson EF, Leeds NE. Quantitative morphology of the corpus callosum in children with neurofibromatosis and attention-deficit hyperactivity disorder. *J Child Neurol*. 15:2 (2000) 90-96.
- Keller EL, Lee KM, Park SW, Hill JA. Effect of inactivation of the cortical frontal eye field on saccades generated in a choice response paradigm. *J Neurophysiol*. 100:5 (2008) 2726-2737.
- Kogan CS, Bertone A, Cornish K, Boutet I, Der Kaloustian VM, Andermann E, Faubert J, Chaudhuri A. Integrative cortical dysfunction and pervasive motion perception deficit in fragile X syndrome.

- Neurology. 63:9 (2004) 1634-1639.
- Lasker AG, Denckla MB, Zee DS. Ocular motor behavior of children with neurofibromatosis 1. *J Child Neurol.* 18:5 (2003) 348-355.
- Laycock R, Crewther SG, Crewther DP. A role for the 'magnocellular advantage' in visual impairments in neurodevelopmental and psychiatric disorders. *Neurosci Biobehav Rev.* 31:3 (2007) 363-376.
- Laycock R, Crewther DP, Crewther SG. The advantage in being magnocellular: a few more remarks on attention and the magnocellular system. *Neurosci Biobehav Rev.* 32:8 (2008) 1409-1415.
- Lee TS. Computations in the early visual cortex. *J Physiol Paris.* 97:2-3 (2003) 121-139.
- Levine TM, Materek A, Abel J, O'Donnell M, Cutting LE. Cognitive profile of neurofibromatosis type 1. *Semin Pediatr Neurol.* 13:1 (2006) 8-20.
- Li B, Thompson JK, Duong T, Peterson MR, Freeman RD. Origins of cross-orientation suppression in the visual cortex. *J Neurophysiol.* 96:4 (2006) 1755-1764.
- Martinez A, Hillyard SA, Dias EC, Hagler DJ, Jr., Butler PD, Guilfoyle DN, Jalbrzikowski M, Silipo G, Javitt DC. Magnocellular pathway impairment in schizophrenia: evidence from functional magnetic resonance imaging. *J Neurosci.* 28:30 (2008) 7492-7500.
- Moore BD, 3rd, Slopis JM, Jackson EF, De Winter AE, Leeds NE. Brain volume in children with neurofibromatosis type 1: relation to neuropsychological status. *Neurology.* 54:4 (2000) 914-920.
- Murre JM, Sturdy DP. The connectivity of the brain: multi-level quantitative analysis. *Biol Cybern.* 73:6 (1995) 529-545.
- Nelson S, Toth L, Sheth B, Sur M. Orientation selectivity of cortical neurons during intracellular blockade of inhibition. *Science.* 265:5173 (1994) 774-777.
- Osaki H, Naito T, Sadakane O, Okamoto M, Sato H. Surround suppression by high spatial frequency stimuli in the cat primary visual cortex. *Eur J Neurosci.* 33:5 (2011) 923-932.
- Passingham RE. Anatomical differences between the neocortex of man and other primates. *Brain Behav Evol.* 7:5 (1973) 337-359.
- Pouget P, Wattiez N, Rivaud-Pechoux S, Gaymard B. A fragile balance: perturbation of GABA mediated circuit in prefrontal cortex generates high intraindividual performance variability. *PLoS One.* 4:4 (2009) e5208.
- Priebe NJ, Ferster D. Mechanisms underlying cross-orientation suppression in cat visual cortex. *Nat Neurosci.* 9:4 (2006) 552-561.
- Ribeiro MJ, Violante IR, Bernardino I, Ramos F, Saraiva J, Reviriego P, Upadhyaya M, Silva ED, Castelo-Branco M. Abnormal achromatic and chromatic contrast sensitivity in neurofibromatosis type 1. *Invest Ophthalmol Vis Sci.* 53:1 (2012) 287-293.
- Rose D, Blakemore C. Effects of bicuculline on functions of inhibition in visual cortex. *Nature.* 249:455 (1974) 375-377.
- Roy A, Roulin JL, Charbonnier V, Allain P, Fasotti L, Barbarot S, Stalder JF, Terrien A, Le Gall D. Executive dysfunction in children with neurofibromatosis type 1: a study of action planning. *J Int Neuropsychol Soc.* 16:6 (2010) 1056-1063.

- Ruppin E, Schwartz EL, Yeshurun Y. Examining the volume efficiency of the cortical architecture in a multi-processor network model. *Biol Cybern.* 70:1 (1993) 89-94.
- Ryvlin P, Bouvard S, Le Bars D, De Lamerie G, Gregoire MC, Kahane P, Froment JC, Mauguiere F. Clinical utility of flumazenil-PET versus [18F]fluorodeoxyglucose-PET and MRI in refractory partial epilepsy. A prospective study in 100 patients. *Brain.* 121 ( Pt 11):(1998) 2067-2081.
- Schiller PH, Tehovnik EJ. Neural mechanisms underlying target selection with saccadic eye movements. *Prog Brain Res.* 149:(2005) 157-171.
- Schmahmann JD, Pandya DN. Disconnection syndromes of basal ganglia, thalamus, and cerebrotectal systems. *Cortex.* 44:8 (2008) 1037-1066.
- Sclar G, Maunsell JH, Lennie P. Coding of image contrast in central visual pathways of the macaque monkey. *Vision Res.* 30:1 (1990) 1-10.
- Shapley RM, Victor JD. How the contrast gain control modifies the frequency responses of cat retinal ganglion cells. *J Physiol.* 318:(1981) 161-179.
- Shilyansky C, Karlsgodt KH, Cummings DM, Sidiropoulou K, Hardt M, James AS, Ehninger D, Bearden CE, Poirazi P, Jentsch JD, Cannon TD, Levine MS, Silva AJ. Neurofibromin regulates corticostriatal inhibitory networks during working memory performance. *Proc Natl Acad Sci U S A.* 107:29 (2010) 13141-13146.
- Sillito AM. Inhibitory mechanisms influencing complex cell orientation selectivity and their modification at high resting discharge levels. *J Physiol.* 289:(1979) 33-53.
- Steen RG, Taylor JS, Langston JW, Glass JO, Brewer VR, Reddick WE, Mages R, Pivnick EK. Prospective evaluation of the brain in asymptomatic children with neurofibromatosis type 1: relationship of macrocephaly to T1 relaxation changes and structural brain abnormalities. *AJNR Am J Neuroradiol.* 22:5 (2001) 810-817.
- Sutherland A, Crewther DP. Magnocellular visual evoked potential delay with high autism spectrum quotient yields a neural mechanism for altered perception. *Brain.* 133:Pt 7 (2010) 2089-2097.
- Swadlow HA. Fast-spike interneurons and feedforward inhibition in awake sensory neocortex. *Cereb Cortex.* 13:1 (2003) 25-32.
- Tsumoto T, Eckart W, Creutzfeldt OD. Modification of orientation sensitivity of cat visual cortex neurons by removal of GABA-mediated inhibition. *Exp Brain Res.* 34:2 (1979) 351-363.
- van Engelen SJ, Krab LC, Moll HA, de Goede-Bolder A, Pluijm SM, Catsman-Berrevoets CE, Elgersma Y, Lequin MH. Quantitative differentiation between healthy and disordered brain matter in patients with neurofibromatosis type I using diffusion tensor imaging. *AJNR Am J Neuroradiol.* 29:4 (2008) 816-822.
- Violante IR, Ribeiro MJ, Cunha G, Bernardino I, Duarte JV, Ramos F, Saraiva J, Silva E, Castelo-Branco M. Abnormal brain activation in neurofibromatosis type 1: a link between visual processing and the default mode network. *PLoS One.* 7:6 (2012) e38785.
- Walker GA, Ohzawa I, Freeman RD. Suppression outside the classical cortical receptive field. *Vis Neurosci.* 17:3 (2000) 369-379.

- Wang PY, Kaufmann WE, Koth CW, Denckla MB, Barker PB. Thalamic involvement in neurofibromatosis type 1: evaluation with proton magnetic resonance spectroscopic imaging. *Ann Neurol.* 47:4 (2000) 477-484.
- Wignall EL, Griffiths PD, Papadakis NG, Wilkinson ID, Wallis LI, Bandmann O, Cowell PE, Hoggard N. Corpus callosum morphology and microstructure assessed using structural MR imaging and diffusion tensor imaging: initial findings in adults with neurofibromatosis type 1. *AJNR Am J Neuroradiol.* 31:5 (2010) 856-861.
- Yoon JH, Maddock RJ, Rokem A, Silver MA, Minzenberg MJ, Ragland JD, Carter CS. GABA concentration is reduced in visual cortex in schizophrenia and correlates with orientation-specific surround suppression. *J Neurosci.* 30:10 (2010) 3777-3781.
- Zamboni SL, Loenneker T, Boltshauser E, Martin E, Il'yasov KA. Contribution of diffusion tensor MR imaging in detecting cerebral microstructural changes in adults with neurofibromatosis type 1. *AJNR Am J Neuroradiol.* 28:4 (2007) 773-776.
- Zilles K, Armstrong E, Schleicher A, Kretschmann HJ. The human pattern of gyrification in the cerebral cortex. *Anat Embryol (Berl).* 179:2 (1988) 173-179.







## LIST OF PUBLICATIONS

**Violante IR**, Ribeiro MJ, Cunha G, Bernardino I, Duarte JV, Ramos F, Saraiva J, Silva E, Castelo-Branco M. Abnormal brain activation in neurofibromatosis type 1: a link between visual processing and the default mode network. *PLoS One*. 7:6 (2012) e38785.

**Violante IR**, Ribeiro MJ, Edden RAE, Guimarães P, Bernardino I, Rebola J, Cunha G, Silva E, Castelo-Branco M. GABA deficit in the visual cortex of patients with NF1: genotype-phenotype correlations and functional impact. *Manuscript submitted for publication*.

**Violante IR**, Ribeiro MJ, Silva E, Castelo-Branco M. Gyrfication, cortical and subcortical morphometry in Neurofibromatosis type 1: an uneven profile of developmental abnormalities. *Manuscript submitted for publication*.

Duarte JV, Ribeiro MJ, **Violante IR**, Cunha G, Silva E, Castelo-Branco M. Multivariate Pattern Analysis Reveals Subtle Brain Anomalies Relevant to the Cognitive Phenotype in Neurofibromatosis Type 1. *Human Brain Mapping* (2012) *in press*.

Ribeiro MJ, **Violante IR**, Bernardino I, Ramos F, Saraiva J, Reviriego P, Upadhyaya M, Silva ED, Castelo-Branco M. Abnormal achromatic and chromatic contrast sensitivity in neurofibromatosis type 1. *Invest Ophthalmol Vis Sci*. 53:1 (2012) 287-293.

Delgado TC, **Violante IR**, Nieto-Charques L, Cerdan S. Neuroglial metabolic compartmentation underlying leptin deficiency in the obese *ob/ob* mice as detected by magnetic resonance imaging and spectroscopy methods. *J Cereb Blood Flow Metab*. 31:12 (2011) 2257-2266.

Rodrigues TB, **Violante IR**, Cerdan S. Unambiguous assignment of the H3S and H3R deuterations of cerebral (2-<sup>13</sup>C) glutamate by <sup>13</sup>C NMR at 18.8 Tesla. *Magn Reson Med*. 63:4 (2010) 1088-1091.

**Violante IR**, Anastasovska J, Sanchez-Canon GJ, Rodrigues TB, Righi V, Nieto-Charques L, Parkinson JR, Bloom SR, Bell JD, Cerdan S. Cerebral activation by fasting induces lactate accumulation in the hypothalamus. *Magn Reson Med*. 62:2 (2009) 279-283.

Ramirez BG, Rodrigues TB, **Violante IR**, Cruz F, Fonseca LL, Ballesteros P, Castro MM, Garcia-Martin ML, Cerdan S. Kinetic properties of the redox switch/redox coupling mechanism as determined in primary cultures of cortical neurons and astrocytes from rat brain. *J Neurosci Res*. 85:15 (2007) 3244-3253.



## AGRADECIMENTOS

Gostaria de agradecer ao meu orientador, Professor Miguel Castelo-Branco, por me ter acolhido no seu grupo e pelo empenho contínuo em proporcionar os meios necessários para possuímos um centro de investigação com qualidades ímpares. Por ter conseguido criar um grupo multidisciplinar onde é possível colaborar e aprender com pessoas vindas de diversas áreas. Acima de tudo, quero agradecer o apoio e a confiança que me foram depositadas ao longo destes anos, essenciais para cultivar ideias, ser criativa e ter vontade de idealizar novos projetos. Muito obrigada por partilhar comigo o seu entusiasmo pela ciência e o dinamismo que põe em tudo o que faz.

Ao Professor Carlos Geraldês, por quem tenho uma elevada gratidão e admiração. Agradeço por me ter ajudado a dar os primeiros passos na ciência e por me ter “indicado o caminho até aqui” tão sabiamente desde a licenciatura.

À Maria, que me orientou desde o primeiro dia. Muito obrigada pela exigência, por me ensinares a ser sempre crítica, pela constante disponibilidade e pela amizade. Obrigada por me despertares para os mistérios da mente humana e a vontade de criar experiências para os explicar.

Quero agradecer a colaboração e disponibilidade dos doentes e das suas famílias e de todas as pessoas que participaram como voluntários neste projeto e o tornaram possível. Muito obrigada às crianças, e aos pais que as acompanharam, e se entusiasmaram por fazer parte desta descoberta.

Muito obrigada ao Doutor Eduardo, à Dra. Fabiana e ao Professor Jorge Saraiva por acreditarem e impulsionarem a importante ligação da ciência à clínica. Obrigada ainda à Dra. Adélia Lourenço, por ser tão disponível, por nos ter recebido e dado um contributo fulcral para a realização deste projeto.

Durante os últimos quatro anos tive a sorte de conhecer e trabalhar com pessoas fantásticas. Acredito com veemência que o meu grupo no IBILI deveria estar qualificado como o melhor grupo para se trabalhar no mundo! A verdade é que quando cheguei aqui em agosto de 2008 estava muito longe de imaginar que faria tantos amigos e que conheceria as pessoas únicas e maravilhosas que conheci. Vocês são o exemplo do que é trabalhar em equipa e do quanto a entreajuda e a camaradagem podem contribuir para se crescer profissionalmente. Queria agradecer especialmente ao Zé (o melhor colega de gabinete de todos os tempos), pela amizade e pela ajuda, às Ineses pelas longas conversas, por todo o apoio e amizade, à Marieke pelas conversas e conselhos, por ser uma

presença tão calma e ponderada, ao Castelhana, pela simplicidade com que sabe estar na vida, à Ana pelos risos, sorrisos e boa disposição, à Filipa, pela originalidade, por ter garra e por ser “responzona”, à Andreia por me ensinar a ensinar e ter vontade de aprender, à Raquel por tantas gargalhadas que me proporcionou e à Susana por amar e odiar coisas como ela só. E a tantas outras pessoas com quem tive o prazer de trabalhar e conviver mais diretamente, nomeadamente o João Duarte, o Gil, a Otília e o Marco. Aos amigos Joana Sampaio, Pedro Serranho e Britta que conheci no IBILI. E ainda ao Carlos e ao João pelo apoio na ressonância, pela boa disposição e profissionalismo.

Aos bons amigos com quem partilhei mais esta etapa e quero partilhar muitas outras: Sílvia, Alberto, Tiago, Rita, Rui, Miguel, Joana, Idália, Zé, Ângela, Né, Cláudio, Denise, Tânia e Henrique. Aos amigos de infância e que serão certamente de velhice, João Goulão, Bruno Dias, Ana Luísa, Rodrigo, Miguel e Jorrrge.

Aos meus pais, à Joana e ao Hugo, por serem a minha família, por tudo o que sempre fizeram por mim, por me apoiarem tanto e tão incondicionalmente.

Ao Tiago, pelo amor, companheirismo, paciência e amizade. Porque soube estar sempre presente e por todos os sonhos e planos que partilhamos e por tudo o que iremos conquistar.

*Inês Violante, Agosto 2012*

## CURRICULUM VITAE

Inês Ribeiro Violante was born on April 10, 1984 in Lisbon, Portugal. Her primary education was done in Recife, Brazil, and her basic and secondary education was completed in Sertão, Portugal. In 2002, she went to the University of Coimbra to study Biochemistry. For her final B.Sc. project she spent one year doing research at the Biomedical Research Institute “Alberto Sols” in Madrid, Spain, as an Erasmus student under the supervision of Professor Sebastián Cerdán. She started working on her Ph.D. project at the Visual Neuroscience Laboratory, IBILI, at the Faculty of Medicine of the University of Coimbra in August 2008.